The Role of MerTK and BAFF in Dendritic Cell-B cell Interactions

Paul Reid Gohlke

A dissertation submitted to the faculty of the University of North Carolina at Chapel Hill in partial fulfillment of the requirements for the degree of Doctor of Philosophy in the Department of Microbiology and Immunology

Chapel Hill
2007

Approved by:

Larry W. Arnold, Ph.D.

Stephen H. Clarke, Ph. D.

Jeffrey A. Frelinger. Ph.D.

Glenn K. Matsushima, Ph.D.

Roland M. Tisch, Ph.D.

ABSTRACT

Paul Reid Gohlke: The Role of MerTK and BAFF in Dendritic Cell-B cell Interactions
(Under the direction of Dr. Glenn K. Matsushima)

Autoimmune disease occurs when the system of cells and molecules designed to protect the host from invading pathogens directs itself towards attacking the host. The development of autoimmunity involves the participation of several cell types each with a distinct role in disease pathogenesis. Systemic Lupus Erythematosus (SLE) is an autoimmune disease in which autoreactive B cells produce antibodies directed against ubiquitous components of the cell nucleus. Although B cells are the effector cell type in this process, specific genetic deletions in mouse models have shown that improper function of the non-B cell components of the immune system can be sufficient to coerce otherwise tolerant B cells into becoming autoantibody-producing cells. Mice lacking a functional version of the receptor tyrosine kinase MerTK (*mertk*^{kd} mice) are one such model. As in SLE, *mertk*^{kd} mice develop autoantibodies to antigens normally found in the cell nucleus such as dsDNA, ssDNA, chromatin, and Sm. While MerTK is not normally expressed by B or T cells, it is expressed by myeloid-lineage cells such as dendritic cells and macrophage. Since dendritic cells are known to both, present antigen to B cells, as well as produce the cytokine BAFF, we decided to investigate the possibility that dendritic cells from *mertk*^{kd} mice are facilitators of B cell autoimmunity. Our experiments demonstrate that MerTK functions to restrict spontaneous BAFF

production by dendritic cells. However we have also determined that dendritic cells have a pro-survival effect on B cells that is independent of both MerTK and BAFF. In an effort to further our understanding of the importance of dendritic cell-derived BAFF *in vivo* we have also generated a targeting construct, DT-BAFF^{flox}, that will permit conditional deletion of the *baff* gene in dendritic cells. Future application of DT-BAFF^{flox} towards creating a *baff*^{flox} mouse, in conjunction with the proper Cre transgenic mouse, will highlight the role that dendritic cell-derived BAFF plays in *mertk*^{kd} mice and other models of autoimmunity.

ACKNOWLEDGEMENTS

First and foremost, I would like to thank Dr. Glenn Matsushima for taking me into his laboratory. Through his mentorship and teaching he has made an invaluable contribution to my professional development. My laboratory co-workers, both past and current, have always fostered an enjoyable and productive work environment. Specifically, I would like to thank Dr. Eric Chen, Vivian Chen, Julie Clarke, Lorelei Taylor, Dr. Andrea Portbury, and Dr. Heather Seitz for their friendship and advice during our years of training together. I would also like to acknowledge the members of our technical staff: Heidi Block, Janell Hostettler, and Cody Schwartz. They carry out many necessary tasks that allow scientific research to proceed smoothly.

I would also like to acknowledge the following contributions of my generous colleagues outside of the Matsushima lab. Dr. Jrgang Chen was an essential source of knowledge, plasmids, and embryonic stem cells during the creation of the DT-BAFF^{flox} targeting vector. Dr. Randy Thresher has also offered advice on this project. I would also like to thank the members of Dr. Barbara Vilen's laboratory for conducting the anti-nucleosome ELISA analysis. Numerous graduate students outside of the Matsushima laboratory have also offered invaluable technical advice on several aspects of my project. These include Kara Conway, Dr. Matilda Nicholas, Dr. Tim Moran, Dr. Mark Wallet, and Dr. Chris Wysocki.

My interest in science and immunology stems from the excellent work of several teachers I have encountered prior to arriving at the University of North Carolina. These include my high school science teacher Dr. Kowalski, My undergraduate immunology professor, Dr. Klaus Elgert, the faculty of the Committee of Immunology at the University of Chicago, and Dr. Åke Lernmark, my former employer at the University of Washington. .

I am very grateful to the Medical Scientist Training Program at the University of North Carolina for brining me to this excellent institution. This program would not be so successful if not for the tireless efforts of Dr. Eugene Orringer, Dr. David Siderovski, and Elizabeth Garman. The Faculty and staff that make up the Microbiology and Immunology department have been extremely supportive throughout my time in graduate school. Finally, I am extremely humbled to be in the company of so many bright minds among my fellow graduate and M.D./Ph.D. students.

A large part of navigating through a research project is choosing which paths to take your work through among the seemingly infinite arbor of research directions. I would like to thank the members of my thesis committee for their guidance in this navigation.

I would like to thank my parents, Martha and James Gohlke, for their endless support in all of my educational endeavors, from kindergarten through medical and graduate school. Likewise, my brother Ken and sister Jennifer have been incredibly supportive throughout my life as well. My stepmother Lisa Hoffmann has been continuous source of courage, comfort and inspiration throughout my life as well. My

parents and brother in-law have also contributed significantly to this work through their support throughout my time in the M.D./Ph.D. program.

Most importantly, nothing that I have accomplished over the past 6 years here would have been possible were it not for my loving wife Julia. Her tireless efforts to raise our children while simultaneously pursuing her own scientific career amaze me daily. Finally, our children Chase and Lake have contributed by filling every moment spent outside of the laboratory with happiness.

TABLE OF CONTENTS

LIST OF TABLES

LIST OF FIGURES

LIST OF ABBREVIATIONS AND SYMBOLS

Ab	Antibody
Ag	Antigen
APC	Antigen presenting cell
APRIL	A proliferation inducing ligand
ATP	Adenosine triphosphate
autoAb	Autoantibody
BAFF	B cell activating factor belonging to the TNF family
BAFFR	BAFF receptor
Bcl	B cell lymphoma
BCR	B cell receptor
BCMA	B cell maturation antigen
BMDC	Bone marrow derived dendritic cell
bp	base pair
∆BAFF	delta BAFF
CVID	Common variable immunodeficiency
DAG	Diacyl glycerol
DC	Dendritic cell
dsDNA	Double stranded deoxyribonucleic acid
dsRNA	Double stranded ribonucleic acid
ECR	Evolutionary conserved region
EGF	Epidermal growth factor

ERK	Extracellular signal regulated kinase
FAK	Focal adhesion kinase
Fc	Fragment (constant) of an antibody
FcR	Fc receptor
Fo	Follicular
Foreign-Ag	Foreign antigen
Gas6	Growth arrest specific gene 6
GEF	Guanine nucleotide exchange factor
Gla	Glutamic acid rich
IFN	Interferon
IKK	IκB kinase
IL	Interleukin
Ig	Immunoglobulin
IP_3	Inositol triphosphate
IκB	Inhibitor of kappa B
JNK	c-jun N-terminal kinase
LPS	Lipopolysaccharide
MAPK	Mitogen activated protein kinase
$MerTK^{kd}$	MerTK kinase dead
MHC	Major histocompatibility complex
mRNA	messenger ribonucleic acid
MZ	Marginal Zone
MΦ	Macrophage

neo^r	neomycin-resistance
NK-κB	Nuclear factor kappa B
nM	nanomolar
PAMP	Pathogen associated molecular pattern
PI3K	Phosphotidlylinositol 3-kina
PKC	Protein kinase C
PLC	Phospholipase C
NK	Natural killer
NKT	Natural killer T
PRR	Pattern recognition receptor
PS	Phosphotidylserine
rBAFF	recombinant BAFF
RCS	Royal college of surgeons
RPE	Retinal pigmented epithelium
RTK	Receptor tyrosine kinase
Self-Ag	Self antigen
SHBG	Sex hormone binding globulin
SLE	Systemic lupus erythematosus
SLEDAI	Systemic lupus erythematosus disease activity index
Sm	Smith
snRNP	Small nuclear ribonucleoprotein
SOCS	Suppressor of cytokine signaling
spDC	Splenic dendritic cell

ssDNA	single stranded deoxyribonucleic acid
T1, T2, T3	Transitional stage 1, 2, or 3
TAM	Tyro3, Axl, MerTK family
TACI	Transmembrance activator and CAML interactor
TCR	T cell receptor
TI	Thymus independent
TM	Transmembrane
TNF	Tumor necrosis factor
Tc	Cytotoxic T cell
Th	Helper T cell
TLR	Toll like receptor
TK	Tyrosine kinase
TRAF	TNF receptor associated factor
μM	micromolar
WT	Wildtype
↑*loxP*	Upstream *loxP*
↓*loxP*	Downstream *loxP*

CHAPTER 1: Introduction

Part I. CELLS OF THE IMMUNE SYSTEM AND AUTOIMMUNITY

The mammalian immune system is comprised of several specialized cell types and molecules that work together to protect the body from pathogenic organisms. These components are broadly divided into the innate and the adaptive immune systems. The innate immune system is the more ancestral of the two and typically represents the body's initial response to infection. Cell types belonging to the innate immune system include: granulocytes (neutrophils, basophils, and eosinophils), mast cells, natural killer (NK) cells, macrophage (MΦ), and dendritic cells (DC), which are discussed in greater detail below. These cells express a variety of receptors that aid in the recognition of broad classes of pathogens. Some of these cell types can also destroy and remove pathogens, while others specialize in alerting the adaptive immune system to their presence [1].

Section 1: B and T Lymphocytes

B and T lymphocytes: Basic physiology

Lymphocytes, also known as B and T cells, are the cell types of the adaptive immune system [1]. What differentiates the evolutionarily nascent adaptive immune system from the innate immune system is the ability of B and T cells to reorganize their genomic DNA in order to generate proteins that recognize very specific molecular structures, or antigens (Ag). On B cells these rearranged genes are known as immunoglobulins (Ig), or antibodies (Ab). Antibodies are found on both the B cell surface, where they are referred to as the B cell receptor (BCR), and as secreted proteins that circulate throughout the body. T cells rearrange the genes coding for the T cell receptor (TCR), which is found only on the cell surface and is

not secreted. The process of BCR and TCR gene rearrangement is highly complex and random, resulting in millions of different B and T cell clones, each specific for a different Ag. This allows the adaptive immune system to focus a given immune response to a specific target by mobilizing only the B and T cell clones that are specific for a given Ag. The process of BCR and TCR gene rearrangement takes place early during B and T cell development in the bone marrow and thymus, respectively.

Mature B and T cells can be subdivided into different types of cells with specialized functions. B cells can be divided into B-1 B cells, B-2 B cells, and marginal zone (MZ) B cells [2-4]. B-1 B cells express a more limited set of BCR specificities and reside primarily in the peritoneal cavity. In the spleen the majority of mature B cells are B-2 B cells which reside in the follicle and thus also referred to as follicular (Fo) B cells. MZ B cells are a smaller subset that reside in the splenic marginal zone, a thin border which separates the red and white pulp.

Mature T cells exit the thymus expressing one of two co-receptor molecules on their surface, CD4 or CD8 [1]. $CD4^+$ T cells are also referred to as “helper” (Th) cells because their primary function is to activate and assist the activities of other lymphocytes and innate immune cells. This help is achieved both through the secretion of various cytokines, and specific surface protein interactions via cell-to-cell contact. $CD8^+$ T cells are also known as cytotoxic T cells (Tc), Once activated, $CD8^+$ T destroy other cells in the body that harbor intracellular foreign-Ag such as viruses.

Recognition of specific Ag by B and T cells takes place differently [1]. The BCRs, and Ab for that matter, bind to their cognate Ag in their native, or unprocessed form. This means that Ag does not need to be modified in any way by another cell type for it to be recognized by a B cell. This is not the case for T cell recognition of Ag through its TCR. The TCR can only recognize short peptides of whole Ag, and these pieces must be located within major histocompatability complex (MHC) proteins on the surface of another cell. Therefore, each T cell clone with its unique TCR is specific, not just for a given Ag, but for a specific piece of that Ag contained within a specific MHC molecule. $CD8^+$ T cells have a TCR that recognizes peptides within MHC class I molecules, which ubiquitously found throughout the body. The TCR on $CD4^+$ T cells, on the other hand, responds to peptides contained within MHC class II molecules, which are only found on a select set of cells in the immune system namely MΦ, DC, and B cells.

B and T lymphocytes: Autoimmunity

In a healthy immune system B and T cells are able to discriminate between molecules normally found in the body (self-Ag) from those that are derived from invading pathogens (foreign-Ag). The lack of an immune response to self-Ag is known as tolerance. There are several different mechanisms built into the immune system to insure that tolerance to self-Ag is maintained, when these mechanisms fail the result is what German microbiologist Paul Ehrlich first described100 years ago as *horror autotoxicus*, also known as autoimmunity [1].

While there are many autoimmune diseases that differ in their severity and target tissue, the commonality among all of them is the involvement of B and/or T

cell clones specific for self-Ag. Autoreactive B cell clones cause tissue damage by producing antibodies against self-Ag, or autoantibodies (autoAb). In some autoimmune diseases autoAb cause impaired function or destruction of specific target cells [1, 5]. Examples of this autoimmunity include: Hemolytic Anemia, Myasthenia Gravis, Hashimoto's Thyroiditis, and Graves disease. However, autoAb can also damage tissues by forming insoluble complexes of autoAb and target Ag (Immune complexes) that deposit in various tissues and lead to inflammatory damage. Systemic lupus erythematosus (SLE) is an example of this type of autoimmune disease. Autoreactive T cells are harmful in one of two ways [1]. Autoreactive $CD8^+$ T cells can directly attack tissues where their cognate self-Ag is found. Type 1 diabetes mellitus and Multiple Sclerosis are examples of this. Alternatively, self-Ag specific $CD4^+$ T cells are harmful because they aid in the activation of both autoreactive B and $CD8^+$ T cells. For this reason $CD4^+$ T cells likely participate in most autoAb-, and $CD8^+$ T cell -mediated autoimmune diseases.

Section 2: Dendritic Cells

Dendritic cells: Origins and subsets

Dendritic cells (DC) are bone marrow-derived innate immune cells residing in both lymphoid (thymus, lymph node and spleen) and peripheral tissues. Rather than a single cell type DC are actually a very heterogenous group of cells comprised of multiple subsets that differ in anatomical location and function. There are also notable differences in what we know about mouse and human DC, this is likely due to differences in the source of cells used in experiments for each [6]. This discussion will primarily focus on the subsets of DC found in the mouse spleen in the

steady state. It is important to note, however, that during non-steady state (inflammatory) conditions, such as blood-borne infection, new DC are generated from blood monocytes and enter the spleen [7]. Resident splenic DC (spDC) are non-migratory cells whose primary function is to capture Ag passing through the spleen and subsequently activate resident B and T cells. Aside from their primary derivation from the bone marrow [8], the nature of spDC precursors is a controversial subject [9, 10]. One set of evidence suggests that spDC are continuously replenished from precursor cells in the blood [9, 11]. However, there is also evidence suggesting that their numbers are maintained by a dividing resident splenic precursor [12].

Conventional splenic DC are identified based on their $CD11c^{hi}$ and MHC II^{+} surface phenotype. These DC can be broken down into $CD8\alpha^{+}$ $CD11b^{-}$ (also called lymphoid DC) and $CD8\alpha^{-}$ $CD11b^{+}$ (also called myeloid DC) subsets, with the later outnumbering the former in the spleen by roughly 3:1[6]. The $CD8\alpha^{-}$ DC population can be further divided based on their expression of CD4. A separate population of DC known as plasmacytoid DC can also be found in the spleen. They are distinguished from other DC by lower levels of CD11c and expression of the B cell marker B220.

Dendritic cells: Maturation and antigen presentation

DC continuously sample the environment for the presence of potentially harmful substances and foreign-Ag [13, 14]. When such material is encountered, DC are responsible for activating immune effector cells, such as T and B cells, so that an Ag-specific response to the foreign Ag can be initiated. This activity is known

as antigen presentation, and thus DC are often referred to as professional antigen presenting cells (APC). .

Uptake of extracellular material by DC requires that they are able to discriminate between substances normally found in the body (self-Ag) versus those that are derived from invading pathogens (foreign-Ag). The failure to make this distinction could lead to induction of a B and/or T cell response against self-Ag, potentially triggering pathogenic autoimmunity. Although DC lack rearranged Ag-specific receptors, such as BCR and TCR, they do have several receptors that recognize molecular structures common to large groups of pathogens. These pattern recognition receptors (PRR) and the pathogen-associated molecular patterns (PAMPS) they recognize constitute an evolutionarily ancient mechanism of host defense shared by non-vertebrates. The toll-like receptor (TLR) family of proteins are PRRs on many cells of the immune system. DC express TLR2, TLR3, TLR4, TLR5, TLR7, and TLR9 although there is variation among the various DC subsets [15]. Examples of PAMPS include lipopolysaccharide (LPS), a TLR4 ligand found on gram$^-$ bacteria, and double stranded RNA (dsRNA), a TLR3 ligand that is an intermediate in the replication cycle of viruses.

When foreign-Ag is encountered by DC it is usually accompanied by some type of PAMP that serves as a “danger signal”. PRR recognition of its cognate PAMP alerts the DC that it is time to activate its APC capabilities, a process referred to as “maturation” [16]. Typically, the events which are used to define DC maturation include: increased surface expression of costimulatory molecules such as CD40, CD80, and CD86, processing and loading of antigen-derived peptides onto

surface-bound major histocompatability (MHC; class I and/or class II) proteins, production of inflammatory cytokines such as interleukin-12 (IL-12), and the ability to activate Ag-specific T cells [13]. However, the term “DC maturation” has been broadly used in the literature to indicate any individual, or combination, of the above events [17].

Dendritic cells: Activation of T and B cells

The mechanism used by DC to activate T cells (both $CD4^+$ and $CD8^+$) has been deeply investigated and is well understood. Activation of T cells by mature DC occurs through two sets of molecular interactions or signals [18, 19]. Signal 1 occurs when Ag-derived peptides and MHC molecules on the DC surface are recognized by T cell clones via their unique T cell receptor (TCR). Signal 2 involves ligation of CD28 on T cells by CD80 and CD86 on DC. When T cells are exposed only to signal 1 without signal 2 they are not fully activated and are, in effect tolerized to the specific Ag that is present by the DC. Therefore the requirement for signal 2 by mature DC is a critical mechanism by which the activation of self-reactive T cells is prevented. This is especially important considering that, in the steady state, DC readily take up self Ag in the form of apoptotic cells, which is discussed below.

In addition to their critical role activating T cells recent evidence suggests that DC are also capable of retaining captured antigens in their native confirmation and making them available to stimulate antigen-specific B cells. In several different *in vitro* and *in vivo* model systems B cell-DC interactions have resulted in outcomes consistent with B cell activation including: upregulation of CD86 and MHC class II

[20, 21], proliferation [20], calcium release [21, 22], cytoskeletal rearrangement [22], differentiation into plasmablasts [23], and antibody production [24].

Since DC presentation of Ag to B cells is a rather new area of investigation many mechanistic questions remain unanswered. At a minimum it seems that Ag internalized by DC via phagacytosis [23], pinocytosis [21], or as immune complexes via FcγR-mediated endocytosis [20] can all be redisplayed on the cell surface with their B cell epitopes intact. If this is indeed the case, then what receptors, in addition to FcγR, are involved in the uptake of Ag by DC? What cellular organelles are involved in returning native Ag to the cell surface? How is the decision made by DC to process some Ag into T cell epitopes, while leaving others in their native format for recognition by B cells?

Another important question is whether or not the properties of mature DC that make them proficient at activating T cells, such as upregulation of peptide:MHC, CD80, CD86 and CD40, also make them better at presenting Ag to B cells, which lack TCR, CD28, and CD40L. This in turn leads to the following question: if the signal 1 equivalent of DC Ag presentation to B cells is the recognition of native Ag by the BCR, what, if any, signal 2 is required for full B cell activation and differentiation into Ab-secreting cells? DC production of the cytokine B cell activating factor belonging to the TNF-family (BAFF) is an intriguing possibility for the provision of signal 2 to B cells and is discussed later in this chapter.

Dendritic cells: Handling of Apoptotic cells

Dendritic cells are also part of the body's phagocytic system that is responsible for clearing the continuous burden of apoptotic cells [25]. Apoptotic cells

are a source of self-Ag. Their engulfment by DC could potentially lead to presentation of self-Ag to, and activation of, autoreactive B and T cell clones. However despite their ability to collect self-Ag and transport it to draining lymph nodes, in non-inflammatory conditions DC do not trigger autoimmunity [26, 27]. Two aspects of DC physiology insure that this does not occur [27]. First is the finding that immature DC are much more capable at apoptotic cell phagacytosis than mature DC [28]. This means that self-Ag are not acquired by DC already poised to activate T cells. Secondly, the act of apoptotic cell phagacytosis itself does not cause DC maturation [29, 30]. On the contrary, the phagacytosis of apoptotic cell has been shown to make DC refractory to future stimulation [29-31]. This effect can be replicated by PS liposomes suggesting that a PS receptor on DC, such as MerTK (indirect via Gas6) is responsible for triggering the inhibition [32]. However, the outcome of this interaction is likely modified by other molecules besides PS since the stage of apoptosis that a dying cell is at can determine the outcome of its engulfment by DC. Unlike the phagacytosis of early apoptotic cells, when DC eat late apoptotic cells they mature and become proficient at T cell activation [33].

For the prevention of autoimmunity the importance of retaining DC in an immature state is compounded by some observations suggesting that they display complexes of MHC class II and apoptotic cell-derived Ag on their surface [34-37]. It should be noted however that some investigators have reported that DC do not present apoptotic cell-derived Ag in MHC molecules [27]. This position was recently elevated by a recent report in which DC did not in fact load MHC class II with apoptotic cell-derived antigens unless a maturation stimulus (such as LPS) was

simultaneously encountered [38]. Although this is a critical issue that needs to be investigated further, the T cell stimulatory capacity of DC that have phagocytosed apoptotic cells is limited by their immature state (low expression of costimulatory molecules). Whereas inducing DC maturation simultaneously with the phagacytosis of apoptotic cells, by either CD40 ligation, tissue inflammation, or FcR engagement, will provoke robust T cell responses [26, 34, 37]. In the latter report the apoptotic cells were opsonized with autoAb before being eaten by DC. This FcR-mediated phagacytosis led to efficient Ag-specific T cell stimulation. This suggests that a positive feedback loop may exist whereby autoAb from self-reactive B cells can indirectly drive the activation of autoreactive T cells via activated/apoptotic cell-bearing, DC [34].

In summary, dendritic cells function as Ag collection and presentation cells for the adaptive immune system. In the absence of infection their continuous uptake of self-Ag requires that DC regulate their capacity to activate T and B cells. This regulation is accomplished, at least regarding T cell tolerance, by keeping self-Ag containing DC in an immature state. Failure to regulate DC APC function can result in pathogenic autoimmunity driven by self-reactive T and B cells.

Section 3: Systemic Lupus Erythematosus

Systemic lupus erythematosus (SLE) is an autoimmune disease characterized by the production of autoAb and deposition of immune complexes in tissues throughout the body [39]. A wide range of organs and tissues can be damaged in SLE, the combination of which varies from patient to patient. Major target organs (with frequency among SLE patients) include: joints (85%), skin (78%),

kidney (74%), vasculature (56%), central nervous system (54%), and lung (30%)[40]. Once immune complexes form and deposit in target organs the ensuing inflammation and activation of complement components damage the surrounding tissue. Although not present in all patients, kidney disease, or lupus nephritis, is the most life-threatening consequence of SLE. Typically in lupus nephritis the damage is focused at the glomerulus (glomerulonephritis), as opposed to tubuluar or interstitial areas. At the microscopic level several different patterns of glomerulonephritis are found in SLE patients, with different patterns being associated with different prognoses for eventual kidney failure [39]. In addition to kidney failure from active SLE, infection and atherosclerosis are also common causes of mortality in SLE [41].

SLE is typically diagnosed according to the SLE disease activity index (SLEDAI) [40]. The SLEDAI is a list of 11 possible symptoms including: malar rash, discoid rash, photosensitivity, oral ulcers, arthritis, serositis (heart or lung), renal disorder (nephritic syndrome or cells in urine), neurological disorder (psycosis or seizure), hematologic disorder (anemia, leuko-, lympho-, or thrombocytopenia), immunological disorder (autoAb to dsDNA, Sm, or phospholipids), and anti-nuclear antibodies. The presence of 4 out of 11 of these symptoms is sufficient to make a diagnosis of SLE. Epidemiologically, SLE is seen is approximately 1/2000 people, mostly of whom are women of childbearing age. There is a 10:1 ratio of female:male lupus patients in this age group, while that ratio is only 2:1 in pediatric and geriatric patients [40]. This has led to the widely held belief that female sex hormones play a significant role in disease etiology.

The self-Ag targeted by autoAb in SLE are predominantly located in the nucleus of all cells. Targets of autoAb can either be nucleic acid or protein in nature. Anti-dsDNA, anti-nucleosome (complex of dsDNA and histone), anti-histones, or small nuclear ribonucleoproteins (snRNPs) such as Sm, Ro, and La, are all targets of autoAb in SLE [42]. If these self-Ag are sequestered in the nucleus how then do they become the target of autoimmunity? When cells die they undergo a tightly controlled process of programmed cell death known as apoptosis [43, 44]. Part of this process involves fragmentation of the nucleus into smaller pieces known as blebs. Extensive studies have documented that during apoptosis components of the cell nucleus, are relocated to the surface of dying cells [45-50]. Thus, the process of apoptosis results in cell nuclear components becoming accessible to the immune system and potentially triggering autoimmunity. For this reason the rapid clearance of apoptotic cells is of the utmost importance for preventing an immune response to nuclear antigens.

The production of autoAb indicates that a loss of tolerance to self-Ag by lymphocytes is central to the immune dysfunction that leads to SLE. While B cells are obvious effector cells in the disease due to their secretion of autoAb, $CD4^+$ T cells also play an important part in SLE. Mouse models of SLE have shown that $CD4^+$ T cells participate in disease since depletion by anti-CD4 Ab treatment, thymectomy, or MHC class II-deficient mice, are all proctective [51-53]. Moreover autoreactive T cell clones specific for histones and/or Sm have been found in both SLE patients and mouse models [54-57]. These T cells are probably important early during SLE to help push autoreactive B cells over self-tolerance barriers, after which

time new self-Ag is targeted. For example, anti-dsDNA is the classic SLE autoAb, yet it does not contain any T cell epitopes and thus may arise only after a primary response to protein-DNA complexes [42]. Indeed, anti-nucleosome Ab arise before anti-dsDNA in MRL/*lpr* mice [58].

PART II. IN-DEPTH ANALYSIS OF MERTK AND BAFF: TWO MOLECULES THAT EXTRINSICALLY REGULATE B CELL TOLERANCE

Section 1: The MerTK Receptor Tyrosine Kinase

MerTK: Structure and Expression Pattern

MerTK is a 994 amino acid receptor tyrosine kinase (RTK) belonging to the Tyro3, Axl, MerTK (TAM) family [59]. This RTK family is defined by a C-terminal intracellular region containing intrinsic tyrosine kinase activity, and a signature $KWA^{I}/_{L}A^{I}/_{L}ES$ sequence, a single transmembrane domain, and an N-terminal extracellular region containing 2 fibronectin type-III domains and 2 immunoglobulin (Ig)-like domains [59, 60]. Proteolytic shedding of the extracellular domain has been demonstrated for both MerTK and Axl [61, 62].

Initially, human MerTK was so named because it was found to be expressed among monocytic (MerTK), epithelial (MerTK), and reproductive (MerTK) cells and tissues [63]. Further analysis in the mouse also revealed that MerTK is expressed among both hematopoetic (spleen and thymus) and non-hematopoetic tissues (heart, brain, lung, skeletal muscle, kidney, testis, retina, and liver) [59, 64, 65]. Among hematopoetic cell types MerTK is expressed by monocytes, macrophage, dendritic cells (DC), natural killer (NK) cells, NKT cells, and platelets [63, 64, 66]. Although not a hematopoetic-lineage cell type, it is relevant that bone marrow stromal cells also express MerTK [67]. MerTK is known to be absent from normal B cells, T cells, and granulocytes [59, 63, 66], but has been detected in various lymphoid leukemias [63, 68, 69]. A myeloid, rather than lymphoid, distribution pattern for MerTK is also seen histologically in various lymphoid organs (thymus,

spleen, and lymph node). Within the spleen, cells expressing MerTK are primarily restricted to the red pulp and marginal zone, with little among the white pulp areas harboring the majority of T and B lymphocytes [66, 70].

MerTK: Ligands

RTK's typically bind to, and are activated, by soluble growth factors [71]. The TAM family of RTK's bind to the vitamin K-dependent serum protein growth arrest specific gene 6 (Gas6) [72-77]. Gas6 was originally described as a gene upregulated in serum-starved NIH3T3 cells, and is most closely related to the anti-coagulant Protein S [78]. Affinity measurements have demonstrated that Gas6 binds strongest to Axl ($K_d \approx$ .4-1.6 nM), followed by Tyro3 ($K_d \approx$2.7-3.6 nM), and then MerTK ($K_d \approx$ 9.7-29 nM) [72, 73].

Binding of Protein S to TAM family members is controversial. Initial findings describing an interaction were based cross-species ligand-receptor pairs [76], while later analyses of interactions between human Protein S with human TAM receptors refute this interaction [72, 74]. More recently, in one mouse study recombinant Protein S was found to induce phosphorylation of Tyro3 and MerTK [65], but our work has demonstrated that serum derived Protein S binds only to Tyro3 [65, 79]. A model in which murine Protein S binds only to Tyro3, which indirectly leads to MerTK phosphorylation is consistent with both of these results. We have also shown that MerTK is not phosphorylated in macrophage lacking both Axl and Tyro3 [79]. This finding is consistent with the above model. Since this dissertation is primarily focused on MerTK, and since Gas6, but not Protein S, have been demonstrated to

physically bind to MerTK in the mouse system, Protein S will not be discussed further here.

Structurally, Gas6 is made from 678 amino acids arranged into an N-termial glutamic acid rich (Gla) domain, 4 epidermal growth factor (EGF)-like domains, and a C-terminal sex hormone binding globulin (SHBG) domain [80]. Experimental findings and crystal stucture analysis have led to a model in which the SHBG domain of Gas6 binds to the Ig-like domains of Axl resulting in the gathering of 2 ligand-receptor pairs into a single complex, culminating in tyrosine phosphorylation of Axl [81-83]. The N-terminal Gla domain of Gas6 binds to phosphatidylserine (PS) exposed on the outer surface of apoptotic cells [84, 85]. Similar to other Gla-containing proteins which bind to cell membranes, this process is dependent upon the γ-carboxylation of the Gla domain by a Vitamin-K dependent enzyme [84, 86]. These structural features of Gas6 have led to the proposal that it functions as a molecular bridge between PS on apoptotic cells and TAM family members [80, 87]. Although this 3-part interaction has yet to be proven experimentally, it is supported by a significant body of evidence describing a role for TAM family members in the phagacytosis of apoptotic cells (discussed below).

MerTK: Downstream Signaling

Due to the initial lack of a confirmed ligand, early studies of cell signaling pathways activated by MerTK involved overexpression of chimeric receptors made up of the extracellular region of an established recetor-ligand pair, and the cytoplasmic region of MerTK. MerTK tranduces signals from the external environment to the cell interior via its tyrosine kinase (TK) activity. MerTK's potential

as a kinase was initially suggested based on a TK-homology domain found during the cloning of the gene [59, 63]. Experimental verification of this kinase activity demonstrated that MerTK undergoes autophosphorylation and subsequently phosphorylates several unknown target proteins as well [88-90]. The ATP-binding lysine residue (K_{614}), and 3 tyrosine residues (Y_{744}, Y_{748}, and Y_{749}) are all required for MerTK kinase activity (Note: For simplicity, residues numbered here are based on the murine MerTK protein sequence. If the primary study involved human MerTK the residue number was converted to its homologous murine counterpart) [89, 91].

Multiple signaling pathways were reported to be activated by a chimeric MerTK construct including: phosphotidylinositol 3-kinase (PI3K), phospholipase Cγ (PLCγ), and the mitogen-activated protein kinase (MAPK) pathways [88]. Some of these early findings have been advanced or challenged by others, both in cells lines with chimeric receptors or with primary cells and Gas6.

Graham et al. made the initial observation of the existence of a putative PI3K p85 subunit binding motif ($Y_{825}xxM_{828}$) in MerTK's cytoplasmic tail [63]. Initial attempts to verify this interaction in transfected cell lines were unsuccessful [91]. Recently, however, MerTK was found to associate with the p85 and p110δ subunits of PI3K in dendritic cells following their engagement with apoptotic cells [31]. MerTK was also shown to bind to, and induce phosphorylation of, the adapter protein Grb2 via Y_{867} (on MerTK) [88, 91]. In one of these studies Y_{867} on MerTK was also required for Grb2 to associate with, and induce phosphorylation of, the p85 subunit of PI3K [91]. This suggests that the recruitment of PI3K by MerTK may take place at 2 different locations: direct binding of PI3K to the $Y_{825}xxM_{828}$ site, or indirectly via

Grb2 associated with the Y_{867} site. Which location is involved in the interaction of PI3Kδ with MerTK in dendritic cells is currently unknown.

MerTK Y_{867} was also required for binding of an unknown 95 kDa phosphorylated protein to PI3K p85 [91]. Although the identity of this 95 kDa protein is unknown, a potential candidate is the guanine nucleotide exchange factor (GEF), Vav1 (97 kDa) which has also been shown to bind MerTK [92]. In the absence of ligand Vav1 constitutively bound to the cytoplasmic tail of MerTK in a region containing the autophosyphorylation-target residues: Y_{744}, Y_{748}, and Y_{749}. Upon ligand addition Vav1 was phosphorylated, dissociated from MerTK, and went on to carry out its GEF function on RhoA-family members. Because the RhoA-family of proteins are known to mediate rearrangment of the cytoskeleton during phagacytosis [93], the MerTK-Vav1 interaction was postulated to be a mechanism by which cells are triggered to initiate the engulfment of Gas6 bound-apoptotic cells [92].

Vav1 is involved in activating PLCγ, also a binding partner of MerTK [94]. In primary macrophage and J774 cells apoptotic thymocytes cause PLCγ to bind endogenous MerTK and become phosphorylated [95]. Since PLC proteins generate the second messenger molecules, diacyl glycerol (DAG) and inositol triphosphate (IP_3), which in turn activate protein kinase C (PKC) and mobilize calcium ions from intracellular stores, respectively [96], these downstream events may also be triggered by MerTK.

Another signaling pathway by which MerTK initiates phagacytosis has also been described. A constitutively active form of MerTK was found to activate Rac1 via a cascade that proceeded through a Src-family kinase, FAK, $p130^{CAS}$, CrkII, and

Dock180. Although the region of MerTK needed to activate this response was not identified, MerTK kinase activity was required. This pathway also involves the cytplasmic tail of the β_5 integrin [97]. The $\alpha_v\beta_5$ integrin uses the same FAK, $p130^{CAS}$, CrkII, Dock180, Rac1 machinery to initiate the phagacytosis of apopototic cells [98]. Furthermore, $\alpha v\beta 5$ integrin has been shown necessary for MerTK activation during RPE phagocytosis in the eye [99]. Therefore MerTK likely cooperates with other receptors to fully induce the cytoskeletal rearragements that are needed to engulf apoptotic cells.

Early studies in transfected cell lines implicated MerTK in activating the MAPK signaling pathway [88]. However, more recently Sen et al demonstrated that the MAPK pathway members JNK, ERK and p38 are not activated by apoptotic cell treatment of dendritic cells [31].

Another example of conflicting findings is the effect of MerTK on the transcription factor nuclear factor κ B (NF-κB). Initiation of the canonical or "classical" NF-κB pathway begins with activation of the IκB Kinase (IKK) complex (consisting of IKKα, IKKβ, and IKKγ). The IKK proteins phosphorylate the inhibitor of κB (IκB), which targets it for proteolytic destruction. Since the function of IκB is to retain NF-κB family members in the cytoplasm, its destruction allows NF-κB homo- or heterodimers to enter the nucleus and regulate the transcription of a wide range of genes critical for inflammation and proper immune system function [100].

Georgescu et al. found that MerTK activated an NF-κB luciferase reporter construct, partially through PI3K, in a pro-B cell line [91]. In contrast, macrophage from mice lacking a functional MerTK protein (*mertk*^{kd} mice) are hypersensitive to

LPS-induced NF-κB activation [101]. This was advanced when it was found that pretreatment of dendritic cells with apoptotic cells prevents LPS–induced activation of IKK proteins, IκB destruction, and nuclear localization of NF-κB by a MerTK-dependent mechanism [31]. In addition to inhibiting the IKK signaling complex MerTK may also promote regulation of NF-κB activity at target genes. Twist proteins inhibit NF-κB activity by binding to nearby *cis*-acting site on NF-κB target promoters [102]. Recently, an Axl-dependent mechanism of inhibition by upregulating Twist was described [103]. It is currently unknown if and how MerTK modulates the expression and activity of Twist proteins. To review, evidence collected using primary cells collectively describe an *inhibitory* role MerTK in NF-κB function. Earlier results describing an NF-κB-*activating* role for MerTK are either artifactual, due to the super-physiologic levels of ectopic/chimeric MerTK constructs used in the earlier experiments, or reflect the differential usage of MerTK by different cell types.

In summary, MerTK is a receptor tyrosine kinase that initiates several downstream pathways in response to apoptotic cells and/or Gas6. Based on evidence compiled over the past 12 years signal transduction events from MerTK can be grouped into 2 distinct functional outcomes. First, MerTK initiates a signaling cascade that culminates in activation of RhoA family members, leading to cytoskeletal rearrangement and, presumably, the phagacytosis of apoptotic cells. Downstream mediators such as Vav1, PLCγ, and the FAK/ $p130^{CAS}$/ CrkII/Dock180 complex are likely involved in this outcome. In the second outcome, engagement of MerTK by apoptotic cells also leads to negative regulation of dendritic cells by preventing future activation of NF-κB. The interaction of PI3K with MerTK is likely a

commonality between both of these downstream pathways. PI3K is both required for the phagacytosis of apoptotic cells [104, 105], and participates in the negative regulation of dendritic cells [31, 106, 107]. Which functional outcome results from MerTK activation may depend on which isoform of p110 is used. During the phagacytosis of apoptotic cells p110β and p110δ localize to the phagocytic cup, but only p110β is required for actual engulfment [108]. The presence of p110δ at the site of engulfment, however, may indicate its interaction with MerTK in response to apoptotic cells [31].

MerTK: Functions

Functional studies of MerTK have been greatly enhanced by the generation of *mertk*^{kd} mice. This mouse line was generated by insertion of a neomycine-resistance cassette into the exons of the *mertk* gene that code for the tyrosine kinase domain [101]. This results in an unstable protein product that is not detectable on the cell surface or in cell extracts [79, 109]. The initial phenotype attributed to *mertk*^{kd} mice was a hypersensitivity to LPS-induced toxic shock, resulting in excessive systemic production of tumor necrosis factor alpha (TNF-α) and poor survival. Coincidently, cultured MΦ from *mertk*^{kd} mice also secrete high levels of TNF-α and display elevated levels of NF-κB binding to a minimal *tnfa* gene promoter [101].

The heightened activation state of MΦ lacking MerTK indicated that it functions as a negative regulator of myeloid lineage cells belonging to the innate immune system. In line with this premise, MerTK was also found to regulate NF-κB in DC [31]. However in *mertk*^{kd} DC the lack of negative regulation is only manifest in

cells that have had prior exposure to apoptotic cells. *Mertk*^{kd} DC display normal levels of activation markers such as CD80, CD86, CD40, and MHC class II [79, 109]. However, where apoptotic cell pretreatment prevents upregulation of these markers by LPS in WT DC, this does not occur in *mertk*^{kd} DC[109]. The same is true for DC secretion of the cytokines interleukin-12 (IL-12) and TNF-α [31, 109]. As described earlier, the inhibitory effect of apoptotic cells on WT DC, which does not occur in *mertk*^{kd} DC, takes place by preventing activation of the IκB kinase (IKK) in response to later stimuli [31].

The most well described function of MerTK is its involvement in the phagacytosis of apoptotic cells. The sequence of discoveries that led to this discovery began, not in the immune system, but in the retina. MerTK having an important function in the retina was initially alluded to by the observation of blindness in mice lacking all 3 TAM family members (TAM mice) [110]. This finding was soon corroborated by studies involving the Royal College of Surgeons (RCS) rat, a model for the human disease retinitis pigmentosa [111]. In the outer retina, the pigmented epithelial layer is made of phagocytic cells that continuously engulf apoptotic photoreceptor cells. This process does not occur in RCS rats due to an autosomal recessive mutation, leading to degeneration of photoreceptors and blindness [112]. In the year 2000 two independent groups discovered that the genetic lesion responsible was a large deletion at the 5' end of the *mertk* gene [113, 114]. Genetic rescue of phagacytosis by RPE cells from RCS rats was then achieved *in vitro* by introduction of a WT allele of the rat *mertk* gene [115]. Given that TAM mice are blind, the relative contribution of MerTK, Axl and Tyro3 to maintenance of the retina

was investigated. Retinal degeneration takes place in mice solely lacking *mertk*, while mice lacking Axl, Tyro3, or both, are unaffected [79, 116, 117]. Importantly, mutations in *mertk* have also been found in retinitis pigmentosa patients [118, 119].

The efficient phagacytosis of apoptotic cells by specialized cells is also an important process in tissues besides the retina. In the spleen where large numbers of apoptotic cells are removed from the systemic circulation daily, this job is filled by MΦ and DC [120, 121]. Given that macro express MerTK, and that Gas6 binds to PS on the surface of apoptotic cells, MerTK's importance in macrophage phagacytosis was investigated by our group in 2001. $Mertk^{kd}$ mice were found to be deficient in the clearance of apoptotic cells from the thymus and spleen, as were their MΦ in *in vitro* [117, 122]. All phagocytic capabilies were not impaired, however, as latex beads or opsonized apoptotic cells were engulfed with WT efficien cy by $mertk^{kd}$ MΦ [79, 117]. This phenotype is shared by other members of the TAM family in some, but not all, cell types and tissues. Loss of Axl and Tyro3, individually or in combination, also results in a reduced ability of MΦ to phagocytose apoptotic cells [79]. However, in the thymus, as in the retina, these receptors are redundant while MerTK is not [79]. Alternatively, Axl and Tyro3 are the critical receptors for phagacytosis by DC, while MerTK is not required [66, 79, 109]. Thus DC have relegated MerTK to the specialized function of inhibiting activation when apoptotic cells are present, while relying on Axl and Tyro3 for the actual engulfment of dying cells [79]. Since DC are proficient at collecting self antigens and activating the adaptive immune system, the specialized function of MerTK in this cell type has probably developed as a mechanism to prevent autoimmunity.

Several findings illustrate that MerTK does indeed regulate immune homeostatsis and tolerance *in vivo*. TAM mice have enlarged secondary lymphoid organs containing elevated numbers of activated B and T cells [70]. Since TAM receptors are not expressed by B and T cells, their increased numbers is likely secondary to an increased activation state of cells that do express TAM receptors. Indeed, MΦ and DC from TAM mice displayed elevated levels of MHC class II, particularly after administration of LPS *in vivo.* Furthermore transferred WT B and T cells underwent several rounds of cell division in TAM, but not WT, recipient mice [70]. Thus, TAM family members are negative regulators of myeloid lineage cells, and a heightened activation state of these cells leads to activation of bystander B and T cells. At this time it is unclear if *mertk*^{kd} mice also have enlarged lymphoid compartments.

Both TAM and *mertk*^{kd} mice display signs of autoimmunity, as evidenced by their spontaneous production of antibodies to self-antigens (self-Ag) commonly targeted in the disease systemic lupus erythematosus (SLE). The list of antigens targeted by autoantibodies (AutoAb) in *mertk*^{kd} mice includes:dsDNA, ssDNA, chromatin, Smith (Sm), heterogeneous nuclear ribonucleoprotein P2 (hnRNP P2), cardiolipin, IgG (rheumatoid factor) [49, 117, 122, 123]. AutoAb against dsDNA, collagen and phospholipids are produced in TAM mice [70]. For some of these autoAb it has been demonstrated that titers are low in younger mice and increase steadily with age [122]. In SLE organ damage is caused by deposition of immune complexes made up of self-Ag and autoAb in highly vascular structures such as the glomerulus of the kidney[5, 40]. Deposition of IgG in the glomerulus occurs in TAM,

and to a lesser degree, *mertk*^{kd} mice [70, 122]. However, *mertk*^{kd} mice do not progress to severe kidney pathology or proteinuria. Increasing levels of autoAb with age, minus the complication of renal failure (as seen in more robust SLE mouse models), make the *mertk*^{kd} mouse a valuable model for studying age-associated autoimmunity.

Aside from regulating DC and being required for the phagacytosis of apoptotic cells, MerTK has important functions on other hematopoetic lineage cell types as well. MerTK is expressed by platelets, while the presence of Axl and Tyro3 on these cells is disputed [64, 124]. Gas6-MerTK signaling is required for proper platelet degranulation and aggregation, and loss of function in either of these genes is protective in mouse models of thrombotic disease [64, 125]. A soluble form of the extracellular domain of MerTK, generated by proteolytic clevage, is found in serum [62]. Addition of exogenous soluble MerTK was found to be protective in a thrombosis model, suggesting that this system may autoregulate itself to preserve normal hemostasis *in vivo*.

NKT cells from *mertk*^{kd} mice have an intrinsic defect in cytokine production. Perhaps this is related to the newly described role for TAM family members in NK cell development [67]. Differentiation of NK cells *in vitro* is enhanced by Gas6 and protein S. Furthermore, development of functional NK cells in the bone marrow was reduced in TAM mice, as was their killing capability and IFNγ production. In functional assays partial phenotypes were observed in NK cells singly, or doubly deficient in TAM family members, suggesting some redundancy in their function [67].

Section 2: BAFF

BAFF: Structure

The B cell activating factor belonging to the TNF family (BAFF, also known as BlyS, TALL-1, THANK, CD257 and zTNF4) is a 309 amino acid protein that plays a critical role in homeostasis of mature B cells [126-129]. BAFF is a type II transmembrane protein consisting of a short (48 residue) N-terminal cytoplasmic region, a 21 residue transmembrane (TM) region, and a 240 residue extracellular TNF-homology domain at the C-terminus [126]. In the stalk region between the TM and TNF-homology domains a conserved sequence ($R_{125}NRR_{128}$) serves as a proteolytic clevage site, releasing the C-terminus of BAFF as a soluble cytokine [126, 130]. The sequence of this clevage site implicates a furin-type protease as responsible for proteolytic cleavage of BAFF, although the exact enzyme has yet to be identified experimentally. In addition, a mechanism for soluble BAFF secretion that bypasses the cell membrane has been shown to take place in neutrophils [131]. X-ray crystalography of soluble BAFF shows that it is capable of forming homotrimers, similar to other TNF-family members [132]. There are also reports that BAFF trimers can further multimerize into “virus-like” structures made up of over 60 BAFF molecules [132, 133]. The existence of such a structure *in vivo*, and its biological relevance, is unverified at this point.

A splice variant for BAFF in which exon 4 (in mouse, exon 3 in human) has also been described (∆BAFF). When coexpressed in cell lines, ∆BAFF can form multimers with full length BAFF and interfere with its receptor binding and biological activity [134]. Transgenic expression of ∆BAFF can also block the activity of

endogenous BAFF *in vivo* [135]. However, although mRNA for ΔBAFF was found in several cell lines and primary cells, and although ΔBAFF protein can be made by transfected cell lines [134], there is no evidence yet that ΔBAFF protein is made from endogenously spliced transcripts.

BAFF: Function

BAFF has several functions on B cell homeostasis and activation, most important of which is its role as a pro-survival factor. This is best evidenced by the drastic reduction in mature B cells seen in *baff*-null mice [136, 137]. B cell maturation begins in the bone marrow where pre-B cells rearrange and test their BCR. Only B cells that have a functional BCR are allowed to leave the bone marrow and migrate to the spleen. Newly formed B cells entering the spleen are still considered immature until they pass through a series of transitional stages T1→T3, after which they become mature B-1, Fo, or MZ B cells. Most B1 B cells relocate to the peritoneal cavity, whereas Fo and MZ B cells reside in the spleen and lymph node cells[2]. Mice lacking BAFF have a block in B cell maturation beginning at the T2 stage. This is manifest as a drastic, albiet not complete, reduction of mature B cells [136-138]. The B cell compartment can be rescued by providing *baff*-deficient mice with a *bcl2* transgene, indicating that promoting survival is the mechanism responsible for maintaining the size of the mature B cell pool [139].

Gain-of-function experiments confirm BAFF's ability to promote B cell survival. Mice harboring BAFF as a transgene have greatly enlarged B cell compartments [127, 140, 141]. Similar results are also seen when recombinant BAFF is given to mice [128, 142].The pro-survival effect of BAFF has also been demonstrated

repeatedly on *ex vivo* B cell cultures [143]. Early *in vitro* experiments demonstrated that BAFF enhances the proliferation of B cells stimulated through their BCR, or with fixed *Staphylococcus aureus* [128, 130, 144]. However, later analyses both, in vitro and in vivo, have established that BAFF itself is not mitogenic [145, 146]. Thus observations of enhanced proliferation likely result primarily from the survival signal given to daughter cells. This survival benefit afforded to replicating B cells by BAFF may result from its induction of cyclooxygenase 2, and subsequent production of prostaglandin E2, which itself enhances B cell viability *in vitro* [147]. However, it has also been proposed that BAFF may prime cells for division without actually pushing them into S-phase [148].

Coincident with BAFF's pro-survival function is it's role in setting the tolerance threshold of the mature B cell pool. As B cell pass through the transitional stages interclonal competition for a limited amount of BAFF governs the final autoreactive makeup of the mature B cell compartment [149]. When found as a monoclonal population autoreactive B cells successfully pass through this checkpoint. However, once they are forced to compete with a full repertoire of clones for BAFF autoreactive B cells fail to enter the mature pool. Autoreactive B cells in a mixed population can, however, be rescued when excess BAFF is provided systemically [150, 151]. Thus BAFF functions as a sort of B cell tolerance "stat". Under homeostatic conditions BAFF levels are set at a point at which a toleragenic B cell pool is maintained. When excess BAFF is present this set point is adjusted so that autoreactive B cells are able to survive through the transitional stages [152].

Several observations fit with a model in which regulating the level of BAFF is critical to maintaining a non-autoreactive B cell population and preventing autoimmunity. First, BAFF transgenic mice develop an SLE-like autoimmunity marked by autoAb and kidney pathology [127, 140, 141, 152]. Second, BAFF levels are elevated in SLE mouse models [127], and in some SLE patients during disease [153, 154]. Elevated BAFF levels have also been found in patients with rheumatoid arthritis [155, 156], Sjögrens syndrome [157, 158], and idiopathic thrombocytopenic purpura [159]. However, BAFF is not elevated in autoimmune diseases with a destructive T cell component, such as insulin-dependent diabetes mellitus and primary biliary cirrhosis [160].

In addition to providing a survival signal, BAFF also influences class switching and secretion of antibody. Ab class switching was classically thought to require interactions between CD40 on B cells and CD40L (CD154) on T cells. However, BAFF provided by DC and MΦ can also induce switching to IgG, IgA, and IgE isotypes independent of CD40 [161, 162]. Aside from switching, BAFF can also enhance the secretion of several Ig isotypes *in vitro* [161-163]. These events are also mediated by BAFF *in vivo* since mice given excess BAFF, exogenously or as a transgene, have elevated circulating levels of IgE, IgA, and all of the IgG sub-isotypes in addition to IgM [127, 128, 140, 142]. It is difficult to fully delineate how much of these elevated titers are due to the BAFF-driven Ab secretion versus enhanced B cell survival. Plasmablasts are Ag-stimulated B cells that are precursors to fully differentiated plasma cells. They also represent a relatively late stage in the lifespan of B cells at which autoreactive cells can be regulated and

prevented from progressing to autoAb secreting cells [164]. BAFF has been shown to enhance the survival of human plasmablasts [165] and may be responsible for the differentiation of mouse plasmablasts as well [23, 165].

Early results with *baff*-deficient mice suggested that, independent from promoting survival, BAFF is also required for the differentiation of MZ B cells. This is because among the limited pool of mature B cells that do remain in these mice, the MZ population was completely absent. This conclusion relied on the identification of MZ B cells based on their expression profile of CD21 and CD23 [136, 137]. Later analyses, however, found that there are B cells in the anatomic marginal zone and that they can be identified using flow cytometry by their IgD and IgM pattern [166], but that their numbers are still reduced [138]. Their earlier perceived absence it turns out was due to the fact that BAFF upregulates the expression of CD21 and CD23 [166].

BAFF: Receptors

BAFF binds to 3 different receptors. BCMA (B cell maturation antigen), and TACI (transmembrane activator and CAML interactor) were the first to be identified and also bind to a closely related ligand APRIL (a proliferation-inducing ligand) [127, 167, 168]. A third receptor, which binds BAFF exclusively, was later identified and named BAFFR [169, 170]. BAFF binds to TACI and BAFFR strongly (low nM), but weakly to BCMA (low μM). This may indicate that BCMA is not a physiological receptor for BAFF but is for APRIL, to which it binds with low nM affinity [171]. This premise is corroborated by the fact that, while mice lacking either BAFF or BAFFR

have very similar phenotypes in terms of their lack of most mature B cells, mice lacking BCMA are seemingly normal in this regard [137, 172].

Immature B cells first become responsive to BAFF during passage through the transitional stages (T1→T3) in the spleen [173]. In line with this TACI and BAFFR expression are first apparent at the T2 stage, and progressively increase thereafter [146]. Among mature splenic B cells, BAFFR is highly expressed by both MZ and FO B cellls, while TACI is expressed at low levels on FO B cells and highly on MZ B cells [138, 174, 175].

Functionally, BAFFR and TACI have opposing roles on B cell survival. Evidence from *baffr*-null mice and A/WySnJ mice, which carry a natural mutation in *baffr*, indicate that BAFFR is the principal receptor responsible for mediating BAFF's pro-survival effect on B cells and the maintenance of the mature B cell pool [138, 170, 176]. TACI on the other hand, has an inhibitory effect on the size of the mature B cell pool [177-179]. Aside from these opposing effects on B cell numbers BAFFR and TACI also have opposing effects on activated B cells [180]. TACI's effects are not all negative, however, as *taci*-null mice display impaired Ab responses to thymus-independent (TI) Ag [177], and impaired IgA class switching [162]. Further complicating the picture is the recent identification of patients with common variable immunodeficiency (CVID) who carry mutations in *taci* [181, 182].

BCMA is expressed by T1 cells but not by subsequent transitional or mature B cells [146, 183]. Instead, BCMA likely becomes important after differentiation of activated B cells since it is expressed by plasmablasts and is required for the maintenance of resident bone marrow plasma cells [163, 165, 184].

BAFF: Survival signaling in B cells

BAFF initiates signaling events in B cells that are consistent with its pro-survival function. Chief among these is activation of both the classical and alternate NF-κB signaling pathways. The alternative pathway is different from the classical pathway (described in Part II, section 1) in that it is initiated upon proteolytic processing of NF-κB2 (p100) to p52 which enters the nucleus as a heterodimer with RelB. Activation of the alternate NF-κB pathway proceeds through NF-κB-inducing kinase (NIK) and IKKα, rather than IKKα in complex with IKKβ and IKKγ [100]. Initially, BAFFR was thought to preferentially activate the alternate NF-kB pathway [185, 186]. This preference is due to an atypical TNF receptor associated factor (TRAF) binding motif in BAFFR [187]. Later, however, it was discovered that both NF-κB pathways are in fact involved in BAFF-mediated survival signals in B cells [145, 146, 188,enzler, sasaki, 189, 190].

In addition to NF-κB, BAFF is also known to activate the ERK [191], and PI3K-Akt signaling pathways. The latter was also shown to involve a novel mechanism for activation of Akt by protein kinase Cβ (PKCβ) [192].

Signaling events initiated by BAFF cause a shift in the balance of pro- and anti-apoptotic proteins in B cells. BAFF downregulates the activity of pro-apoptotic proteins. Activation of B cells through their BCR activates the pro-apoptotic protein Bim. Simultaneous provision of BAFF, however, prevents this [191]. Furthermore, in *bim*-deficient mice tolerance to self-Ag is lost, and the survival of *ex vivo* B cells is BAFF-independent [193]. Autoreactive B cells, which are chronically stimulated through their BCR, contain elevated levels of Bim [150]. This may explain why they

have a higher requirement for BAFF and therefore compete poorly with non-autoreactive B cells. BAFF also prevents accumulation of PKCδ in the nucleus, where it would otherwise participate in apoptosis by phosphorylating histones [194].

In contrast to inhibiting Bim and PKCδ, BAFF promotes the function of anti-apoptotic genes [195]. mRNA and/or protein for Bcl-2, Bcl-xL, Pim-1 and -2, Mcl-1 and A1 have all been shown to be upregulated by BAFF in resting and activated B cells *in vitro* [145, 146, 188, 195-197]. At the protein level the induction of bcl-2 by BAFF seems to not take place in resting B cells, but rather is limited to CD40L-activated B cells only [145, 188]. Furthermore, levels of A1 protein are not elevated by BAFF, and *a1*-deficient B cells do not show a decreased survival response to BAFF [188].

BAFF: Sources

Sources of BAFF can be divided into two groups of cells, hemotopoetic and stromal [198]. Radiation-sensitive hematopoetic BAFF sources include MΦ, DC, and neutrophils [131, 144, 161, 199, 200]. BAFF is not made by normal (untransformed) B cells, but has been reportedly produced by activated T cells. The radiation-resistant stromal cell types that produce BAFF are ill-defined at this point but likely include follicular DC which are known to produce BAFF [201] and are highly radiation-resistant [202, 203]. Bone marrow chimera experiments involving *baff*-deficient mice (referred to as KO here for simplicity) have illustrated the relevance of these two BAFF-producing populations *in vivo* [198]. In terms of maintaining a full B cell compartment under homeostatic conditions, stromal cell-derived BAFF (KO→WT) is both necessary and sufficient. This population is also the sole source of

circulating BAFF that can be detected in mouse serum. Upon Ag challenge however, BAFF derived only from hematopoetic sources (WT→KO) is sufficient to induce WT titers of IgG1, and intermediate numbers of *ex vivo* Ab-secreting cells. This is especially impressive considering that WT→KO mice have a 6-fold reduction in total B cells compared to WT or KO→WT mice. This study has led to the paradigm that, while stromal cells produce what BAFF is needed for a full B cell population in the steady state, hematopoetic cells are mobilized to produce excess BAFF during an immune response (desired or pathologic). In agreement with this model BAFF mRNA levels in blood leukocytes from SLE patients correlate more strongly with disease scores than do their serum BAFF levels [204].

Despite this division of responsibility among BAFF-producing cells there is still relatively little evidence that BAFF derived from hematopoetic cell types, such as DC, can modulate B cell responses *in vivo* during infection or autoimmunity. One exception is an important study by Balazs et al, which demonstrated that, after capturing bacteria, circulating DC migrate to the spleen to present Ag to MZ B cells. Activated B cells then differentiated into plasmablasts, and this process could be blocked by addition of a soluble form of TACI [23]. Ag-fed DC could also induce these changes in B cell *in vitro*. However it is premature to assume that *in vivo,* DC, and not stromal cells, were the critical suppliers of the agent that was blocked by soluble TACI. Furthermore, we do not know if this agent was BAFF or APRIL, since TACI binds both with similar affinity [171]. Mice carrying a conditional deletion of BAFF in specific cell types (such as DC) will be needed to fully address their individual contribution to B cell responses *in vivo*.

The majority of published experiments concerning DC and MΦ-derived BAFF come from primary human cells studied *in vitro*. BAFF expression can be detected on the surface of these cells and is secreted into culture supernatants. Inducers of BAFF by these cell types include: IFNγ, IFNα, IL-10, CD40L, LPS, and peptidoglycan [128, 130, 161, 200, 205]. MΦ- and DC- derived BAFF does regulate B cell function *in vitro* by enhancing proliferation, Ab secretion, and inducing Ig class switiching [130, 144, 161].

The information regarding BAFF production by murine myeloid cell types is more limited and not in complete agreement with the human data. For example, TLR agonists such as LPS and CpG oligodeoxynucleotides did not induce BAFF secretion by murine DC [199]. However, in a separate study LPS did cause elevated surface expression of BAFF on DC, but secretion was not measured [205]. What is most intriguing about both of these reports is that, collectively, they suggest a mechanism for a possible positive feedback loop that drives autoimmunity. Diaz-de-Durana et al. found that, in addition to LPS, apoptotic and necrotic cells also increased surface BAFF levels on DC [205]. Thus apoptotic cells can simultaneously serve as both a source of autoAg and a means by which DC can provide excess BAFF to autoreactive B cells. Meanwhile, Boulé and colleagues found that in their system the strongest inducer of BAFF by DC was immune complexes of chromatin and autoAb [199]. Indicating that once autoreactive B cells make autoAb to chromatin, and immune complexes form, DC are provoked to secrete more BAFF, proving further survival and differentiation signals to autoreactive B cells. The ability of excess BAFF to drive autoimmunity in mice, and

the association of higher BAFF levels with various autoimmune diseases would suggest that understanding how BAFF expression is regulated is a worthwhile research endeavor. However, unlike the breadth of data concerning BAFF's effect on B cells, there is little understanding of the molecular players that control BAFF mRNA expression or protein production. DC lacking the suppressor of cytokine signaling-1 (SOCS-1) have constitutively elevated BAFF mRNA and protein levels. They also have an enhanced ability to augment BCR-induced B cell proliferation and Ab secretion, and cause anti-dsDNA to be made when transferred into WT mice [206]. Therefore SOCS-1 seems to be a critical regulator of BAFF production by DC. One of the goals of our work here is to increase our understanding of what other molecules may regulate BAFF production by DC.

The experiments described in this dissertation were designed to test the hypothesis that MerTK regulates DC function in a manner that affects how they interact with B cells. We have specifically addressed the production of BAFF by DC as one potential mechanism by which dysregulated DC can promote the loss of B cell tolerance.

CHAPTER 2: Dendritic Cells Utilize MerTK to Regulate BAFF Production But Not Interactions with B Cells

ABSTRACT

The MerTK receptor tyrosine kinase is an important negative regulator of dendritic cell function and is required to prevent B cell autoimmunity *in vivo*. Since MerTK is expressed by dendritic cells, but not B cells, we sought to test the hypothesis that dendritic cells from mice lacking MerTK (*mertk*^{kd} mice) have characteristics that promote autoantibody production. We found that *mertk*^{kd} mice contain an elevated number of splenic dendritic cells, and that dendritic cells from older *mertk*^{kd} mice contain an elevated percentage of cells secreting the critical B cell survival factor, B cell activating factor (BAFF). Elevated numbers of BAFF secreting cells were also detected among *mertk*^{kd} bone marrow-derived dendritic cell (BMDC) populations. This was seen in both resting BMDC, and BMDC stimulated with lipopolysaccharide (LPS) or treated with exogenous apoptotic cells. We also found that dendritic cells in general have a pro-survival effect on resting B cells in coculture. However, despite containing more BAFF-secreting cells, *mertk*^{kd} BMDC were not superior to C57BL/6 or *baff*-deficient BMDC at promoting B cell survival. These results do not support a model in which *mertk*^{kd} DC promote autoantibody production *in vivo* via excess BAFF production.

INTRODUCTION

Systemic Lupus Erythematosus (SLE) is an autoimmune disease in which a breakdown of tolerance mechanisms permits self reactive B cell clones to produce autoantibodies (autoAb) against a variety of self antigens normally found in the nuclei of intact cells [40]. The genetic etiology of SLE is complex with dozens of susceptibility loci having been established in humans and mouse models [207, 208]. In addition, there are several single gene knockout mouse models in which lupus-like symptoms (autoAb production to nuclear antigens, immune complex deposition, etc.) develop. For some of these genes the primary defect in tolerance mechanisms can be classified as either B cell intrinsic (TLR7 and *Ly108*, for example) [209-211] or B cell extrinsic (MFG-E8 and DnaseI, for example) [212, 213].

MerTK is a member of the TAM (Tyro3, Axl, MerTK) family of receptor tyrosine kinases. Mice lacking all three of these receptors develop splenomegaly, autoAb, and spontaneous lymphocyte activation [110], demonstrating that the TAM family is involved in immune homeostasis and tolerance. Immune dysfunction is also found in mice solely lacking a functional *mertk* gene (*mertk*^{kd} mice). These animals show increased cytokine production [70, 101], and develop autoAb to several nuclear antigens including: dsDNA, ssDNA, chromatin, and Sm [49, 70, 117, 122]. Autoimmunity in *mertk*^{kd} mice is likely to be primarily driven by B cell extrinsic mechanisms as MerTK is expressed in macrophage, dendritic cells (DC), natural killer (NK) cells, and NK-T cells, but is absent in normal B and T cells. [31, 59, 66, 67]. This makes *mertk*^{kd} mice a valuable model for examining how B-cell extrinsic

mechanisms can facilitate self-reactive B cells to bypass tolerance safeguards and produce autoAb.

The TAM family members play a role in the recognition and phagacytosis of apoptotic cells. This recognition likely takes place through the serum protein growth arrest specific gene 6 (Gas6), a known ligand for TAM family members that also binds to phosphatidlylserine exposed on the surface of apoptotic cells [72, 73, 214]. These receptors have non-overlapping functions in the phagacytosis of apoptotic cells depending on the tissue and cell type involved [79]. Interestingly, unlike macrophage and retinal pigmented epithelial cells, DC do not require MerTK for the phagacytosis of apoptotic cells [31, 66, 79]. Instead, MerTK is used by DC to transduce inhibitory signals in response to apoptotic cells. Apoptotic cells render DC refractory to LPS-induced maturation and inefficient at antigen presentation to T cells [29-31, 109]. Mechanistically, this inhibition proceeds through PI3Kδ and culminates in impaired activation of the transcription factor NF-κB [31, 109]. *Mertk*^{kd} DC lack the ability to inhibit the NF-κB signaling pathway in response to apoptotic cells [31].

Dysregulated DC in *mertk*^{kd} mice are potential facilitators of B cell autoreactivity for two reasons: DC have the ability to capture and present native antigen to B cells, and DC produce the cytokine BAFF (also known as BLyS, TALL-1, and CD257). It is well established that DC are potent stimulators of antigen specific T cell responses via their ability to capture, process, and display antigenic peptides on their cell surface within MHC molecules for recognition by T cell receptors [13]. More recently, however, evidence has accumulated suggesting that

DC are also capable of retaining captured antigens in their native confirmation and making them available to stimulate antigen-specific B cells [20-24]. Although the exact mechanism responsible for this “native” antigen presentation has yet to be defined, there is evidence that antigens are first internalized by DC prior to being re-displayed on the surface [20, 21].

One mechanism by which DC have the potential to modify B cell behavior is through their production of BAFF. BAFF is a type II transmembrane protein that contains a C-terminal cytokine domain which is released upon proteolytic clevage at an extracellular site [126, 130]. Functionally, BAFF fills a critical role during the later stages of B cell life history, ranging from the late transitional stages to differentiated plasma cells. Perhaps most striking is BAFF’s ability to regulate the size and repertoire of the mature B cell pool by delivering a necessary pro-survival signal to resting B cells [152, 163, 215]. *Baff*-deficient mice have severely reduced numbers of mature splenic B cells [136, 137], whereas mice carrying a *baff* transgene display elevated B cell numbers and signs of autoimmunity [127, 140, 141]. Furthermore BCR-transgenic mouse models have been used to demonstrate that limiting BAFF availability is a mechanism by which the immune system excludes autoreactive B cell clones from the mature B cell repertoire [150, 151]. *In vitro,* recombinant BAFF promotes B cell survival by up regulating pro-survival molecules and down regulating pro-apoptotic pathways [145, 146, 188, 191, 194].

DC-derived BAFF has been shown to have several effects on B cell function *in vitro* including: enhanced proliferation [144], plasmablast differentiation [23], Ig class switching [161], and Ig secretion [161, 206]. However, direct evidence that DC

promote B cell survival, either *in vitro* or *in vivo,* via a BAFF-dependent mechanism is lacking. Furthermore, bone marrow chimera studies involving *baff*-null mice have demonstrated that systemic BAFF levels and the maintenance of a normal B cell compartment require BAFF derived from radiation-resistant (stromal), but not radiation-sensitive (bone marrow derived), cell populations. Thus the influence that DC-derived BAFF has on *in vitro* B cell survival and overall B cell homeostasis *in vivo* is unclear.

Given the following observations: 1) *mertk*^{kd} mice make autoAb, 2) excess BAFF promotes B cell autoimmunity, 3) DC normally express BAFF and 4) MerTK functions as a negative regulator of DC activation, we examined the hypothesis that MerTK regulates BAFF production and therefore influences DC-B cell interactions. We found that DC lacking MerTK have an enhanced capacity to secrete BAFF, both at rest and in response to LPS or apoptotic cells. A novel B cell survival assay was then designed to study the biological significance of DC-derived BAFF. Unexpectedly, excess BAFF production by *mertk*^{kd} DC did not translate into an enhanced ability to augment B cell survival *in vitro*. In fact DC support of B cell survival was found to occur through a BAFF -independent mechanism. These results suggest that aberrant secretion of BAFF by DC may not be responsible for autoAb production in *mertk*^{kd} mice.

MATERIALS AND METHODS

Mice C57BL/6 mice were purchased from Jackson Laboratories and then bred in house. *mertk*^{kd} mice have been describe previously [101]. The animals used in these experiments were backcrossed to C57BL/6 for 6 generations. Mice lacking a functional *baff* gene (*baff* mice) (also backcrossed to C57BL/6, n=8) were kindly provided by Biogen Idec and have been described previously [137]. All mice were kept under pathogen-free conditions in our UNC Division of Laboratory Animal Medicine facilities and in accordance with the Institutional Animal Care and Use Committee approved protocols.

Autoantibody ELISA Assays For the anti-dsDNA ELISA calf thymus dsDNA (Promega) was pre-treated with S1 nuclease (Promega) to remove contaminating ssDNA. Maxisorp plates (NUNC) were then filled with 10 µg of S1-treated dsDNA in 100 µl water, which was evaporated overnight in a 37°oven. Plates were blocked for 2 hours at room temperature with 4% fetal bovine serum. After washing, sample sera (diluted 1:100) and standards were added in triplicate and incubated for 2 hours at room temperature. After washing anti-mouse IgG^{HRP} (R&D Systems) was added and incubated for 1 hour at room temperature. ABTS (Sigma) was used as a substrate and absorbance at 405 nm was measured on a microplate reader (Bio-Tek Instruments). The standard curve consisted of sera pooled from multiple 6 month old MRL/*lpr* mice. A 1:100 dilution of this serum was arbitrarily designated as 100 Units/ml, 2-fold serial dilutions were then made down to 1:6400 or 1.56 Units/ml. This was the limit of detection for the assay. A semi-logarithmic plot was used to derive the standard curve equation ($y=mLn(x)+b$).

The anti-nucleosome assay was performed by Barbara Vilen's laboratory. ELISA plates (Dynatech) were coated with 100 µl of 100 µg/ml histones (Immunovision) and incubated overnight at 4°C. Plates were washed with boric acid-buffered saline (BBS) and wells were then coated with 100 µl of 10 µg/ml dsDNA (Sigma) for 3 hours at room temperature. Plates were washed with BBS and blocked with 200 µl of BBS-0.5% BSA-0.4% Tween for 1 hour at room temperature. After washing, samples and standards were added (50 µl/well) and incubated overnight. Samples were detected with goat anti-mouse Ig-alkaline phosphatase at 1:1000 and developed with p-nitrophenyl phosphate in buffer. Wells were read at 405 nm

Ex vivo splenic dendritic cells DC were enriched from spleens using anti-CD11c microbeads (Miltenyi Biotech) according to manufacturer's instructions. Recovered cells were typically 75-95 % $CD11c^+$, as assessed by flow cytometry.

Bone marrow derived dendritic cell (BMDC) culture To generate DC *in vitro* femurs were collected from 2-3 month old mice. Following a brief ethanol wash and PBS rinse femurs were flushed with RPMI 1640 (Gibco) to extract marrow which was then dissociated with gently pipetting. After osmotic red blood cell lysis, remaining cells were washed in PBS, suspended in media and counted. $2x10^6$ bone marrow cells were plated in 4 ml of media in 6-well ultra low cluster plates (Corning). BMDC media consisted of RPMI 1640 containing 10% FBS (Atlanta Biologicals), 50 U/ml penicillin, 50 µg/ml streptomycin, 1 mM sodium pyruvate, 0.1 mM non-essential amino acids, 0.05 mM β-Me (all from Gibco), 10 ng/ml GM-CSF and 10 ng/ml IL-4 (both from Peprotech). Cells were maintained at 37°C with 5% CO_2. On day 1 of

culture non-adherent cells were removed, diluted approximately 2-fold with fresh media containing 20 ng/ml GM-CSF and 20 ng/ml IL-4, and plated in 2 new 6-well ultra low cluster plates. Cultures were fed on day 4 by adding 2 ml of fresh media containing 30 ng/ml GM-CSF and 30 ng/ml IL-4. On day 7 cultures were fed again by removing 2 ml of old media and replacing with 2 ml of fresh media containing 30 ng/ml GM-CSF and 30 ng/ml IL-4. BMDC culture was harvested for experiments on day 8 at which time $CD11c^{+}$ cells comprised 85-95% of the culture.

Apoptotic cells Apoptotic cells were prepared by dissociating mouse thymi in RPMI 1640 and then irradiating (600 Rads) in a calibrated ^{137}Cs gamma irradiator. Irradiated thymocytes were incubated at 37°C for 12 hours before using in experiments.

Flow Cytometry Before staining cells were treated with Fc-block (anti-CD16/CD32) from either BD Biosciences or Caltag. Cells were then stained with monoclonal antibodies to the following surface markers where applicable: $I\text{-}A^{FITC}$, $CD3^{FITC}$, $CD11c^{PE}$, $CD11c^{PE\text{-}Cy7}$, $CD8\alpha^{APC}$ (BD Biosciences), $CD19^{PE\text{-}Cy5}$, $CD80^{FITC}$, $CD86^{FITC}$, $CD11b^{PE\text{-}Cy5}$ (e-Bioscience) or $CD8\alpha^{PE}$, anti-rat IgG^{PE} (Invitrogen), TACI and $BAFFR^{FITC}$ (R&D Systems). Polyclonal anti-MerTK, and anti-goat IgG^{PE} (both from R&D systems) were also used. All antibodies were diluted in 1% fetal bovine serum (Atlanta Biologicals). All washes were done with phosphate buffered saline (Gibco).

BAFF real time PCR Total RNA was isolated from spleen tissue, *ex vivo* splenic DC, or cultured BMDC with TRIZOL reagent (Invitrogen). Further purification, as well as DNase digestion, was carried out with RNeasy columns (Qiagen). Total RNA was quantiated and then converted to cDNA using Superscript II reverse

transcriptase with random hexamer primers (Invitrogen). cDNA was used as template in each Real Time PCR reaction, which also included 2x Master Mix (Applied Biosystems) and the following primer/probe sets: *baff* fwd-primer (5'CCC AAAACACTGCCCA ACA3'), *baff* rev-primer (5'CTCATCTCCTTCTTCCAG CCTC3'), *baff* TaqMan probe (5'TTCCTGCTACTCGGCTGGCATCG3') or endogenous control HPRT fwd-primer (5'GCA AACTTTGCTTTCCCTGG3'), HPRT rev-primer (5'TTCGAGA GGTCCTTTTCA CCA3'), HPRT TaqMan probe (5'AAGCTTGCAACCTTAACC ATTTTGGGGCT3') (all from Applied Biosystems). 96-well reaction plates were run on either the ABI 7700 or ABI 7500 Real Time PCR machine. Relative quanitation of *baff* expression was made using the comparative $2^{-\Delta\Delta Ct}$ method, with HPRT serving as the endogenous control. This method was validated for equal efficiency of *baff* and HPRT amplification by a cDNA titration experiment. For the time course measurements of *baff* expression in the spleen a total of 5 reactions plates were run. A pool of spleen cDNA from 1-month old B6 mice was made and served as the calibrator sample on each reaction plate. However, each data point in the spleen time course represents 5 mice whose *baff* expression was measured independently (unpooled).

BAFF ELISA and ELISPOT The matched pair of monoclonal anti-murine BAFF antibodies 5A8 (capture) and biotinylated 1C9 (detection) from Apotech were used for both the ELISA and ELISPOT assays. ELISA measuring serum BAFF was carried out according to manufacturer's instructions in Maxisorp plates (Nunc). Recombinant murine BAFF (Apotech) was used to generate a standard curve ranging from 0.75 to 48 ng/ml. Mouse sera were diluted 1:2 and pre-cleared with

Protein G (Amersham) before analysis. For BAFF ELISPOT sterile 96-well Multiscreen plates (Millipore) were coated at 4°C overnight with 5 μg/ml 5A8 antibody, then washed with PBS and blocked at room temperature for 2 hours with 1% BSA (Sigma). BMDC were plated at $1x10^5$/well in BMDC media with or without the indicated concentration of LPS (O11:B4, UltraPure, Invivogen), or with apoptotic cells. In some experiments apoptotic cells were also pre-incubated with 100nM recombinant murine Gas6 (R&D Systems) and washed three times in PBS before adding to BMDC. After 3 days plates were washed with PBS, followed by PBS-tween, then 2 μg/ml biotinylated 1C9 antibody was added and plates incubated overnight at 4°C. After washing with PBS-tween strepavidin-HRP (BD Biosciences) was added and plates incubated overnight at 4°C. Plates were developed with 3-amino-9-ethyl carbazole and counted on an ELISPOT plate reader (CTL).

B cell survival assays Resting B cells were isolated from mouse spleens by negative selection using a B cell Isolation kit (Miltenyi Biotec). B cell purity was assessed by flow cytometry to determine CD19 expression and was routinely >95%. B cell survival was assessed on B cell only cultures or B cell:BMDC cocultures. In some assays B cell survival was enhanced by recombinant BAFF (Peprotech). This effect could be blocked using soluble BAFFR-Fc or TACI-Fc decoy receptors (kindly provided by Zymogenetics).

The B cell:BMDC coculture was carried out in 24-well Ultra Low Cluster plates (Corning) in the RPMI-based media described for culturing BMDC. Cocultures consisted of $5x10^5$ total cells comprised of varying numbers of B cells and BMDC depending the ratio. For example, a B cell:BMDC ratio of 4:1 consisted of $4x10^5$ B

cells and $1x10^5$ BMDC, while a 16:1 ratio consisted of $4.71x10^5$ B cells and $.29\ x10^5$ BMDC . In some experiments BMDC were stimulated for 20 hours prior to adding to co-culture. For LPS and IFNγ stimulations, upon harvest BMDC were prepared for coculture by washing 3 times in PBS (Invitrogen). Alternatively, when BMDC were treated with fresh apoptotic cells, Lympholyte-M (Cedarlane) was used to separate apoptotic cells from BMDC prior to using in coculture. Cocultures were incubated at 37°in 5% CO_2 for 3 days. B cell viability was measured as either the percent of VAD-FMK$^-$ B cells or the absolute number of VAD-FMK$^-$ B cells. To determine the absolute number of viable B cells remaining, first the B cells in each coculture well (distinguished from BMDC by size and morphology), were counted on a hemacytometer. The percent of viable B cells was then assessed by staining harvested cells with VAD-FMK^{FITC} (Promega) and CD19$^{PE\text{-}Cy5}$, followed by analysis on a Cyan flow cytometer (Dako Cytomation). The absolute number of viable B cells was determined by the following formula:

Number of viable B cells = (# of counted B cells) x (frequency of VAD-FMK$^-$ among CD19$^+$cells)

Statistics Statistical tests were conducted using JMPIN software (SAS Institute). Due to small sample sizes only non-parametric tests were used. A *p-value* of <.05 was considered significant.

RESULTS

As *mertk*^{kd} mice age they develop progressively elevated titers of autoAbs to ssDNA and chromatin, [122]. To further characterize this pattern we analyzed serum levels of autoAb to two additional self-Ag, dsDNA and nuclesomes. Similar to previous findings, anti-dsDNA and anti-nucleosome IgG levels became manifest between 3-6 months of age and steadily increased throughout the first 12 months of life (Figure 2.1A and B). Thus, the *mertk*^{kd} mutation on the C57BL/6 background promoted the induction of autoAb to dsDNA and nucleosomes .

We also recorded the spleen mass in aging *mertk*^{kd} mice and found them to be elevated over C57BL/6 spleens at all time points tested, with profound splenomegaly by 12 months of age (Figure 2.2A). After 6 months, spleens from *mertk*^{kd} mice were routinely 1.5 to three times the weight as compared to C57BL/6 mice. This suggested that there could be increased numbers of cells in the spleen of *mertk*^{kd} mice. Therefore we next examined whether the cellular components of the spleen in *mertk*^{kd} mice could account for the larger spleen size. Surprisingly, total splenocyte numbers, as well as percentages and numbers of B and T cells, were not significantly elevated in *mertk*^{kd} mice at any age (Figure 2.2 B-D). We did find, however, that the frequency and number of CD11c^{+}, I-A^{+} DC was elevated in *mertk*^{kd} mice of all ages tested (Figure 2.2 E). Among splenic DC subsets, we found increased numbers of CD11b^{+}, but not CD8α^{+} DC (Figure 2.2 F-G). Interestingly, MerTK was expressed at a slightly higher level by the CD8α^{+} subset than the CD11b^{+} subset (Figure 2.2 H), however, the significance of this is unclear. Nonetheless, *mertk*^{kd} mice appear to have greater numbers of CD11c^{+} DC,

particularly the CD11b^{+} DC subset, in the spleen that may have a role in B cell autoimmunity.

Mertk^{kd} mice have a defect in the clearance of apoptotic cells [117, 122]. Given that the antigens targeted in *mertk*^{kd} mice are known to be on the surface of apoptotic cells, and thus exposed to the immune system [45-48], the simplest explanation for autoimmunity in these mice would be that autoAbs result from an overabundance of self antigen due to faulty clearance. However, Cohen et al. found that injection of apoptotic cells into young *mertk*^{kd} mice failed to accelerate the appearance of autoAb [122]. This result argues against the explanation that elevated Ag load alone is sufficient to drive autoimmunity. This led us to question what other age-related changes take place *in vivo* that might correlate with the timing of autoAb in *mertk*^{kd} mice.

We first turned our attention towards the cytokine BAFF. When overexpressed *in vivo* BAFF is known to promote autoAb production and autoimmune disease. Furthermore, our lab has shown dysregulated TNF-α expression in *mertk*^{kd} mice [101], which is in the same gene superfamily as BAFF. An analysis of *baff* mRNA expression in spleen tissue from mice of varying ages revealed a 2-3 fold increase in *mertk*^{kd} compared to C57BL/6 mice beginning at 6 months of age (Figure 2.3 A). Serum levels of BAFF protein were not found to be elevated in older *mertk*^{kd} mice, however (Figure 2.3 B).

When splenic DC (spDC) were examined we found elevated *baff* mRNA levels in most (3 out of 4) preparations of DC taken from *mertk*^{kd} mice compared to those from C57BL/6 mice (Figure 2.3 C). The elevated baff mRNA was

predominantly found in older *mertk*^{kd} mice although this was not always the case. Meanwhile, only one out of four spDC preparations from older C57BL/6 mice had elevated levels of BAFF similar to old *mertk*^{kd} mice. When *ex vivo* spDC were examined for BAFF production by ELISPOT we found that a higher frequency of spDC from *mertk*^{kd} mice made BAFF in culture compared to spDC from C57BL/6 mice (Figure 2.3 D). Unlike *baff* mRNA expression, elevated BAFF protein production was most pronounced in the younger spDC from *mertk*^{kd} mice. However, the trend of increased numbers of spDC producing BAFF also held for the older *mertk*^{kd} mice when compared to older C57BL/6 counterparts. Importantly, this was not due to a general increase in the activation state of these DC, which was assessed by surface expression of I-A, CD80, and CD86. Thus *mertk*^{kd} mice have an increased frequency of BAFF-producing DC in addition to an increase in DC number.

Since *baff* expression was elevated in spDC from older *mertk*^{kd} mice we examined whether the same was true of bone marrow derived DC (BMDC) which could be used as a more obtainable source of DC for further experimentation. We first wanted to compare the efficiency of our BMDC culture method by tracking the differentiation of DC from the various mouse strains. As shown in Figure 2.4 A C57BL/6, *mertk*^{kd}, and *baff* BMDC cultures generated viable CD11c^{+} cells with similar efficiencies. Since day 8 cultures produced the most consistent number of CD11c^{+} DC among the genotypes, we used these cultures for further studies. As expected, MerTK could be identified on the surface of C57BL/6 but not *mertk*^{kd} BMDC (Figure 2.4 B).

It was important to determine whether BMDC from day 8 cultures were similar in phenotype and matured properly upon stimulation The surface expression of I-A and the costimulatory molecules CD80 and CD86 was not different among the three genotypes of day 8 BMDC, nor was it after LPS-induced maturation (Figure 2.4 C). Thus both *mertk*^{kd} and *baff* mutant BMDC differentiate similarly and have a similar maturation status to WT BMDC.

Despite the apparent similar activation status of *mertk*^{kd} BMDC, when the production of BAFF was examined on a per cell basis they were found to contain more BAFF producing cells than C57BL/6 BMDC at rest (Figure 2.5 A, media). LPS, but not IFNγ, stimulation led to the induction of more *mertk*^{kd} BAFF-producing BMDC (Figure 2.5 A). Interestingly, neither of these stimuli induced BAFF production by C57BL/6 BMDC. While this finding differs from studies using human DC [130, 161], it is consistent with previous mouse BMDC results involving LPS [199]. Despite the elevated number of BAFF-producing *mertk*^{kd} BMDC there was no change in the size of the BAFF ELISPOTS. This result indicates that MerTK regulates BAFF production at the population level but does not affect the amount made on a per cell basis. So BAFF production is regulated in an “on/off”, rather than a graded, manner by a subset of BMDC lacking MerTK. The low levels of MerTK observed on C57BL/6 BMDC may indicate that not all BMDC normally express MerTK, and those that do may be the same subset of cells that make BAFF in *mertk*^{kd} BMDC cultures.

MerTK functions as a recognition molecule for apoptotic cells by DC. Although MerTK is not required for the phagocytosis of apoptotic cells by DC [31, 66, 79], it does alter DC physiology in response to apoptotic cells by making them

refractory to LPS-induced NF-κB activation [31]. Since others have shown that apoptotic cells can induce BAFF surface expression on DC [200, 205] we next wanted to see how apoptotic cells affected BAFF expression by C57BL/6 and *mertk*^{kd} BMDC. Apoptotic cells did not induce BAFF production by C57BL/6 BMDC (Figure 2.5, B). Alternatively a greater number of BMDC lacking MerTK were induced to make BAFF following exposure to apoptotic cells (Figure 2.5 B). This result points towards the existence of an apoptotic cell recognition receptor on BMDC that delivers a BAFF-induction signal and is unopposed in *mertk*^{kd} BMDC. Since Tyro3 and Axl bind to the same ligand (Gas6) as MerTK we postulated that they might be participating in the induction of BAFF by apoptotic cells. When apoptotic cells were pre-treated with recombinant Gas6 we observed a small but consistent increase in the number of BAFF producing *mertk*^{kd} BMDC compared to untreated apoptotic cells (Figure 2.5 B). Apoptotic cells alone contributed negligibly to BAFF spots in these wells. As with LPS stimulation, only the number of cells making BAFF, but not the amount of BAFF per BMDC was increased. In summary, these results in Figure 2.5 demonstrate that MerTK is an important negative regulator of BAFF production by dendritic cells.

Given that *mertk*^{kd} DC produce excess BAFF we wanted to examine what, if any, consequences this had on the outcomes of DC-B cell interactions. One of BAFF‘s functions is to provide pro-survival signals for resting B cells [143, 192, 193, 216]. We therefore developed an *in vitro* assay to monitor the survival of resting B cells. The assay involves culturing negatively selected B cells for 3-4 days and then evaluating their viability based on their staining with VAD-FMK^{FITC}. This reagent

binds irreversibly to activated caspase family members and is therefore sensitive to the early stages of the apoptotic process. The isolation of B cells by the negative selection kit routinely resulted in greater than 95% enrichment (Figure 2.6A). Viability was quantified as either the percentage of B cells ($CD19^+$) that were VAD-FMK^-, or in some experiments, the absolute number of VAD-FMK^- B cells (Figure 2.6 B).

First the effect of recombinant BAFF (rBAFF) on B cell survival was evaluated in a titration. As shown in Figure 2.6 C rBAFF elevated both the percentage and absolute number of viable B cells after 4 days in culture. It appears that a minimum concentration of 100 ng/ml of rBAFF was necessary to sustain maximum viability. Using this concentration we found that the pro-survival benefit of BAFF could be blocked with soluble forms of BAFFR (BAFFR-Fc) or TACI (TACI-Fc) (Figure 2.6 D).

We next set out to determine if BMDC could enhance the survival of resting B cells. As shown in Figure 2.7 A, compared to B cells cultured alone, the presence of either C57BL/6 or *mertk*^{kd} BMDC BMDC increased the percentage of VAD-FMK^- B cells. Importantly, the pro-survival benefit could be titrated down by increasing the ratio of B cells to BMDC. At a B cell:BMDC ratio of 4:1 for BMDC from *mertk*^{kd} mice, and 16:1 for BMDC from C57BL/6 mice, the survival benefits were similar to recombinant BAFF. The absolute number of viable B cells present after 3 days in culture was also increased significantly in the presence of BMDC (Figure 2.7B). Unexpectedly, culturing B cells with *mertk*^{kd} BMDC did not improve their viability compared to those cultured with C57BL/6 BMDC. However, very few viable B cells remained if either type of BMDC was absent. When BMDC were pre-stimulated with

LPS or apoptotic cells to boost the percentage of BAFF-producing cells *mertk*^{kd} BMDC still did not outperform C57BL/6 BMDC (Figure 2.7 C). Thus, despite producing excess BAFF *mertk*^{kd} BMDC did not provide enhanced survival signals to resting B cells. In agreement with this, *baff*-deficient BMDC performed similarly to C57BL/6 and *mertk*^{kd} BMDC in supporting the survival of resting B cells. However, BMDC augmentation of B cell survival is an active process that requires functional BMDC since it was eliminated when resting, LPS-stimulated, or apoptotic cell-treated BMDC were fixed with paraformaldehyde prior to adding to the coculture (Figure 2.7D). These results point towards the existence of a BAFF -independent mechanism by which DC enhance B cell survival.

The lack of a requirement for DC-derived BAFF by surviving B cells was not due to the lack of expression of BAFF receptors on B cells in our coculture system. BAFFR expression was seen to varying degrees after culture alone, or with all treatment groups of C57BL/6, *mertk*^{kd}, and *baff* BMDC. Interestingly, we found that a population of TACI^{+} B cells emerged in cultures with BMDC that were pre-treated with media alone (*left* column) or apoptotic cells (*right* column), but not LPS (*middle* column) or when B cells were cultured alone (*top*) (Figure 3.7 E). Conversely, LPS stimulation of BMDC resulted in a higher percentage of BAFFR-expressing B cells compared to media and apoptotic cell-treated BMDC. At this point it is unclear if this phenomenon is due to a population of B cells upregulating TACI on their surface, or to the enhanced survival of this population in culture with unstimulated BMDC.

DISCUSSION

DC are a MerTK-expressing cell type with the capacity to initiate autoantibody production *in vivo* [217-220]. Therefore, we sought to determine if DC are potential contributors to autoimmunity in *mertk*^{kd} mice. In support of this, we found that *mertk*^{kd} mice contain elevated numbers of splenic DC, particularly among the CD11b^{+},CD8^{-} subset. There are several possible explanations for this increase. Within the bone marrow, MerTK may regulate the output of DC progenitors [8]. Alternatively, the differentiation of monocytes or DC precursors into DC may be affected [7, 10, 12, 221]. It is interesting that serum from SLE patients has the ability to induce DC differentiation from monocytes *in vitro* [222]. This was shown to be IFN-α dependent process so it will be informative to determine what the IFN-α levels are in *mertk*^{kd} mice. MerTK may also regulate the survival of resting DC within the spleen [223]. Increased DC survival has been shown to promote autoAb production in mice with a lupus-prone (MRL) genetic background [218] and a similar mechanism may be at work here.

. Despite our findings of a potential role for MerTK in regulating the size of the splenic DC pool it is also important to point out that splenic DC numbers were not elevated when the *mertk*^{kd} allele was moved onto the non-obese diabetic (NOD) genetic background by marker-assisted backcrossing [109]. Our *mertk*^{kd} allele is on the C57BL/6 genetic background (*n=6*). It will be interesting to see if our observations regarding splenic DC numbers persist in mice backcrossed additional generations. The difference between these outcomes may suggest that MerTK's

role in regulating splenic DC populations is dependent upon its interactions with specific alleles (NOD vs. C57BL/6) of other genes.

Contrary to the elevation in splenic DC number, autoAb production in *mertk*^{kd} mice does not begin until later in life. This suggests that some other factor exists which precipitates a breakdown in B cell tolerance in older mice. Since BAFF is expressed by similar cell types as MerTK [130, 144, 161], and can cause autoimmunity when overexpressed *in vivo* [127, 140, 141], we compared BAFF levels in C57BL/6 and *mertk*^{kd} mice of various ages. We found elevated levels of *baff* mRNA in spleen tissue from *mertk*^{kd} mice beginning at 6 months of age. However, this increase was not sufficient to cause an increase in circulating systemic BAFF. This result would not be unexpected if the *mertk*^{kd} mutation causes elevated BAFF expression solely by a bone marrow-derived cell type (such as DC) since detectable levels of serum BAFF are produced exclusively by non-hematopoetic cell types [198]. This is also consistent with normal B cell numbers in *mertk*^{kd} mice, since they are elevated when BAFF levels are systemically elevated [128, 142]. Interestingly, in SLE patient SLEDAI scores and autoAb levels are significantly correlated with blood leukocyte *baff* mRNA levels, but not with serum BAFF protein levels [204]. This fits a model in which myeloid-lineage cells, while not a source of circulating BAFF, are able to influence B cell tolerance when producing BAFF in excess.

Rather than a systemic-wide controller of BAFF expression, MerTK seems to regulate BAFF expression by select cell types. We found that *baff* mRNA was elevated among splenic DC from older *mertk*^{kd} mice, as was the number of DC that

actively produce BAFF *ex vivo,* although the latter finding was more pronounced in younger *mertk*^{kd} mice. Given that *mertk*^{kd} mice have a larger DC population comprised of an elevated number of BAFF -producing cells, DC may be participants in autoAb production in *mertk*^{kd} mice. However, it is also important to consider other cell types that might be involved. Macrophage for example, also express MerTK and BAFF, and populate similar anatomical locations in the spleen as DC [121]. To investigate if dysregulated BAFF expression by DC, specifically, is sufficient to drive B cell autoimmunity in *mertk*^{kd} mice we are currently generating a conditional *baff*-null mouse. Since there are two non-redundant pools of *baff*-producing cells (hematopoetic and stromal) [198] our conditional baff-*null* mouse will be very useful in delineating the relevance of specific cell types, not only in autoimmunity, but in B cell homeostasis and protective responses to foreign antigens as well.

To further our understanding of how MerTK and BAFF regulate DC-B cell interactions we turned our focus towards *in vitro* DC cultures. In line with an inhibitory role for MerTK in DC physiology [31] we found that MerTK is a negative regulator of BMDC BAFF production. However, in contrast to other MerTK-regulated DC activities, the control over BAFF secretion is apparent in the absence of exogenous stimuli. Although the number of BAFF-producing *mertk*^{kd} BMDC could be further increased in the presence of LPS, but not IFNγ. On the contrary we found that C57BL/6 BMDC produced very little BAFF, even in the presence of LPS or IFNγ. Although this stands in contrast to data collected from human DC, it agrees with a previous report regarding BAFF secretion by LPS-stimulated murine BMDC [199]. Importantly, both C57BL/6 and *mertk*^{kd} BMDC upregulate MHC class II, CD80 and

CD86 to a similar degree in the presence of LPS. This demonstrates a) that our C57BL/6 BMDC are not refractory to LPS stimulation, and b) that the reduced control over *baff* expression by *mertk*^{kd} BMDC is not simply due to a general heightened activation state. Thus, BAFF secretion is tightly regulated in mouse DC, and MerTK may be a participant in this regulatory mechanism.

Apoptotic cells deliver a negative signal to DC by preventing LPS- or CD40L-induced activation of the NF-κB signaling pathway by a MerTK-dependent mechanism [31]. Surprisingly we found that, rather than conveying an inhibitory effect, apoptotic cells increased the number of BAFF secreting *mertk*^{kd} BMDC. This insinuates that a) DC may have an apoptotic cell recognition protein that is a positive inducer of BAFF production, and b) the *baff* gene may be regulated independently of NF-κB (this 2nd topic is discussed further in Chapter 4). Regarding the recognition of apoptotic cells, we found that pre-incubating apoptotic cells with Gas6 slightly increased the number of *mertk*^{kd} BMDC producing BAFF. This may indicate that the other two members of the TAM family (Axl and/or Tyro3) may be transducing a *baff* induction signal in the absence of MerTK. An alternative mechanism is illuminated by the finding that BAFF production by DC can be induced by immune complexes of chromatin and IgG [199]. Given that chromatin is exposed on the outer surface of apoptotic cells [48] it may be stimulating *baff* expression via a similar mechanism. Experiments involving DC deficient in multiple TAM family members, or apoptotic cells pre-treated with DNase will help to sort out what mechanism underlies the *baff*-inducing signal provided to *mertk*^{kd} BMDC by apoptotic cells.

Regardless of the receptor(s) involved, the finding that apoptotic cells are delivering a *baff* induction signal to *mertk*^{kd} DC, while simultaneously acting as a source of self antigens [45, 46], defines a potential mechanism by which DC could promote B cell autoimmunity. DC are known to capture, recycle, and display antigens in a way that preserves their epitopes for recognition by cognate B cells [20-22, 24]. While this "native antigen presentation" has yet to be demonstrated for material derived from apoptotic cells, DC pre-fed apoptotic cells are efficient at inducing anti-nuclear antibodies upon injection into C57BL/6 mice, suggesting that antigen was made accessible to B cells [217, 219]. Furthermore, DC have been shown to present antigen derived from ingested apoptotic cells to antigen specific CD4^{+} T cells, leading to their proliferation [34]. In a model where IgM transgenic mice, possessing anti-Sm-specific B cells, were placed onto the *mertk*^{kd} background, there were twice as many marginal zone B cells found compared to littermate control background [49]. It is intriguing to consider the possibility that self antigen-bearing DC are capable of providing both a BCR signal and a BAFFR signal to autoreactive B cells. This is an attractive model for how B cell-extrinsic mechanisms facilitate autoAb production in aging *mertk*^{kd} mice where apoptotic cells may accumulate with age due to inefficient clearance mechanisms [117, 122].

We also found that BMDC have a pro-survival effect on *ex-vivo* cultured B cells. Unexpectedly, this involves a BAFF-independent mechanism as culturing B cells with either C57BL/6 BMDC, which produce very little BAFF under all conditions tested, or *baff*-deficient BMDC resulted in similar numbers of viable B cells compared to those cultured with *mertk*^{kd} BMDC which contain a higher frequency of

BAFF-secreting cells. The augmentation of B cell survival by BMDC may involve other secreted factors or signals delivered by cell-cell contact. Future experimentation using BMDC-conditioned supernatant and/or transwell assays will be needed to uncover the specific mechanism involved.

Although finding that BMDC support of B cell survival is BAFF-independent is unexpected, this is the first study involving DC from *baff*-deficient mice. Our results illustrate how much there is yet to learn about the importance of DC-derived BAFF during *in vitro* and *in vivo* interactions with B cells. Although not a necessary pro-survival signal, DC-derived BAFF may play an important role in the differentiation of antigen stimulated B cells into antibody secreting cells. Such B cells may be autoreactive B cells that exist in *mertk*^{kd} mice and, under chronic exposure to apoptotic cells, these B cells are primed to respond to BAFF or other secondary signals. Our experiments using cocultures of resting B cells with DC can be expanded to include B cells derived from *mertk*^{kd} mice which may be “preactivated”.

In summary, we have found that BAFF expression appears to be regulated by MerTK. In the absence of MerTK, there is an increase in *baff* mRNA expression in the spleen and among splenic DC from aging *mertk*^{kd} mice. Furthermore, BAFF is constitutively produced by *mertk*^{kd} , but not C57BL/6 BMDC. However, this excess BAFF does not appear to increase the viability of resting B cells when cocultured with BMDC. Thus, the augmentation of resting B cells survival by BMDC *in vitro* is likely independent of BAFF and MerTK. It remains to be determined whether MerTK and BAFF influence DC-mediated B cell activation, plasma cell differentiation and autoantibody production.

Figure 2.1

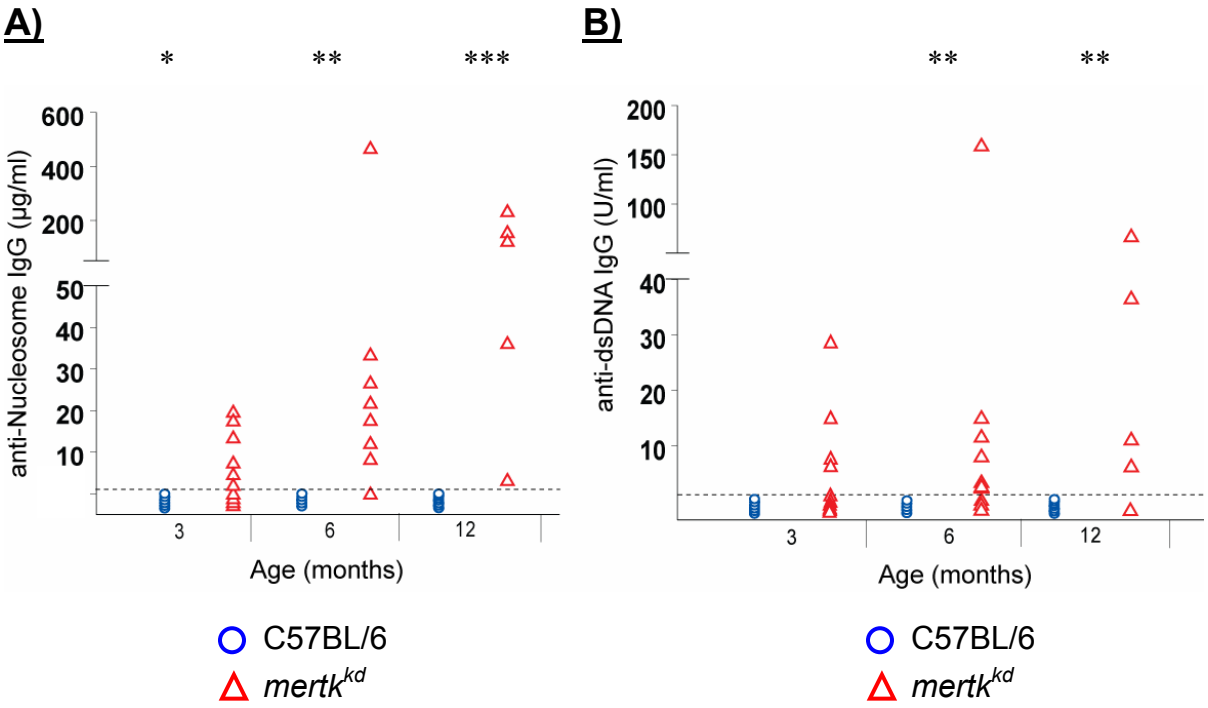

Figure 2.1 Rising autoantibody levels in *mertk*^{kd} mice with age. Levels of anti-nucleosome (A) and anti-dsDNA (B) were measured by ELISA in a cohort of C57BL/6 and *mertk*^{kd} mice. The dotted line represents the limit of detection in each assay. These limits are 15 ng/ml and 1.56 Units/ml for the anti-nucleosome and anti-dsDNA assays, respectively. Statistical significance was determined by Wilcoxon Rank Sum test at each time point (* p<.05, ** p<.001, *** p<.005).

Figure 2.2

A)

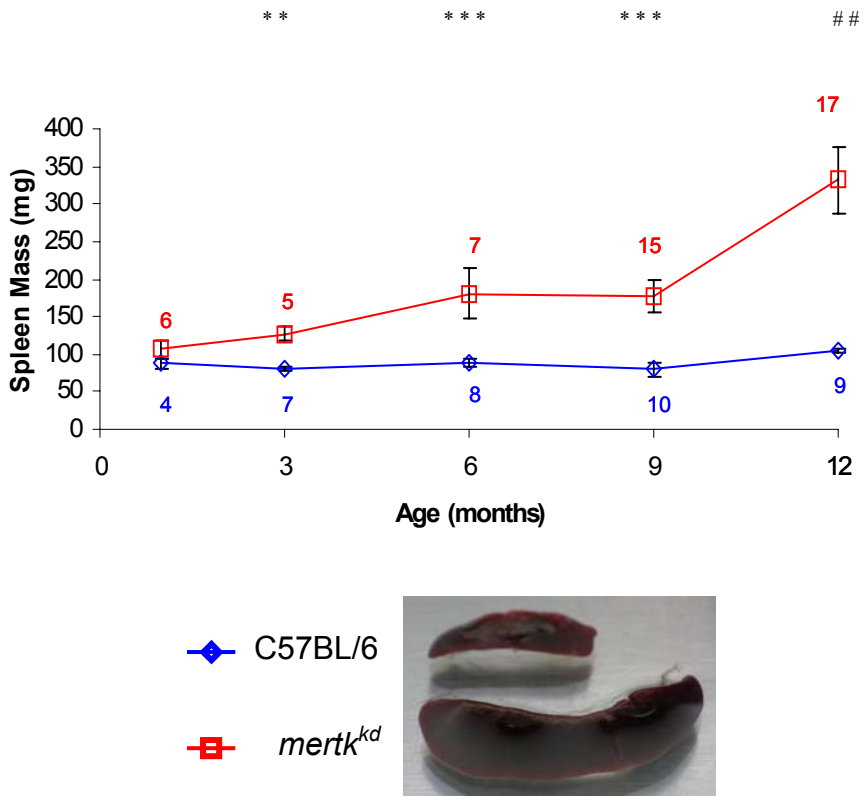
* *
* * *
* * *
# #
Spleen Mass (mg)
400
350
300
250
200
150
100
50
0
0
3
6
9
12
Age (months)
6
5
7
15
17
4
7
8
10
9
C57BL/6
mertk^kd

B)

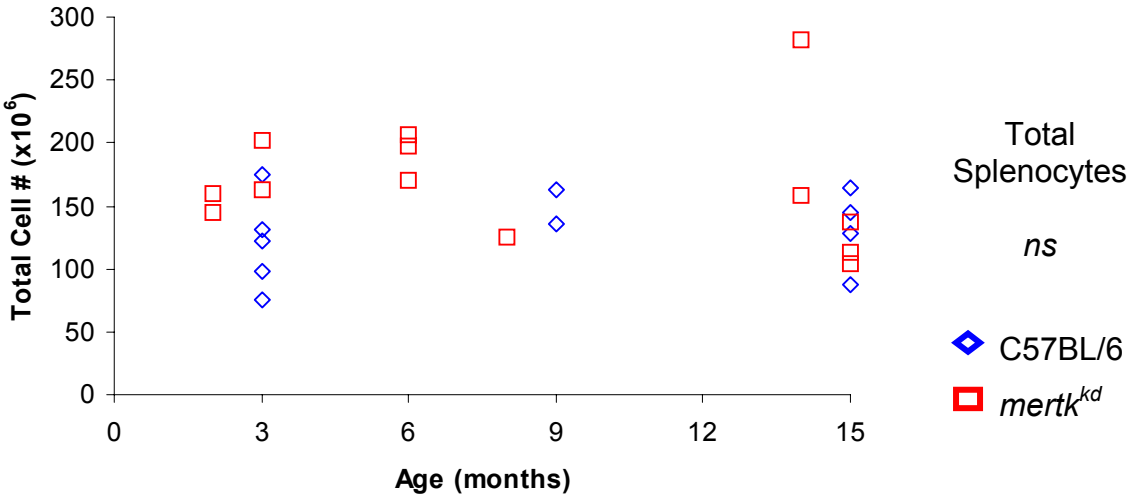
Total Cell # (x10^6)
300
250
200
150
100
50
0
0
3
6
9
12
15
Age (months)
Total Splenocytes
ns
C57BL/6
mertk^kd

Figure 2.2, continued

C)

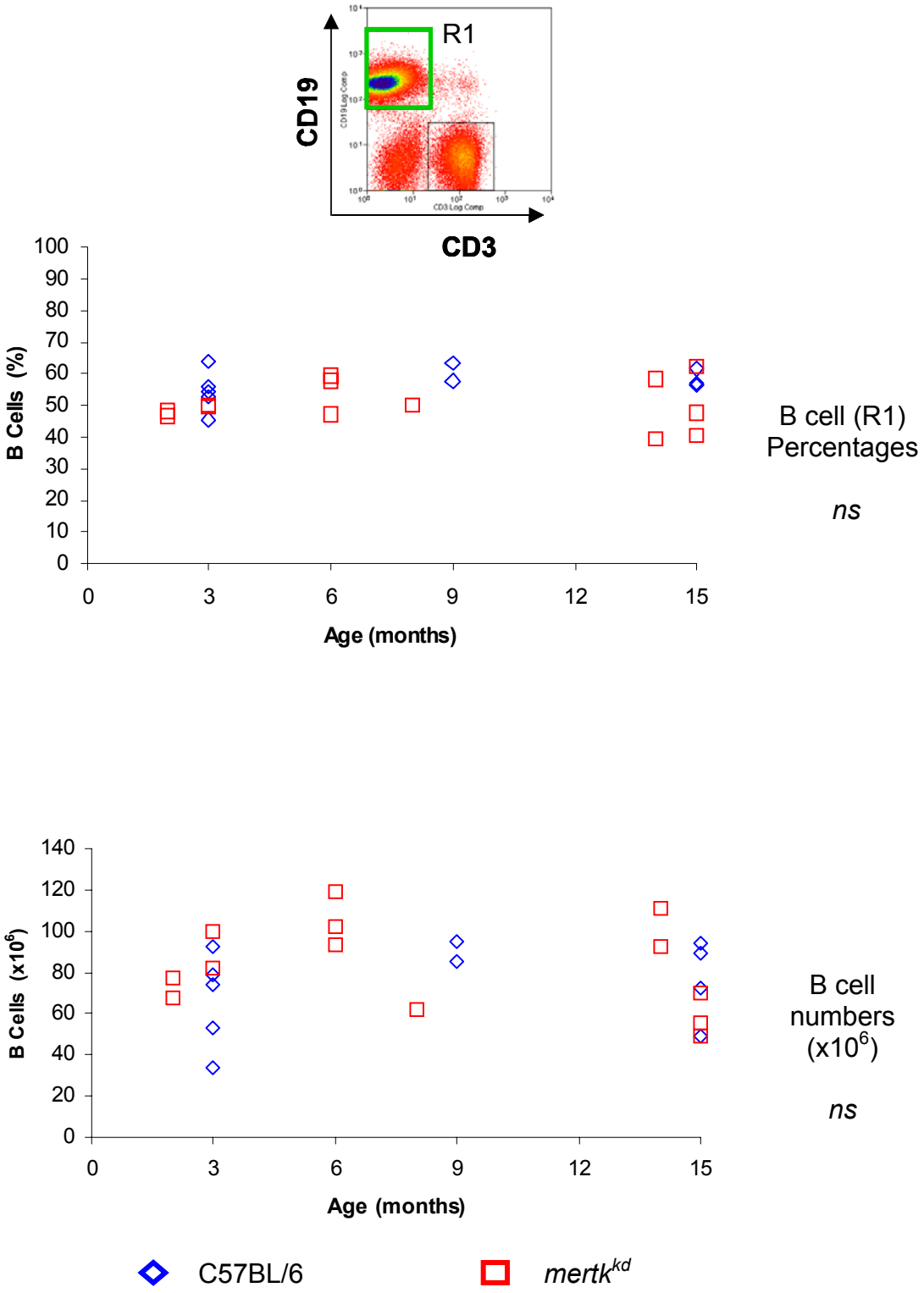

Figure 2.2, continued

D)

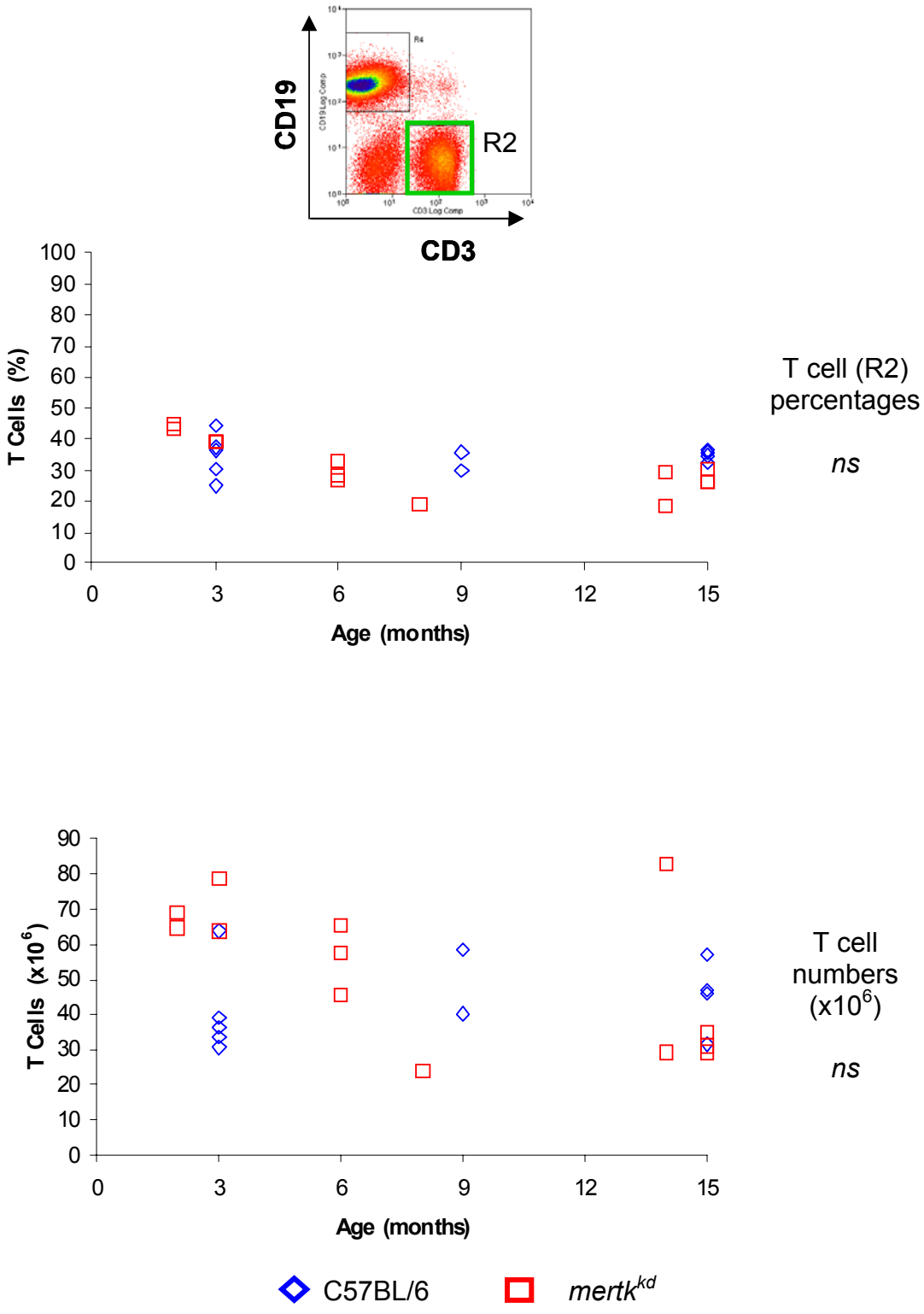

Figure 2.2, continued

E)

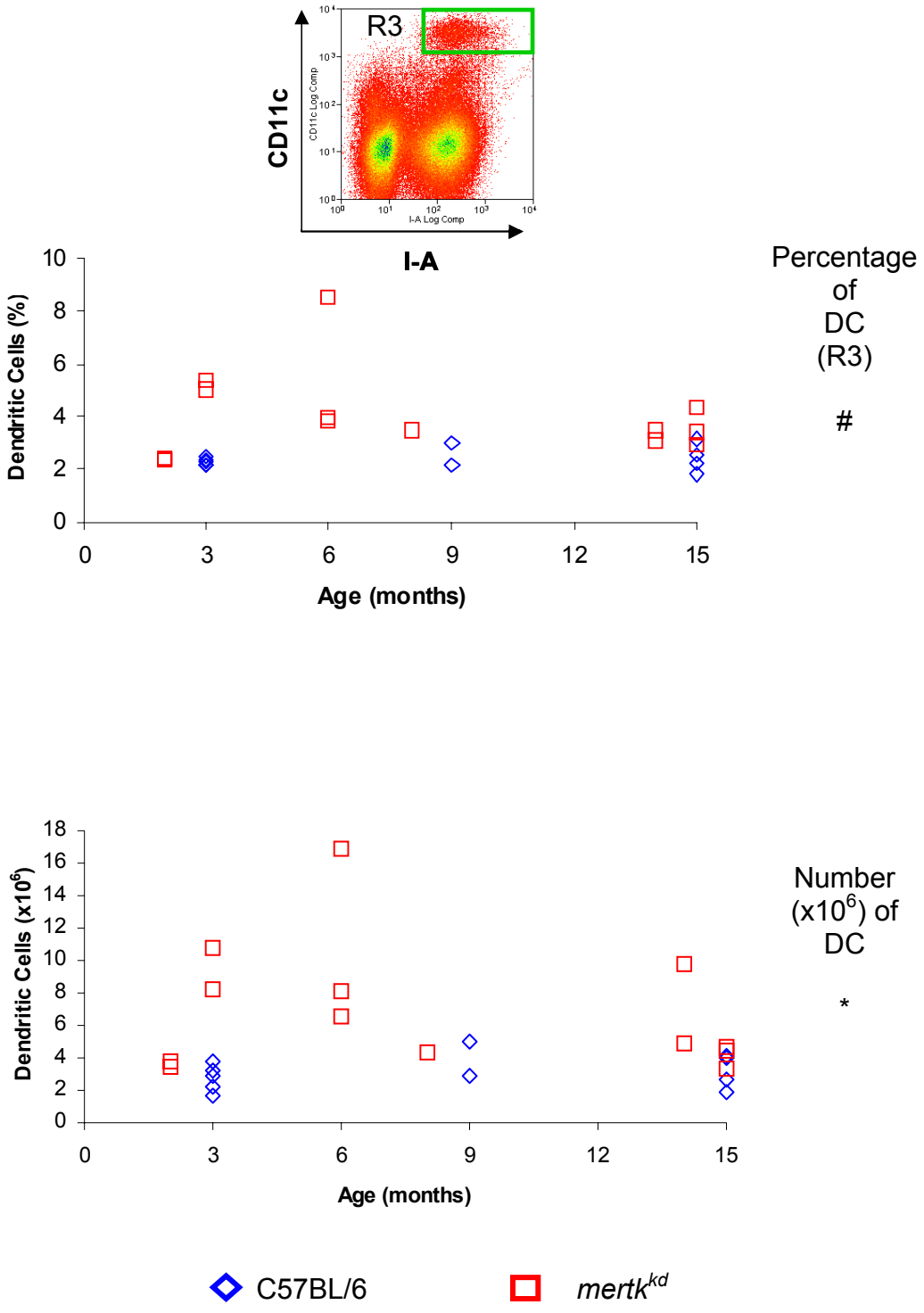

Figure 2.2, continued

F)

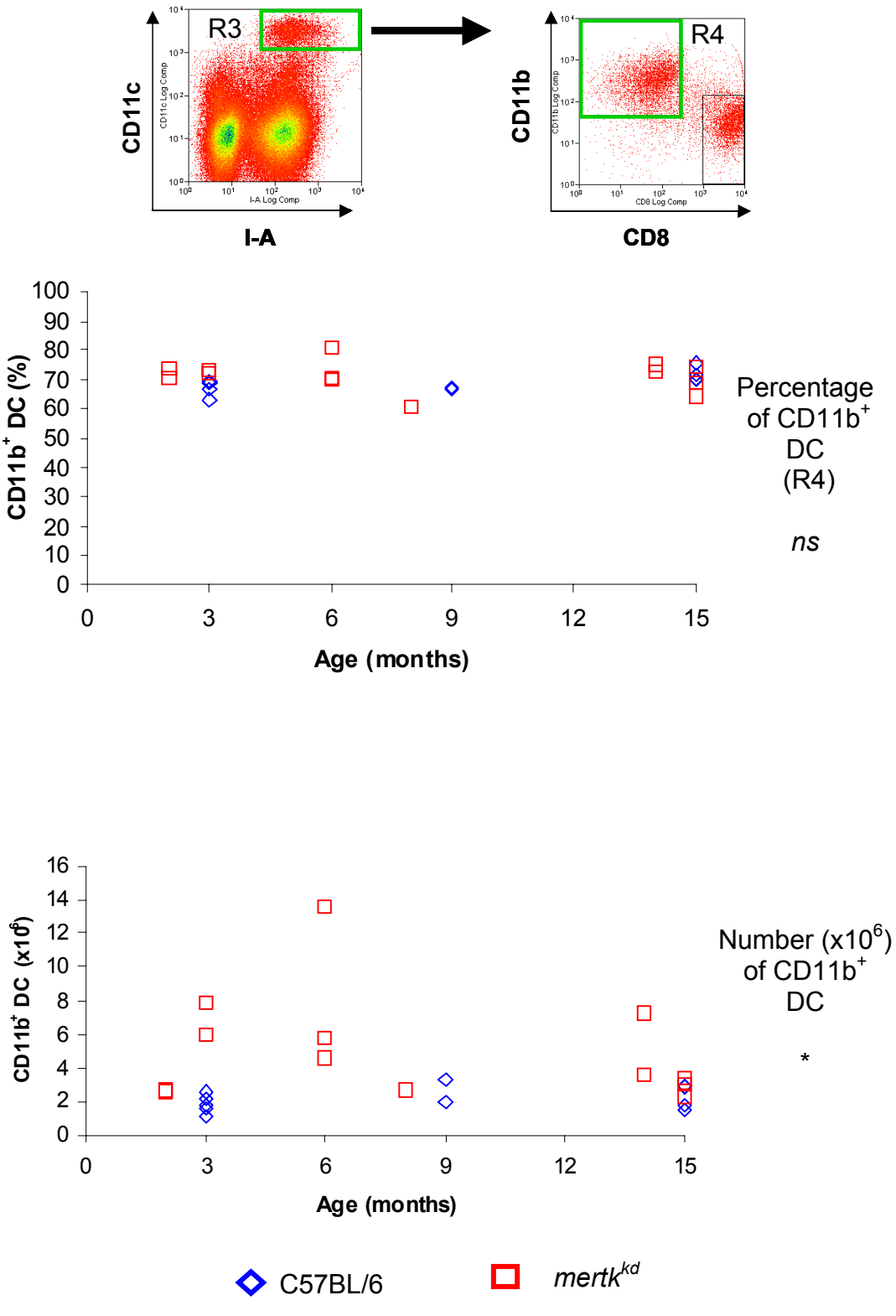

Figure 2.2, continued

G)

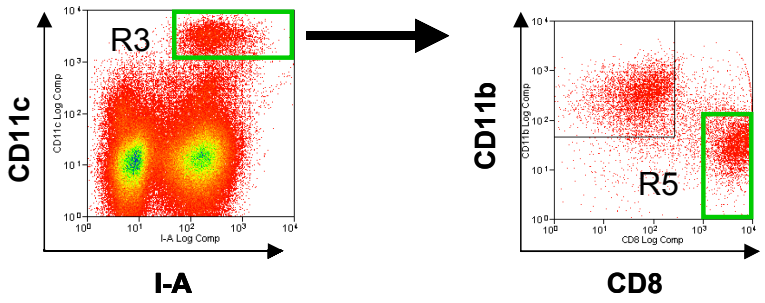

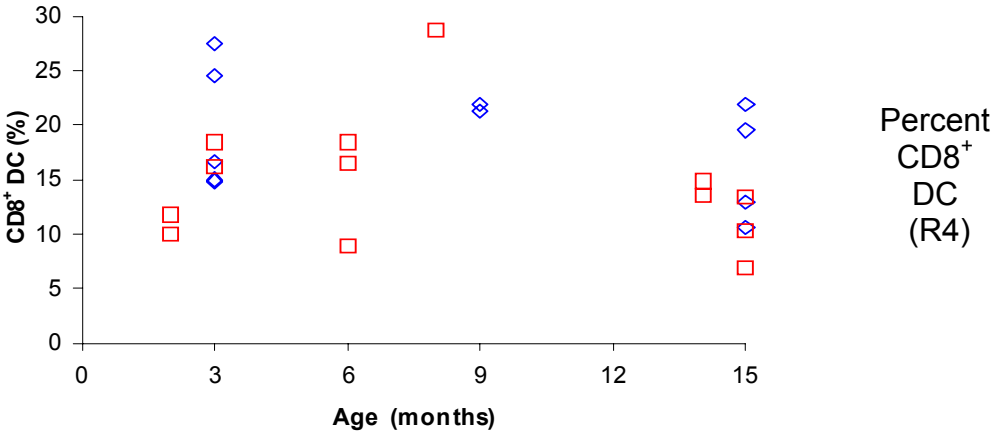

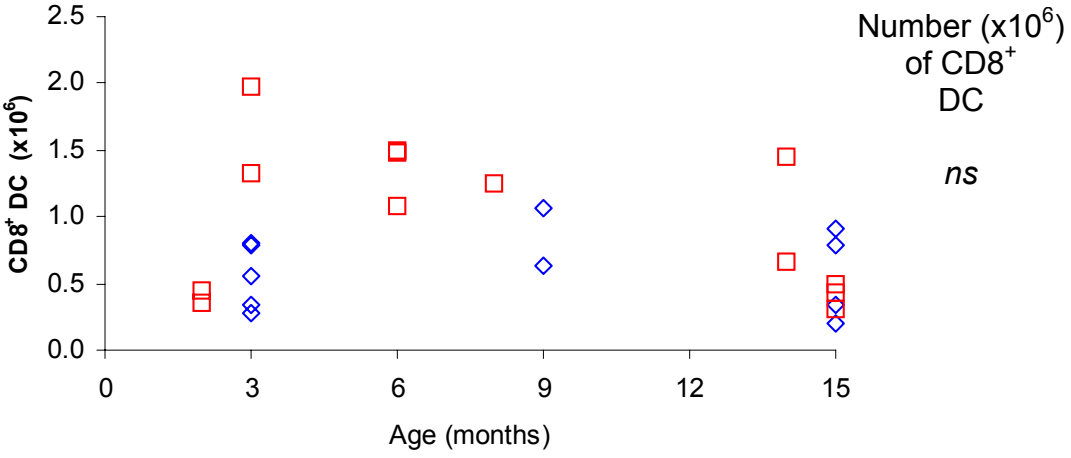

C57BL/6 *mertk*^{kd}

Figure 2.2, continued

H)

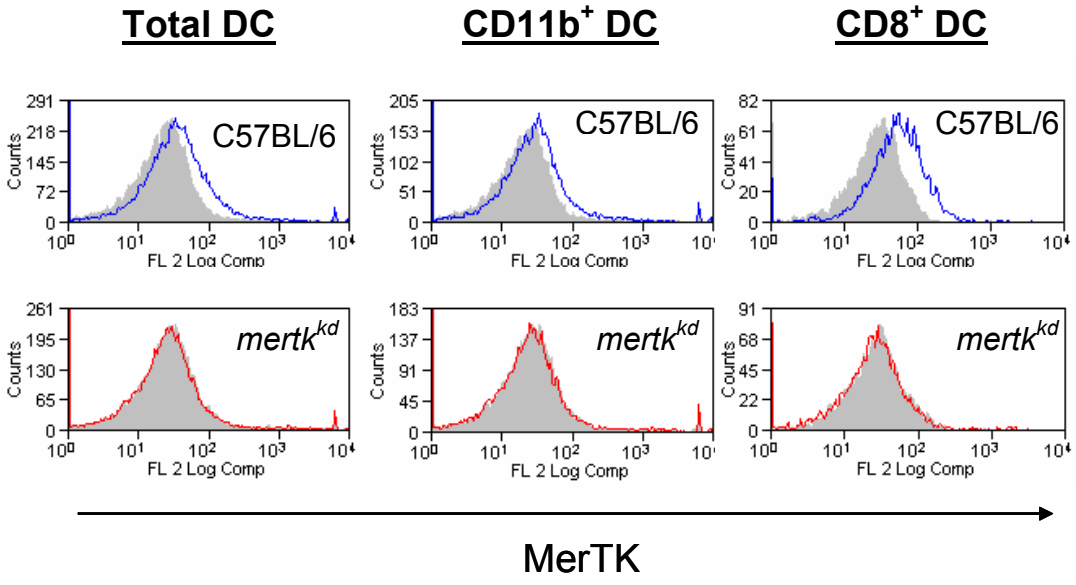

Figure 2.2 Enlarged spleens in *mertk*^{kd} mice contain normal lymphocyte populations but elevated numbers of dendritic cells A) Spleens weights of mice of various ages are shown (mean ± sem). Number indicated number of spleens measured per data point. A photo of representative spleens from 12-month old mice is also shown below. B) Number of total nucleated (post-RBC lysis) splenocytes from mice of various ages are shown. C, D, E) The percent and number of splenic B cells (gate R1), T cells (gate R2), and dendritic cells (gate R3) from the same mice as (B) are shown. F, G) The percent and number of CD11b^{+} (gate R4) and CD8^{+} (gate R5) DC subsets from the same mice as (B) are shown. H) Staining of cell surface MerTK (colored lines) or goat IgG istoype control (gray fill) on splenic DC. Representative of 6-8 mice per genotype. Statistical significance was determined by Wilcoxon Rank Sum test, the results of which can be found to the right of each graph (*ns* not significant, * $p< .05$, ** $p<.01$, *** $p<.005$, $^{\#}$ $p<.001$, $^{\#\#}$ $p<.0001$).

Figure 2.3

A)

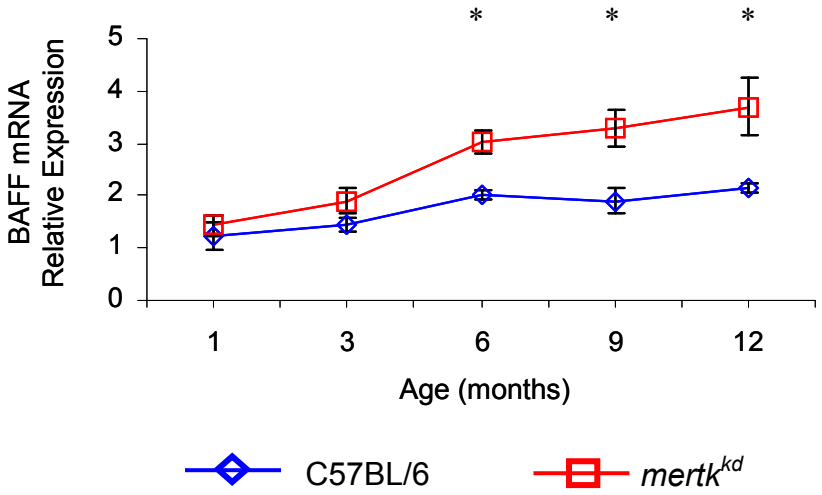
BAFF mRNA
Relative Expression
5
4
3
2
1
0
*
*
*
1
3
6
9
12
Age (months)
C57BL/6
mertk^kd

B)

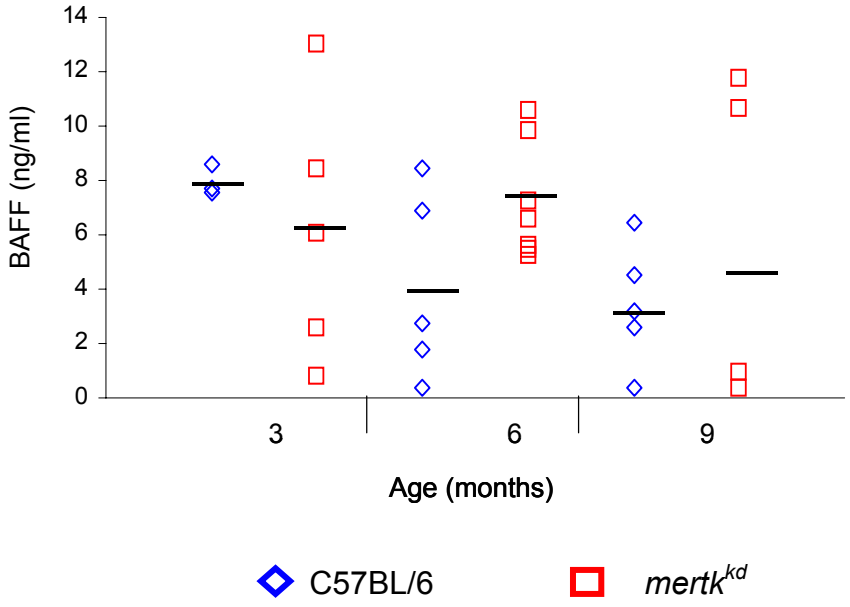
BAFF (ng/ml)
14
12
10
8
6
4
2
0
3
6
9
Age (months)
C57BL/6
mertk^kd

Figure 2.3, continued

C)

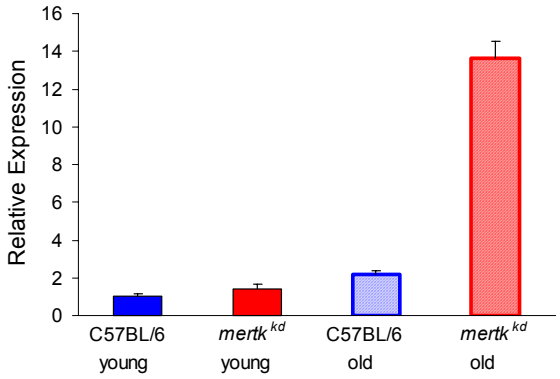

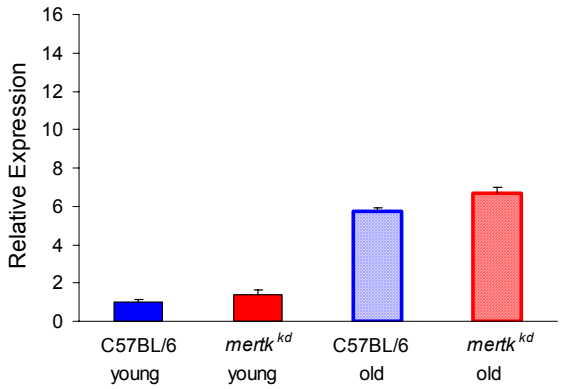

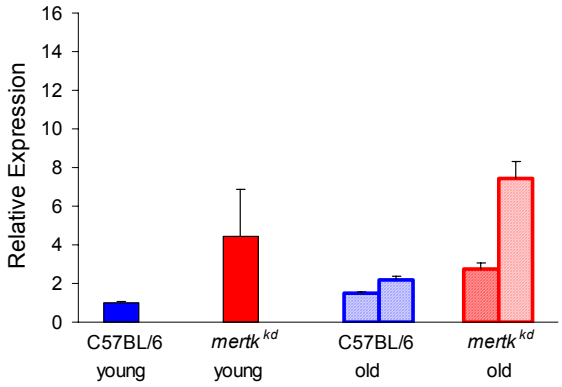

Figure 2.3, continued

D)

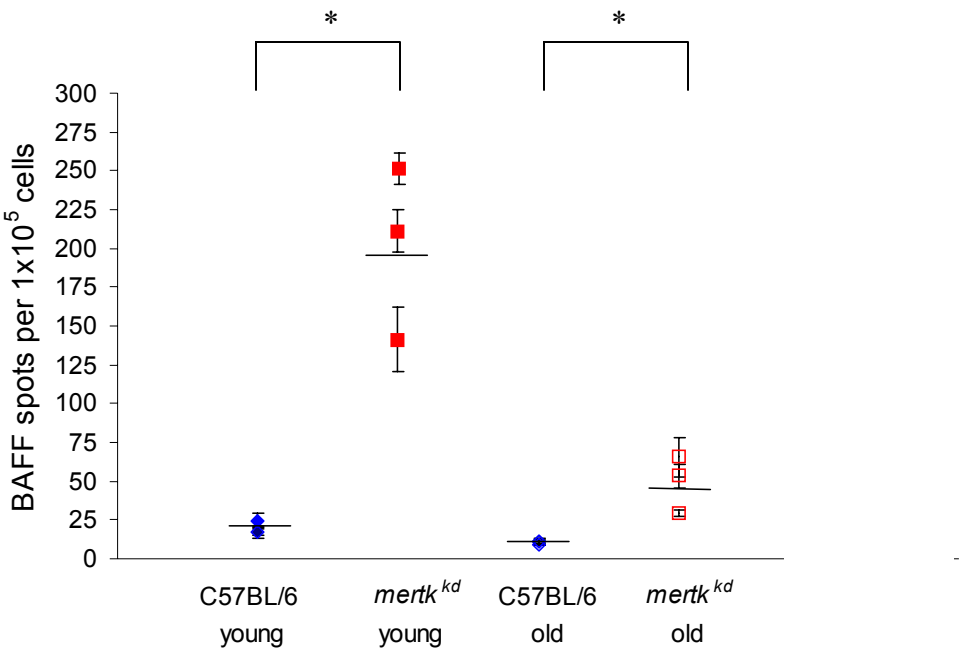

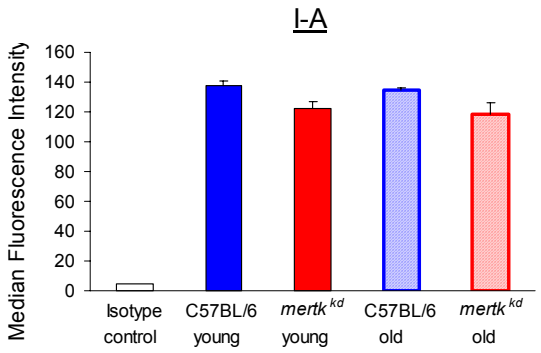

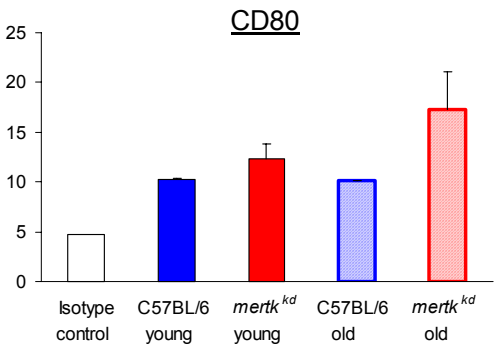

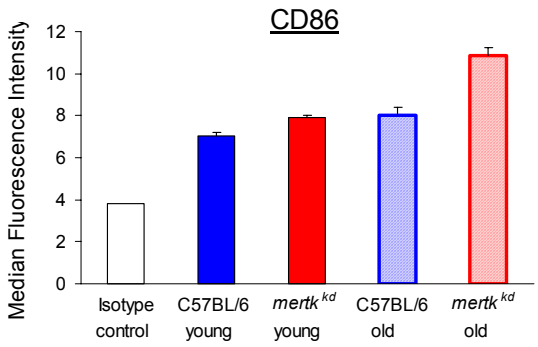

Figure 2.3, continued

Figure 2.3 BAFF is overproduced by DC, but not systemically, in *mertk*^{kd} mice
A) Real time PCR analysis of BAFF expression in the spleen of aging mice. Each data point represents the BAFF expression (mean ± sem) from 5 mice. Wilcoxon Rank Sum test was performed (* $p<.05$). B) ELISA analysis of serum BAFF levels in aging mice. The levels in individual mice and the mean level are shown. Differences are not statistically significant. C) Three independent real time PCR analyses of *baff* expression by spDC taken from young and old mice C57BL/6 and *mertk*^{kd} mice. Each bar represents the relative *baff* expression (+sem) by splenic DC from a single donor mouse. D) ELISPOT analysis (*above*) of *ex vivo* BAFF secretion by splenic DC from young and old C57BL/6 and *mertk*^{kd} mice. Each data point represents the number of BAFF spots counted (mean ± sem) from 4 wells containing spDC from a single donor mouse. Horizontal lines represent the mean number of BAFF spots for the 3 donor mice in each group. Wilcoxon Rank Sum test was performed (* $p<.05$). These same splenic DC were evaluated for expression of I-A, CD80, and CD86. Graphs (*below*) show the median fluorescence intensity of these markers on CD11c^{hi}-gated events. In both (C) and (D) "young" mice were 2-3 months old, while "old" mice were 10-14 months old.

Figure 2.4

A)

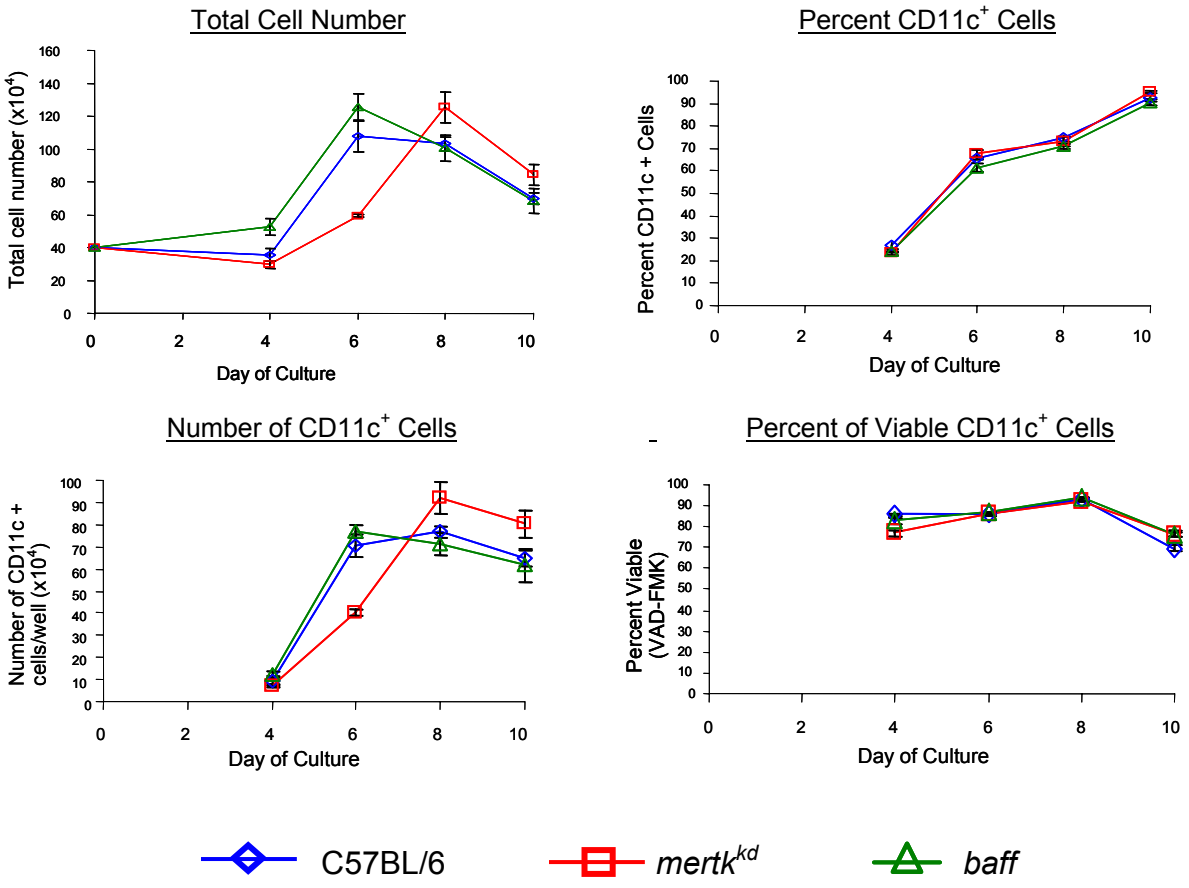
Total Cell Number
Total cell number (x10^4)
Day of Culture
Percent CD11c+ Cells
Percent CD11c + Cells
Day of Culture
Number of CD11c+ Cells
Number of CD11c + cells/well (x10^4)
Day of Culture
Percent of Viable CD11c+ Cells
Percent Viable (VAD-FMK)
Day of Culture
C57BL/6
mertk^kd
baff

Figure 2.4, continued

B)

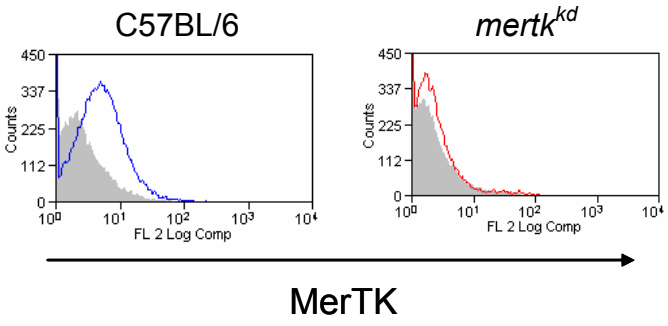

C)

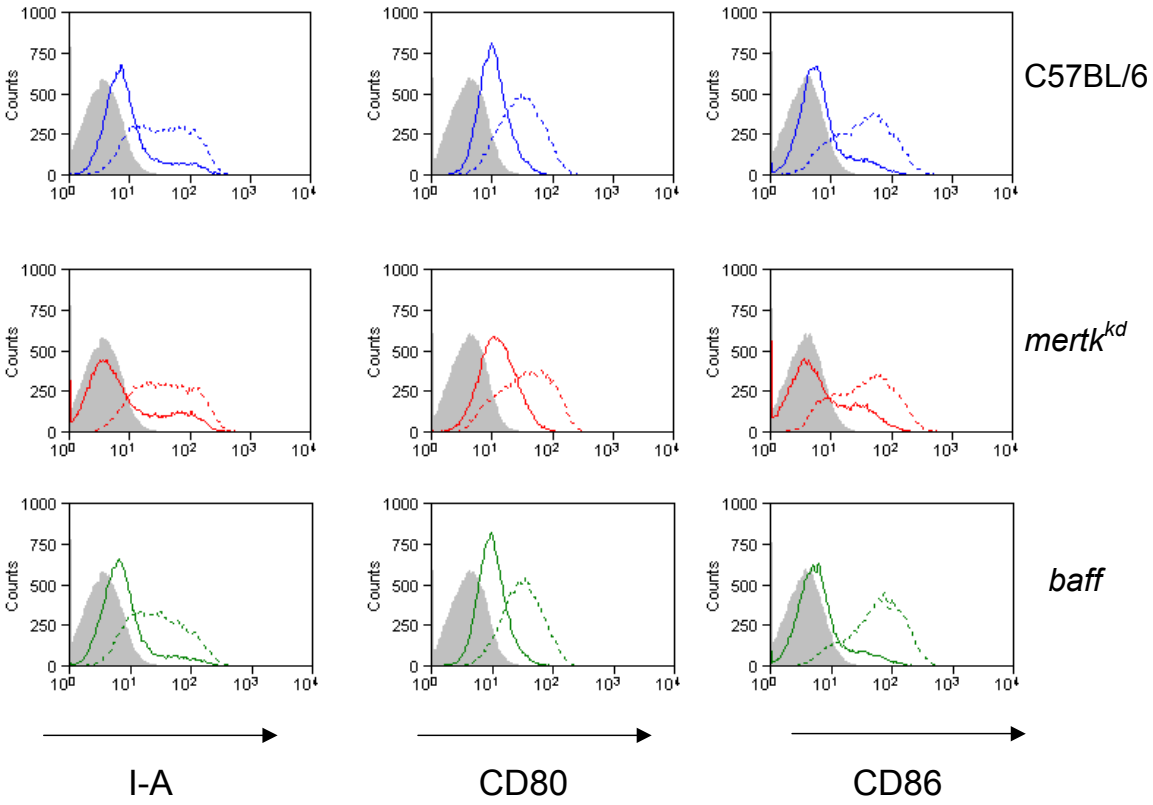

Figure 2.4, continued

Figure 2.4 Characterization of BMDC cultures A) The kinetics of cell growth, DC differentiation and viability in bone marrow cultures from C57BL/6, *mertk*^{kd} and *baff* mice were monitored. Culture conditions were identical to those described in *Materials and Methods* section except that volumes and starting cell numbers were scaled down from 6- to 24-well Ultra Low Cluster plates. Each data point represents the mean (± sem) measurement from three culture wells. Data is representative of three experiments with C57BL/6 and *mertk*^{kd} BMDC cultures, and one with *baff* BMDC included. B) MerTK (colored line) or goat IgG isotype control (gray fill) staining on the surface of day 8 BMDC (gated on CD11c^{+} events). C) C57BL/6, *mertk*^{kd} and *baff* BMDC were cultured in media alone (*solid line*) or with 500 ng/ml LPS (*dotted line*) for 2 days, after which time the change in surface expression of I-A, CD80 and CD86 was analyzed by flow cytometry (gated on CD11c^{+} events). Isotype control staining is also shown (*gray fill*). Data is representative of 2-4 experiments.

Figure 2.5

A)

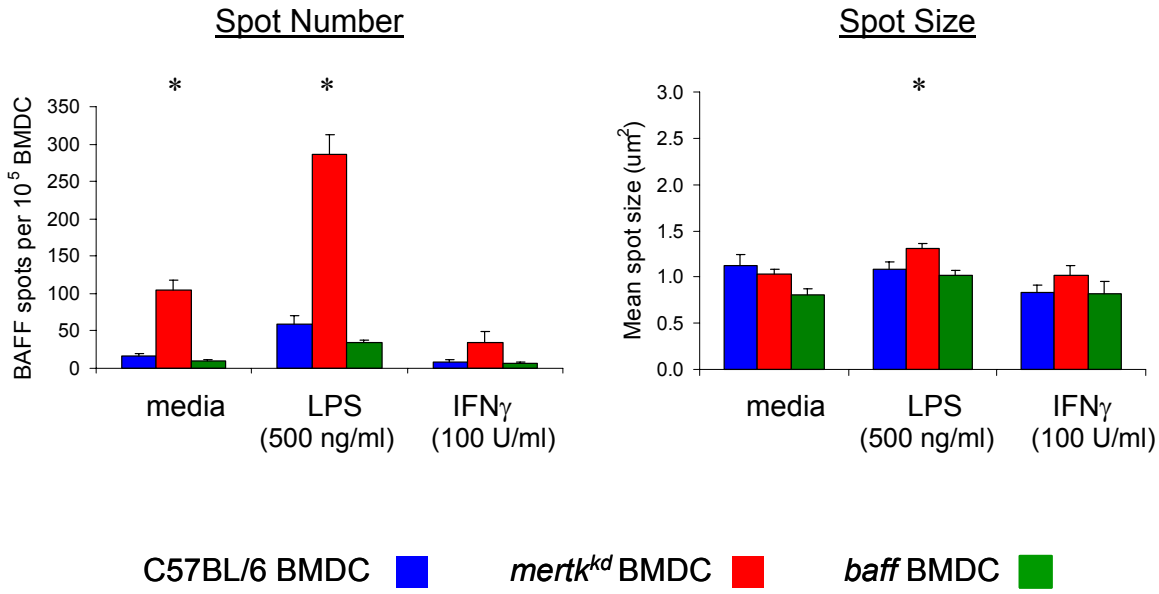
Spot Number
Spot Size
BAFF spots per 10^5 BMDC
Mean spot size (um^2)
media
LPS (500 ng/ml)
IFNγ (100 U/ml)
C57BL/6 BMDC
mertk^kd BMDC
baff BMDC

B)

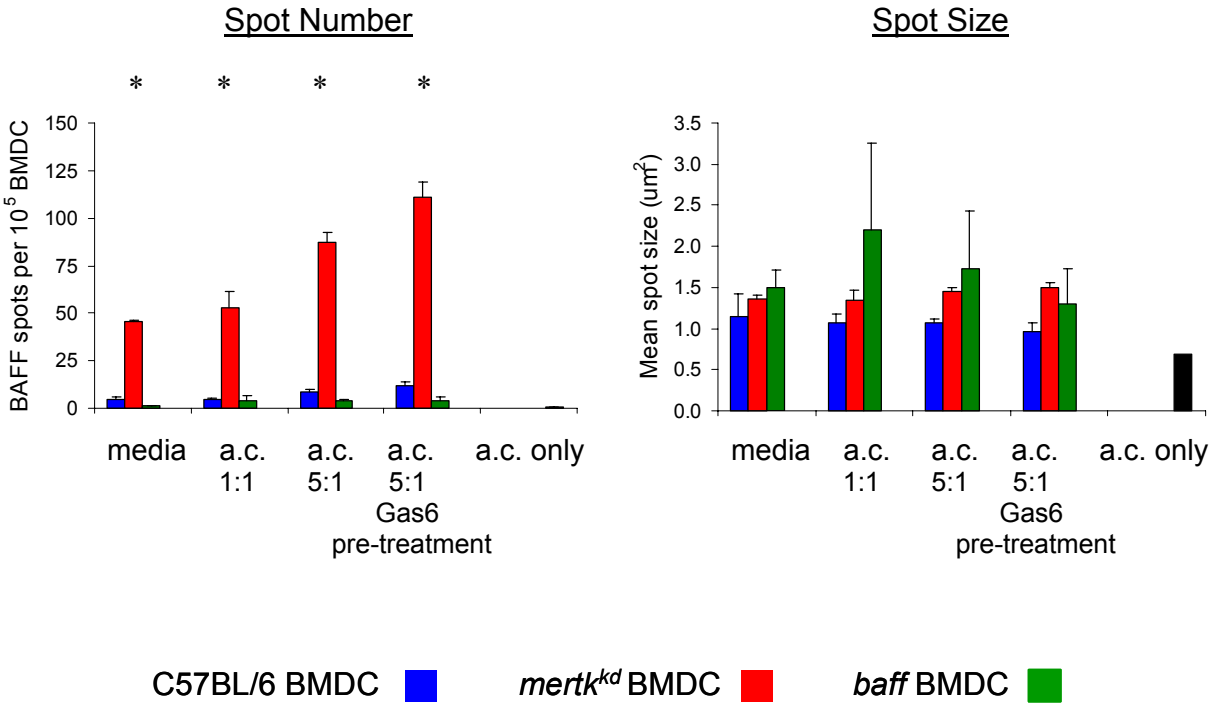
Spot Number
Spot Size
BAFF spots per 10^5 BMDC
Mean spot size (um^2)
media
a.c. 1:1
a.c. 5:1
a.c. 5:1 Gas6 pre-treatment
a.c. only
C57BL/6 BMDC
mertk^kd BMDC
baff BMDC

Figure 2.5, continued

Figure 2.5 *mertk*^{kd}, but not C57BL/6 BMDC readily secrete BAFF in culture
BAFF secretion by BMDC in response to media alone, LPS, or IFNγ (A) or apoptotic cells (a.c.) (B) was measured by ELISPOT. Apoptotic cells were given at a 1:1 or 5:1 ratio to BMDC (5 a.c. per 1 BMDC). Pretreatment of apoptotic cells with rGas6 (30 minutes at 37°, followed by multiple washes) was also tested. Both the spot number and mean spot size are reported. Each bar represents the mean (+ sem) of three ELISPOT culture wells. Data is representative of 3-4 independent experiments. Statistical significance of difference among genotypes within each treatment group were determined by the Kruskal-Wallis test (* p<.05)

Figure 2.6

A)

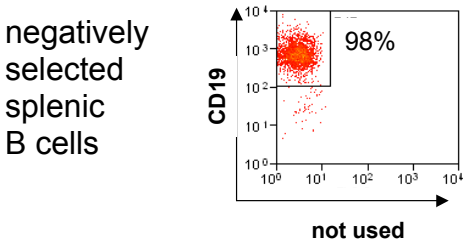

B)

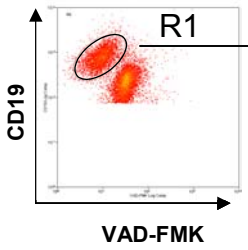

Counted B cells per well
X
Percent viable B cells
(VAD-FMK$^-$ among CD19$^+$ population)

= Absolute Number of Viable B cells

C)

Percent Viable B cells (VAD-FMK$^-$)

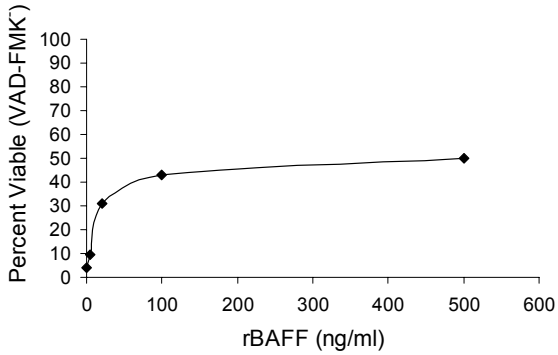

Absolute Number of Viable B cells

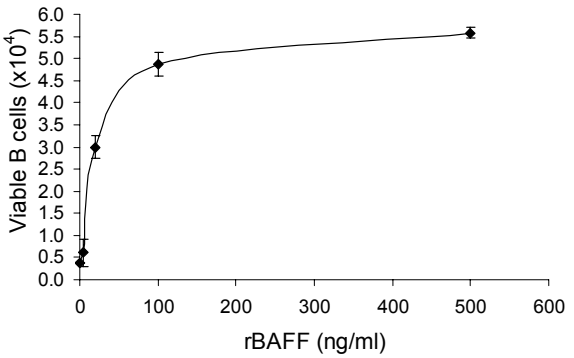

Figure 2.6, continued

D)

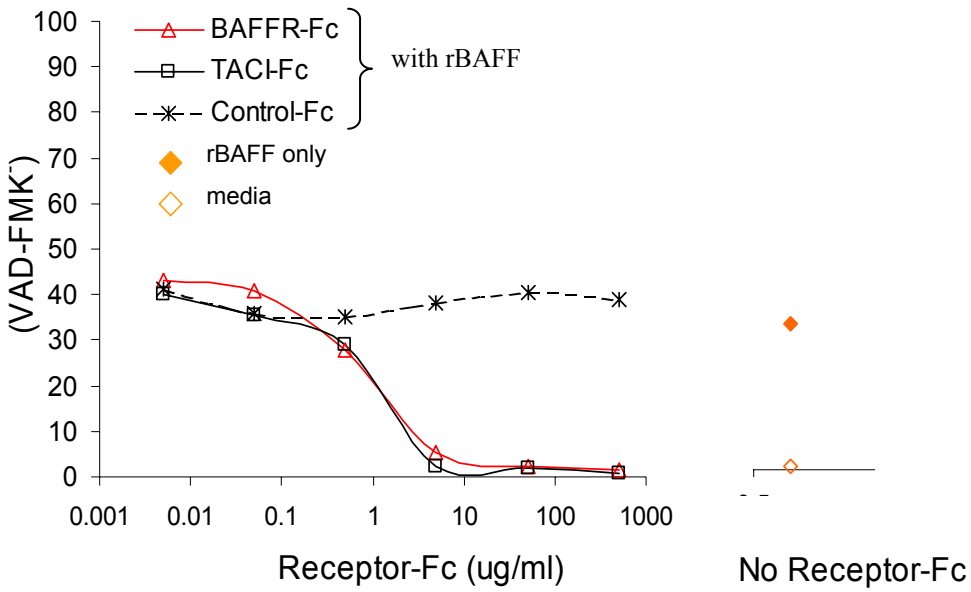

Figure 2.6 An in vitro assay for resting B cell survival A) An example of the splenic B cells obtained after negative selection. B) A sample staining of VAD-FMK^{FITC} among resting B cells (CD19^{+} events) after 3 days in culture. The percentage of VAD-FMK^{-} B cells (gate R1) was also used to determine the absolute number of viable B cells by the formula shown. C) $2x10^{5}$ negatively-selected splenic B cells were cultured with rBAFF (500 ng/ml, 100 ng/ml, 20 mg/ml, 4 ng/ml) or media alone for 4 days. Harvested cells were counted and the percent viability among CD19^{+} events was determined by staining with VAD-FMK^{FITC}. Data (mean $\pm$ sem) is plotted as either the percent of VAD-FMK^{-} B cells (left) or the absolute number of viable B cells (right). D) B cells were cultured in media alone, 100 ng/ml rBAFF, or 100 ng/ml rBAFF plus varying concentrations of the soluble decoy receptors BAFFR-Fc or TACI-Fc, or a control-Fc reagent. After 3 days the viability was measured by VAD-FMK staining of CD19^{+} events. One of two independent experiments.

Figure 2.7

A)

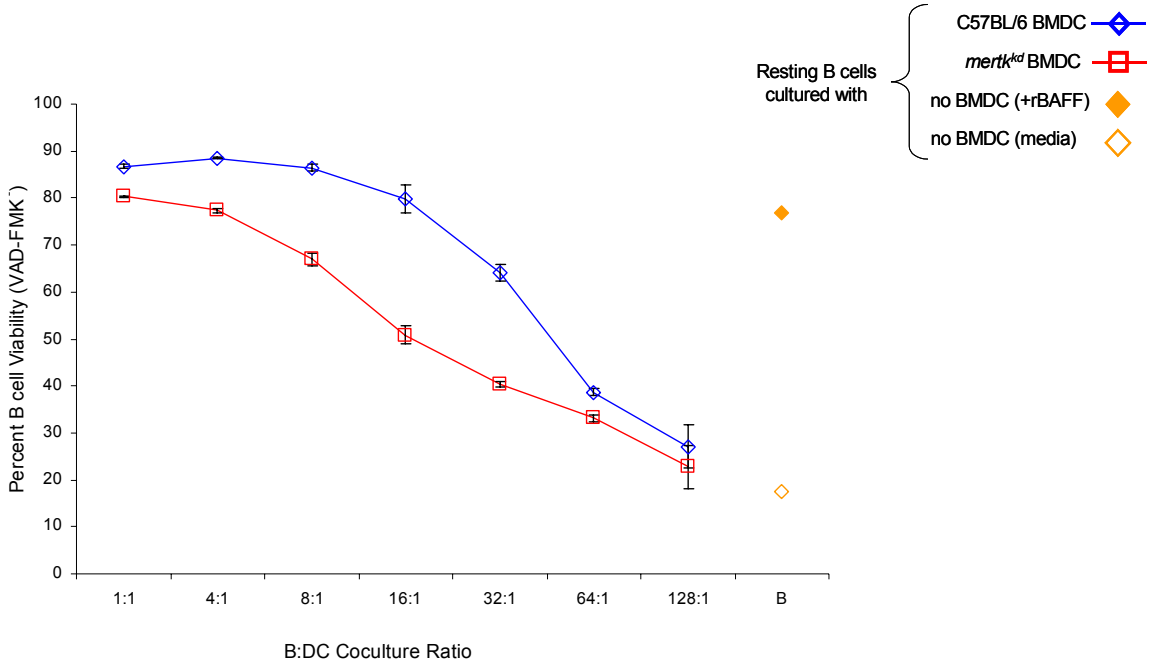
Resting B cells cultured with
C57BL/6 BMDC
mertk^kd BMDC
no BMDC (+rBAFF)
no BMDC (media)
Percent B cell Viability (VAD-FMK-)
100
90
80
70
60
50
40
30
20
10
0
1:1
4:1
8:1
16:1
32:1
64:1
128:1
B
B:DC Coculture Ratio

B)

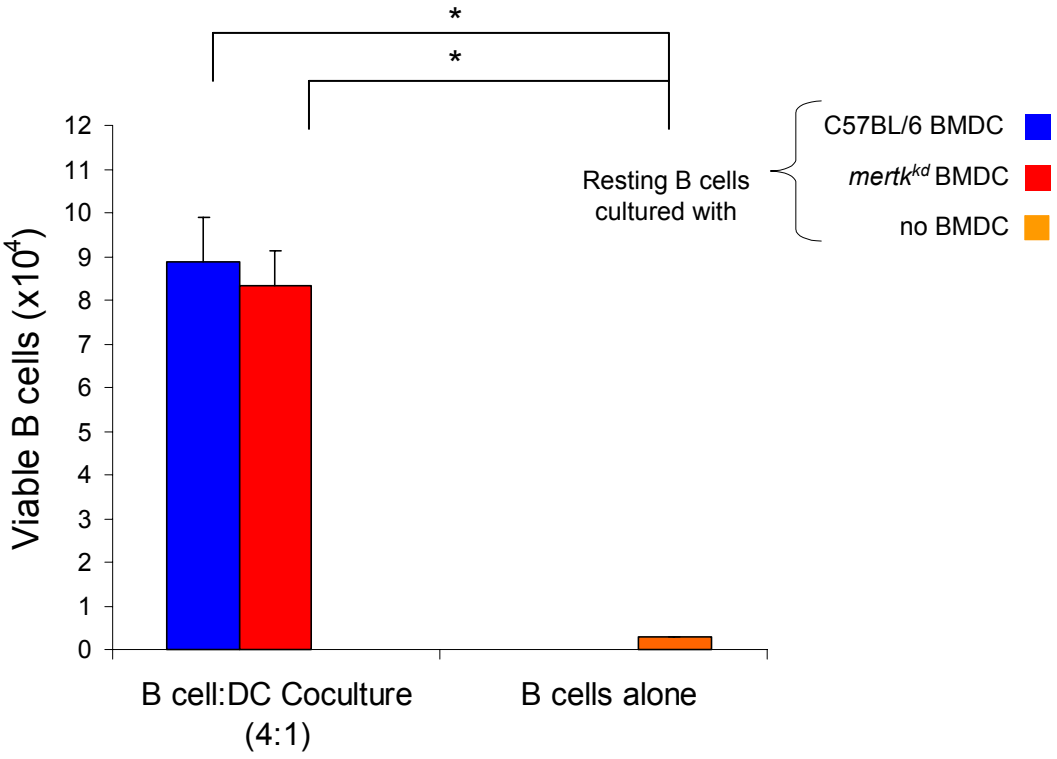
*
*
Resting B cells cultured with
C57BL/6 BMDC
mertk^kd BMDC
no BMDC
Viable B cells (x10^4)
12
11
10
9
8
7
6
5
4
3
2
1
0
B cell:DC Coculture (4:1)
B cells alone

Figure 2.7, continued

C)

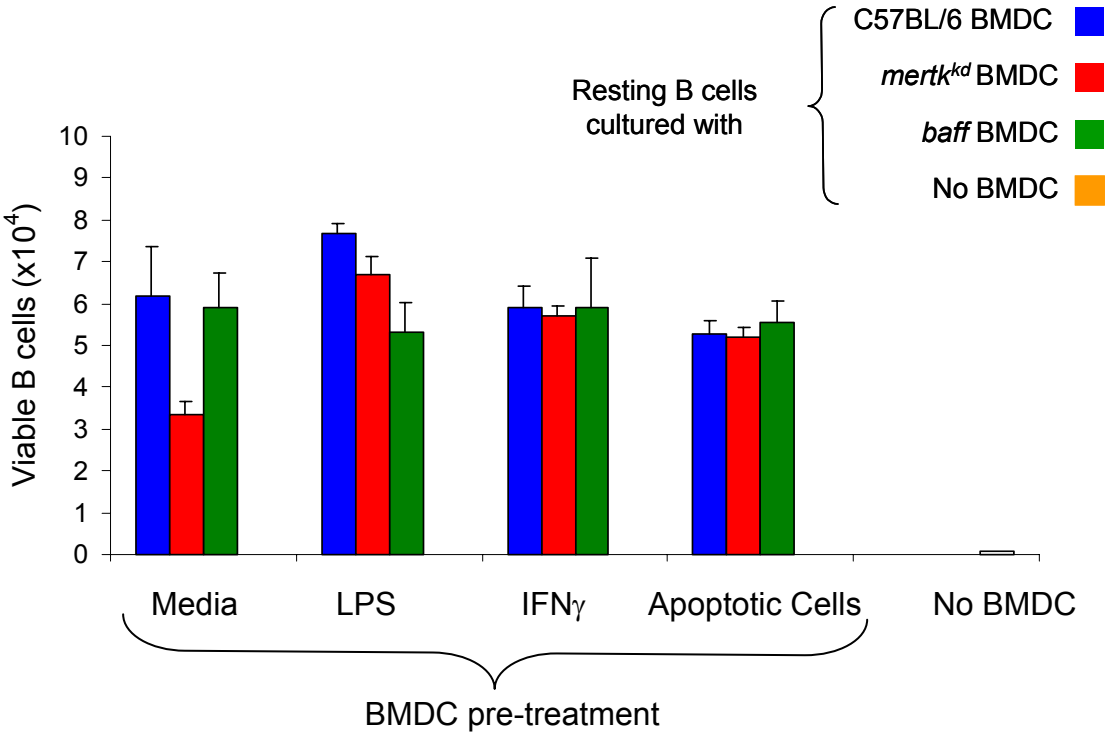

D)

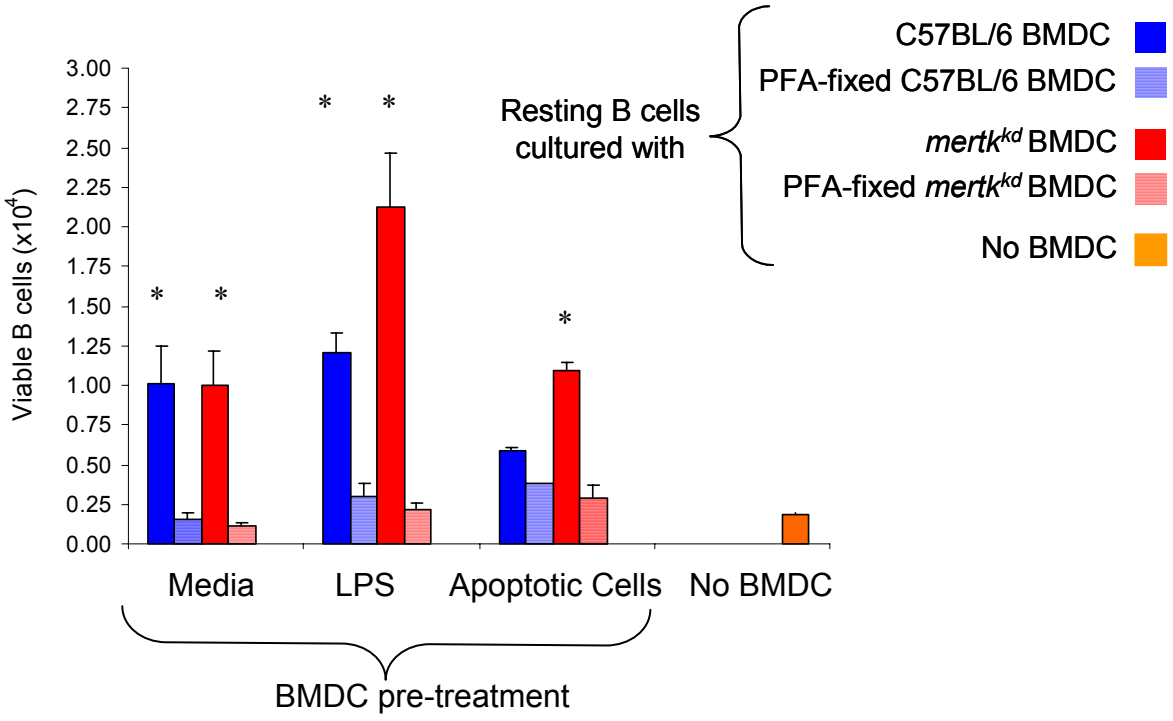

Figure 2.7, continued

E)

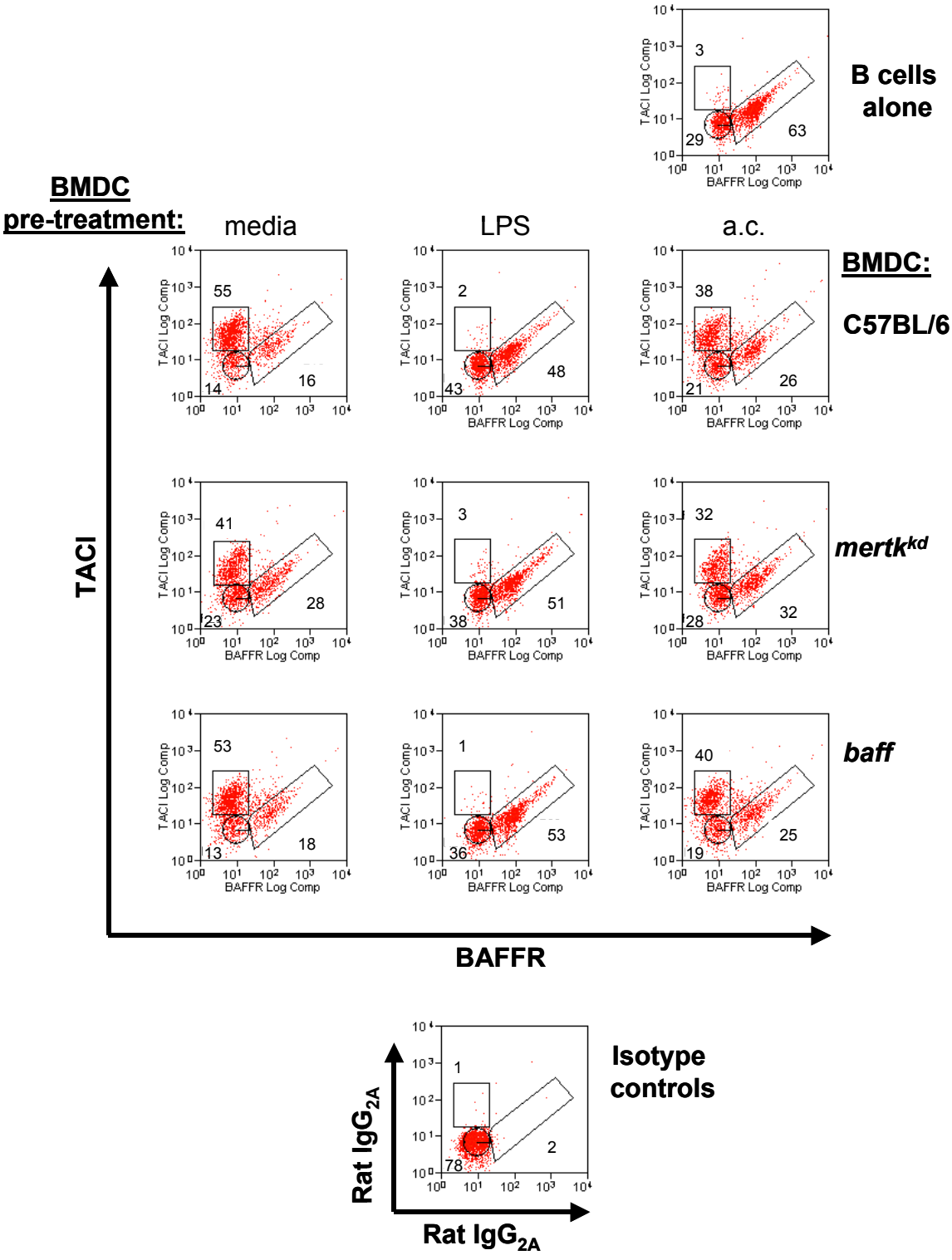

Figure 2.7, continued

Figure 2.7 BMDC augment the survival of resting B cells by a BAFF-independent mechanism A) Negatively-selected B cells were cultured alone in media or 100 ng/ml rBAFF, or with unstimulated C57BL/6 or *mertk*^{kd} BMDC in various ratios for 3 days at which time the percent of VAD-FMK^{-} cells among CD19^{+} events was determined by flow cytometry. Data points represent the mean (± sem) of 3 culture wells. Data is representative of two independent experiments. B) In a separate experiment, the absolute number of viable B cells remaining after culturing alone, or with unstimulated C57BL/6 or *mertk*^{kd} BMDC at a 4:1 ratio ($4x10^5$ B cells : $1x10^5$ BMDC) was determined by the formula shown in figure 2.4 A. Data represent mean (± sem) of 3 culture wells. Statistical significance between BMDC and B cells alone was determined using the Wilcoxon Rank Sum test (* $p<.05$). C) BMDC were pre-treated as indicated for 20-24 hours before washing and culturing with B cells at a 4:1 ratio. Data is representative of two independent experiments. There were no statistically significant differences between BMDC genotypes within each treatment group as determined by the Kruskal-Wallis test. D) Pre-treated BMDC were fixed with 1% paraformaldehyde, or left unfixed, before culturing with B cells at a 4:1 ratio. Statistical significance between the non-fixed and fixed BMDC in each treatment group was determined by the Wilcoxon Rank Sum test (* $p<.05$). E) The expression of TACI and BAFFR on B cells (gated on CD19^{+} events) was evaluated after coculture with BMDC that were pre-treated as indicated.

CHAPTER 3: Creation of a baff^{flox} Targeting Vector

ABSTRACT

Mice lacking the MerTK receptor tyrosine kinase (*mertk*^{kd} mice) spontaneously develop autoantibodies against nuclear antigens beginning around 4-6 months of age. Since MerTK is not expressed by B cells, autoimmunity in these mice might be initiated by other cell types which promote the breakdown of B cell tolerance mechanisms. One such mechanism involves limiting the availability of the pro-survival cytokine BAFF to autoreactive B cells. Dendritic cells (DC) express MerTK and are known to produce BAFF. We have found that mRNA encoding BAFF is elevated in splenic DC from older *mertk*^{kd} mice, suggesting that DC might be promoting B cell autoimmunity *in vivo*. However, *in vitro* experiments have failed to uncover a role for DC-derived BAFF in promoting B cell survival. To define the role that DC-derived BAFF has in autoimmune *mertk*^{kd} mice we decided to create BAFF conditional knockout mice. A targeting vector was made in which *loxP* sites flank exons 5 and 6 of the murine baff gene (DT7-BAFF^{flox}). Initially this vector was used successfully to target the *baff* locus in C567BL/6 embryonic stem (ES) cells, and subsequently generate chimeric mice. However, transmission of the baff^{flox} locus through the germline was not observed among over 140 F1 progeny mice (chimera x C57BL/6). Further attempts to apply DT7-BAFF^{flox} in a new set of ES cells are underway. Once *baff*^{flox} mice are successfully made (and mated to *cd11c*.Cre transgenic and *mertk*^{kd} mice) we will gain new insight into the importance of DC-derived BAFF in promoting B cell autoimmunity *in vivo*.

INTRODUCTION

Mertk^{kd} mice spontaneously develops antibodies against a variety of self-antigens commonly targeted in the disease Systemic Lupus Erythematosus, including dsDNA, ssDNA, chromatin, and Sm[49, 117, 122]. Considering that these mice also have a defect in the clearance of apoptotic cells[117, 122], and that these autoantigens are known to be found on the surface of apoptotic cells[45-50], the simplest explanation for autoimmunity in these mice is that it is driven solely by the presence of excess antigen in the form of unengulfed apoptotic cells. However, there are two arguments in opposition to such an explanation. First is the finding that the appearance of autoAb appears to be age-dependent, as most titers do not begin to rise until after 6 months of age[122]. Given that large numbers of apoptotic cells are generated continuously throughout life[120], a delay in autoAb until 6 months of age would be unexpected if uncleared apoptotic cells alone caused autoAb production in *mertk*^{kd} mice. A second finding that contradicts this explanation is that injections of apoptotic cells failed to accelerate the appearance of autoAbs in young *mertk*^{kd} mice[122].

In an effort to understand what genes or cells types might be driving autoimmunity in *mertk*^{kd} mice we turned our attention towards the cytokine B cell activating factor (BAFF). BAFF and its receptors (BCMA, TACI, and BAFFR) are members of the tumor necrosis factor superfamily. BCMA and TACI also bind to a protein closely related to BAFF known as a proliferation-inducing ligand (APRIL). Several cell types produce BAFF including macrophage, dendritic cells (DC), neutrophils, and non-hematopoetic stromal cells [130, 131, 144, 161, 198, 201]. An

extensive body of literature has led to a model in which, by providing B cells with a necessary pro-survival signal, BAFF's primary role *in vivo* is to maintain both the size and tolerigenic state of the mature B compartment [149, 152, 183, 224]. Under homeostatic conditions limited BAFF levels are thought to deprive autoreactive B cells of the pro-survival signals necessary to compete with non-autoreactive B cells for space in the mature B cell pool. However, when BAFF is present in excess amounts autoreactive B cells are able to differentiate into mature B cells, and ultimately autoantibody secreting cells[150, 151].

Aside from BAFF's role in regulating B cell tolerance our interest also stems from the fact that BAFF is produced by DC, which normally express the MerTK receptor. Numerous *in vitro* studies have demonstrated that BAFF derived from DC can enhance proliferation, plasma cell differentiation, Ig class switching, and Ig secretion from BCR-stimulated B cells[23, 130, 144, 161]. Evidence that DC-derived BAFF can mediate these same effects *in vivo* has been lacking thus far. Balazs et al. were able to demonstrate that, after capturing antigen, blood DC migrate to the spleen and activate MZ B cells, and that this activation was blocked by TACI-Ig delivered in an adenovirus[23]. However, such a systemic-wide blockade in BAFF activity does not discriminate between the importance of BAFF versus APRIL, or BAFF derived from the antigen-bearing DC versus other *in vivo* sources such as stromal cells. Indeed, studies using WT→*baff*$^{-/-}$ bone marrow chimeras indicate that non-bone marrow derived cell types (stromal cells) provide sufficient BAFF for normal B cell homeostasis, while BAFF derived strictly from bone marrow derived sources is incapable of maintaining a full B cell compartment and is

not detectable in serum[198]. While this evidence would suggest that BAFF from DC (or any other bone marrow-derived cell type) is not necessary for maintenance of the resting B cell pool *in vivo*, it does not rule out an important role for DC in providing BAFF to B cells during either a pathogen challenge, or autoimmune syndrome. Aside from this bone marrow chimera evidence, there have been no other *in vitro* or *in vivo* studies in which DC from *baff*$^{-/-}$ mice were studied.

We have recently obtained *baff*$^{-/-}$ mice[137] and intend to generate *mertk*^{kd} */baff*$^{-/-}$ mice. Although we intend to use this line as a source of DC for *in vitro* studies, it will be a poor tool for understanding the role that BAFF play, in the appearance of autoAbs in aging *mertk*^{kd} mice. The severe lack of mature B cells found in *baff*$^{-/-}$ mice at birth makes the prospect of *mertk*^{kd}*/baff*$^{-/-}$ mice developing autoAb with age questionable. Moreover, using a *mertk*^{kd}*/baff*$^{-/-}$ mouse, investigation into the importance of BAFF derived specifically from DC *in vivo* would have to be limited to adoptive transfer experiments.

In order to have more precise control over the cell type or timing of *baff* ablation we decided to generate conditional *baff*$^{-/-}$ mice using a Cre/*loxP* approach. Once a mouse carrying a *baff* gene flanked by *loxP* sites (*baff*^{flox} mice) is made, ablation of BAFF in DC or myeloid lineage cells can be achieved by mating *baff*^{flox} mice to transgenic mice that express the Cre recombinase gene under the control of the *cd11c* or *cd11b* promoters, respectively. Moreover, the importance that BAFF plays in the appearance of autoAbs in aging *mertk*^{kd} mice can be determined by generating *mertk*^{kd}*/baff*^{flox} mice and mating them to mice harboring a tetracycline-inducible form of the *cre* gene. By waiting to delete *baff* until *mertk*^{kd} mice become

positive for autoAb we will circumvent the obstacle that lifelong *baff* ablation poses to addressing this question. This chapter describes the procedures involved in creating a $baff^{flox}$ targeting vector. Replacement of the WT *baff* locus with our $baff^{flox}$ allele in murine ES cells, as well as an initial attempt at generating a $baff^{flox}$ mouse line, are also described.

MATERIALS AND METHODS

Cloning and PCR Reagents BamHI, EcoRI, EcoRV, XhoI, XbaI, and NotI were all purchased from New England Biolabs. Gel purification, column purification, and bacteria mini-prep kits were all purchased from QIAGEN. Taq polymerase was purchased from QIAGEN or Invitrogen, except in the amplification of fragment A' where Expand long range polymerase from Roche was used. dNTPs were purchased from QIAGEN. A list of PCR primers, and their sequences can be found in Table 3.1. A list of the PCR products described in the text can be found in Table 3.2. All primers were purchased from MWG Biotech

Plasmids The BAC clone RP23-92O5 (accession # AC101113) is part of a C57BL/6 mouse genomic library and was obtained from the Childerns Hospital of Oakland Research Institute (http://bacpac.chori.org). pBluescript (Stratagene) and PCR2.1-TOPO (Invitrogen) were used as recipient vectors during the subcloning process. pBS-DT7 is a derivative of pBluescript modified to carry a gene encoding Diptheria toxin. A map of pBS-DT7 can be found in Figure 3.2 B. The plasmids PL451 (contains single loxP and frt flanked neo^r) and PL452 (contains loxP flanked neo^r) were obtained from the National Cancer Institute[225]. Maps of PL451 and PL452 can be found in Figure 3.3.

Cells JM109 (Promega) and TOP10 (Invitrogen) cells are chemically competent E.coli strains used during subcloning. They were transformed according to manufacturer's instructions. DY380 and its derivative EL350 are electro-competent E.coli from the National Cancer Institute [225]. Both strains contain 3 genes (exo, bet, gam) that make them proficient at homologous recombination. These genes are

under the control of a temperature-sensitive repressor: they are repressed when DY380 cells are grown at 32°C, but become active when the repressor is inactivated at 42°C. EL350 also possess an arabinose-inducible cre gene encoding Cre recombinase. All bacteria were propagated with LB agar and broth. C57BL/6 embryonic stem (ES) cells were purchased from ATCC. Their propagation and transfection was conducted by Dr. Jrgang Cheng at the BAC Engineering Core Facility in the UNC Neuroscience Research Building.

Southern Blot A probe (probe 4) was prepared by PCR amplifying from BAC RP23-92O5, and then cloning into PCR2.1-TOPO (Invitrogen). Probe 4 was then excised from PCR2.1-TOPO by EcoRI digest. Gel purified probe 4 was then radiolabeled with $dCTP^{32}$ using a Random Primed DNA Labeling Kit (Roche). 10 µg of DNA from one WT ES cell and the 6 putative $BAFF^{flox}$ targeted ES cells was digested with XbaI for 24 hours. Digested samples were separated on an agarose gel and then transferred onto a Zeta-Probe membrane (Bio-Rad) using a vacuum blotter. Pre-hybridization and hybridization were conducted using QuickHyb solution (Stratagene). Hybridization with radiolabeled probe 4 (approximately $4x10^7$ total cpm) was carried out for 4 hours at 68°C. After extensive washing the membrane was exposed to film (Kodak).

Mice FLP-Tg mice were obtained from Jackson Laboratories and were described as backcrossed to C57BL/6 n>4 upon arrival. We have continued backcrossing this line to C57BL/6 in our colony, having reached n>7 as of March 2007. The FLP transgene is driven by an actin promoter.

Bioinformatic Software The DNA alignment program Squecher (Genecodes Corporation) was used throughout the design and construction of DT-BAFF^{flox}, and to make many of the schematic diagrams in this chapter. All PCR primers were picked using the free web-based tool Primer3[226] (http://fokker.wi.mit.edu/primer3/input.htm). Target sites for primers and probes were screened for repetitive elements using the free web-based tool RepeatMasker[227] (http://www.repeatmasker.org/)

RESULTS

In designing a Cre/*lox* conditional BAFF knockout mouse our initial concern was choosing a region of the gene which, when deleted, would result in a non-functional transcript or protein product. The murine *baff* gene consists of seven exons spread over approximately 30 kb (Figure 3.1). The first 3 exons consist of the N-terminal cytoplasmic tail, the transmembrane region, and the extracelluar stalk of the BAFF protein. The amino acid sequence that serves as the cleavage site (RNRR) to release soluble BAFF is also located in exon 3[126]. Residues encoded for by exons 4-7 make up the soluble cytokine domain of BAFF, and therefore are likely to be the most important for allowing BAFF to bind to its receptors. Although removing this entire portion of the gene would provide the best chance of ablating BAFF function, flanking this large region (14.6 kb) by *loxP* sites would not allow for efficient removal by Cre recombinase.

A closer examination of the genomic layout of the *baff* gene, however, points toward exons 5 and 6 as ideal targets for flanking *loxP* sites. The distance from the start of exon 5 to the end of exon 6 is only 347 bp, yet this region codes for 87 of the 166 residues that make up the soluble BAFF secondary structure. More importantly, a significant body of empirical evidence indicates that this region of the protein plays an important role in BAFF binding to its receptors. Crystalography studies indicate that a majority of the BAFF residues in direct contact with BAFF-R are located within exons 5 and 6[228-230]. Furthermore, in binding assays with BCMA and TACI, most of the BAFF peptide fragments bound to the either receptor spanned exons 5 and/or 6[132]. This information suggests that if a functional mRNA transcript was

generated from a *baff* gene lacking exons 5 and 6, and if this mRNA were translated into a stable protein, such a protein would likely be biologically inactive.

Subcloning the homology region of BAFF gene

The BAC clone RP23-92O5 (Accession number: AC101113) contains a 70 kb region of mouse chromosome 8, including the entire BAFF gene. Within the BAFF gene, an 8,333 bp fragment (referred to as fragment D) containing exons 5 and 6 as well as 5.4 kb of upstream sequence (long arm) and 2.6 kb of downstream sequence (short arm) was selected as the homologous region to be used in the BAFF targeting vector. Fragment D is defined at the 5' end by a *HindIII* site upstream of exon 5, and at the 3'end by an *EcoRV* site (Figure 3.1).

A combination of restriction digest and PCR were used to subclone fragment D from RP23-92O5 as separate adjoining fragments (Figure 3.2). Initially a sub-library of RP23-92O5 was made by shotgun cloning into pBluescript (pBS). A HindIII and XhoI double digest of RP23-92O5 was ligated into pBS that had previously been cut with HindIII and XhoI, treated with CIP (calf intestinal phosphatase), and column purified. Ligation products were used to transform JM109 competent cells. Subclones of RP23-92O5 were screened for fragment A (6449 bp) and fragment B (3972 bp) using the ↑*loxP* and ↓*loxP* PCR assays, respectively. Fragment B was identified in this manner and was further verified as the correct insert by a triple restriction digest with HindIII, XhoI, and SacI (Figure 3.2, C). Since fragment B (*XhoI→HindIII*) contains more downstream sequence than is desirable for our final BAFF targeting vector it was shortened from 3972 bp to 1905 bp by subjecting fragment B-pBS to an EcoRV restriction digest. A 4905 bp fragment containing pBS

(3000 bp) and the 1905 bp piece of fragment B was gel purified, re-ligated and used to transform JM109 competent cells. This shortened piece of fragment B, now known as fragment C, was verified by an XhoI / EcoRV restriction digest and the ↓*loxP* PCR assay (Figure 3.2 D and data not shown).

Fragment A was not recovered from the *HindIII / XhoI* library of RP23-92O5. Therefore a PCR-based cloning approach was used to isolate this region from RP23-92O5. PCR primers (fragment A'-f1 and fragment A'-r2) were designed in such a way that a region slightly larger than fragment A could be amplified, this PCR product was designated as fragment A' (6965 bp) (Figure 3.2 E). Fragment A' was cloned by a topoisomerase-based TA cloning method into PCR2.1-TOPO, and subsequent transformation into TOP10 competent cells. Clones carrying fragment A' were identified by the ↑*loxP* PCR assay and a HindIII / XhoI restriction digest. Importantly, this digest also liberated fragment A from the excess flanking pieces of DNA (approximately 400 bp and 100 bp) that were part of fragment A'. Fragment A was then isolated from PCR2.1-TOPO and these smaller fragments by gel purification (Figure 3.2 F).

Fragments A and C were joined to form the final 8.3 kb BAFF region of interest (Fragment D) by ligating both fragments into the targeting vector backbone, pBS-DT7, simultaneously. Fragment C was first isolated from pBS by an XhoI / EcoRI digest and gel purified (Figure 3.2 F). (Note: EcoRI was chosen over EcoRV, which was used to originally clone Fragment C into pBS, due to the more-specific ligation product expected with a sticky vs. blunt ended fragment. This approach added 6 bp of the pBS multiple cloning site to the 3' end of fragment D). pBS-DT7

was prepared by a HindIII / EcoRI digest, followed by CIP treatment, and column purification (Figure 3.2 F). This preparation of pBS-DT7 was ligated to the gel purified fragments A (*HindIII→XhoI*) and C (*XhoI→EcoRI*) and used to transform TOP10 cells. Ampicillin-resistant colonies were screened for both fragments A and C using the ↑*loxP* and ↓*loxP* PCR assays, respectively (data not shown). Four clones that were positive in both of these PCR assays were selected for subsequent screening by restriction digest with EcoRV. All 4 of these clones gave the 3 expected bands in this digest (pBS-DT7 (4170 bp), and fragment D (5863 bp and 2470 bp)), indicating that fragment D had been successfully cloned (Figure 3.2 G). For further verification of fragment D, the presence of exons 5 and 6 were verified by PCR and the integrity of their coding region sequences was found to be intact. The targeting construct consisting of fragment D + pBS-DT7 was designated DT7-BAFF (Figure 3.2 A). This construct contains an ampicillin-resistance cassette.

Introduction of loxP sites

Our strategy for integrating *loxP* sites into the sequence surrounding exons 5 and 6 of DT7-BAFF involves obtaining the *loxP* sites from donor plasmids, attaching short pieces (~100bp) of DNA from the desired location of the BAFF gene to each end, and then allowing homologous recombination to insert them in the correct location (Figure 3.3). The *loxP* site that was directed to the region upstream of exon 5 will be referred to as ↑*loxP*, while the site placed downstream of exon 6 will be referred to as ↓*loxP*. The *loxP* sequences themselves came from the donor plasmids PL452 and PL451. PL452 contains 2 *loxP* sites flanking a neomycin-resistance (*neo*^{r}) cassette. PL451 contains a single *loxP* site, and 2 *frt* sites flanking

a *neo*^{r} cassette. Both donor plasmids contain these regions within a *BamHI* / *EcoRI* fragment, which were excised and purified. These *BamHI* / *EcoRI* fragments of PL452 and PL451 will be referred to as, PL452$^{EcoRI\ /\ BamHI}$ and PL451$^{EcoRI\ /\ BamHI}$, respectively (see Figure 3.3 C).

. The site-specific integration of PL452 and PL451 into DT7-BAFF was achieved by flanking each cassette with short pieces of DNA from the desired location of the *baff* gene (see Figure 3.3). These flanking pieces were generated and attached as follows. Each *loxP* site has 4 primers associated with it. The primer pairs ↑*loxP*-f1 / ↑*loxP*-r1 and ↑*loxP*-f2 / ↑*loxP*-r2 were used to generate the PCR products ↑*loxP*-1 and ↑*loxP*-2, respectively, using RP23-92O5 as a template (see Table 3.2). These PCR products contain the novel restriction sites *EcoRI* on ↑*loxP*-1, and *BamHI* on ↑*loxP*-2 due to the addition of these sites to the 5' ends of the ↑*loxP*-r1 and ↑*loxP*-f2 primers respectively (see Table 3.1). The ↑*loxP*-1 and ↑*loxP*-2 PCR products were digested with the appropriate enzyme and then column purified. An identical process was carried out to generate PCR products to flank the ↓*loxP* site: the primer ↓*loxP*-r1 added an *EcoRI* site to the ↓*loxP*-1 PCR product, while the primer ↓*loxP*-f2 added a *BamHI* site to ↓*loxP*-2 PCR product. The flanking PCR products ↑*loxP*-1^{EcoRI} and ↑*loxP*-2^{BamHI} were ligated to PL452$^{EcoRI\ /\ BamHI}$, while ↓*loxP*-1^{EcoRI} and ↓*loxP*-2^{BamHI} were ligated to PL451$^{EcoRI\ /\ BamHI}$. Each ligation product was then PCR amplified using the outermost primer pairs: ↑*loxP*-f1 and ↑*loxP*-r2 in the case of ↑*loxP*(PL452), and ↓*loxP*-f1 and ↓*loxP*-r2 in the case of ↓*loxP*(PL451) (Figure 3.3 B). PCR products (approximately 2.1 kb each) were then gel purified.

The next several steps involved properly integrating the ↑*loxP*(PL452) and ↓*loxP*(PL451) sites into DT7-BAFF by homologous recombination (Figure 3.4). To do this the DT7-BAFF construct was first introduced into DY380 cells by electroporation. Transformants were selected by growth on ampicillin + tetracycline plates (DY380 have *tet*^{r}). DT7-BAFF transformed DY380 were placed in a 42°C water bath for 15 minutes (see *Materials and Methods*), then cooled on ice and centrifuged at 5,000 rpm for 5 minutes. Pelleted bacteria were washed twice in 1 ml of water before ↑*loxP*(PL452) was introduced by electroporation. As a negative control DY380 cells containing DT7-BAFF, but not exposed to 42°C, were also transformed with ↑*loxP*(PL452). Transformants were plated on ampicillin and kanamycin (a surrogate for neomycin), and allowed to grow at 32°C. After 2 days of growth 9 colonies were picked and used to innoculate broth containing ampicillin and kanamycin. The negative control plates did not contain any colonies after 2 days. Minipreps of the 9 colonies were screened for correct integration of ↑*loxP*(PL452) into DT7-BAFF by separate restriction digests with either EcoRI or BamHI and XhoI . Upon EcoRI digest a 1402 bp band results from the novel *EcoRI* site introduced by ↑*loxP*(PL452). This band was present in the same 8 clones and was absent in the parent plasmid. Similarly the novel *BamHI* site introduced by ↑*loxP*(PL452) yields a new 1340 bp band upon BamHI/XhoI digest (Figure 3.4 B). This band was seen in 8 out of the 9 clones, but not in the parent plasmid DT7-BAFF. One of the 8 clones was selected and was renamed DT7-BAFF$^{\uparrow loxP(PL452)}$.

Before the ↓*loxP* site could be properly inserted it was necessary to make DT7-BAFF$^{\uparrow loxP(PL452)}$ neomycin-sensitive by removing *neo*^{r} cassette in the ↑*loxP* site.

Since PL452 consists of 2 *loxP* sites that flank *neo*^{r}, Cre recombination was used to remove *neo*^{r} and leave behind a single *loxP* site. The bacterial strain EL350 is a derivative of DY380 that expresses Cre recombinase when grown on arabinose. EL350 cells were transformed with DT7-BAFF$^{\uparrow loxP(PL452)}$ by electroporation and screened for removal of the *neo*^{r} cassette by PCR. Prior to Cre recombination the primers ↑*loxP*-f1 and ↑*loxP*-r2 sit approximately 2 kb apart due to the presence of the *neo*^{r} cassette. Following Cre/lox recombination of DT7-BAFF$^{\uparrow loxP(PL452)}$ the bulk of this region is excised, leaving 63 bp, which includes a single *loxP* site (↑*loxP* PCR assay, see Table 3,2). The presence of the extra 63 bp can be detected by the ↑*loxP* PCR assay when compared to WT sequence (RP23-92O5). All 11 EL350 clones tested were positive for this size increase. Since most of the PL452 sequence, including the *neo*^{r} cassette, has been removed from our targeting vector it is now referred to as DT7-BAFF$^{\uparrow loxP}$ (Figure 3.4, C).

A single DT7-BAFF$^{\uparrow loxP}$ clone was chosen for the next step, insertion of ↓*loxP*(PL451) to generate DT7-BAFF$^{\uparrow loxP/\downarrow loxP(PL451)}$. In line with the procedure described above for ↑*loxP*(PL452), these EL350 cells were primed for homologous recombination at 42°C and then transformed with ↓*loxP*(PL451) by electroporation. Clones that had integrated ↓*loxP*(PL451) were selected for survival by growing on ampicillin + kanamycin plates. Integration of ↓*loxP*(PL451) was expected to result in the addition of 1 new *EcoRI* site and 1 new *BamHI* site. Therefore, eight ↓*loxP*(PL451)-transformed clones, as well as DT7-BAFF$^{\uparrow loxP}$ (negative control), were subject to EcoRI and BamHI digests. In these digests bands that are diagnostic for DT7-BAFF$^{\uparrow loxP/\downarrow loxP(PL451)}$ include a 1606 bp band following EcoRI digest, and bands

of 2844 bp and 3562 bp in the BamHI digest. As the BamHI digest in Figure 3.4 D shows, these bands were present in the kanamycin-resistant clones and not in the parent plasmid DT7-BAFF$^{\uparrow loxP}$. However these clones also contained bands that were only expected from DT7-BAFF$^{\uparrow loxP}$. This raised a concern that our $\downarrow$*loxP*(PL451)-positive clones may have actually contained 2 plasmids. This situation can arise when not all copies of the parent plasmid integrate the *neo*^{r} cassette, yet the clone survives growth in kanamycin because a sufficient number plasmids have integrated *neo*^{r}. To confirm this, plasmids from our clones were linearized with a *NotI* digest. As predicted, DT7-BAFF$^{\uparrow loxP/\downarrow loxP(PL451)}$ and DT7-BAFF$^{\uparrow loxP}$ could be discriminated as two separate bands within several individual clones (data not shown). To achieve pure clones, one of the NotI digested plasmid preps was re-ligated and used to transform JM109 cells. Clones grown in ampicillin + kanamycin were screened by EcoRI and BamHI digests. Four of 5 JM109 clones examined were pure versions of DT7-BAFF$^{\uparrow loxP/\downarrow loxP(PL451)}$ (Figure 3.4, E). A single clone was chosen and the integrity of exons 5 and 6 was re-validated by sequence analysis. With exons 5 and 6 now flanked by loxP sites the targeting vector was renamed DT7-BAFF^{flox}.

To insure that the loxP sites were functional DT7-BAFF^{flox} was put into Cre-expressing EL350 cells. Cre expression is induced in these cells by plating on arabinose-containing media. A successful loxP recombination event will result in loss of the neo^{r} cassette, therefore cells were grown under ampicillin selection only (no kanamycin). EL350 clones were evaluated for loxP recombination by PCR analysis using the primer pair $\uparrow$*loxP*-f1 and $\downarrow$*loxP*-r2 (hybrid *loxP* PCR assay). In the DT7-

BAFF^{flox} construct these primers sit approximately 3.7 kb away from each other. As expected, recombination of the loxP sites in DT7-BAFF^{flox} resulted in this primer pair being able to generate a 315 bp PCR product. Furthermore, the region of our construct carrying exons 5 and 6 could no longer be amplified by PCR (exon 5/6 PCR assay). Finally, loxP-recombined clones displayed the expected alterations in restriction fragments upon digestion with EcoRI, BamHI, and NotI. These results indicate that the loxP sites flanking exons 5 and 6 in DT7-BAFF^{flox} can undergo recombination when exposed to Cre. More importantly, our construct was now ready to use as a targeting vector for the BAFF gene in mouse ES cells.

Transformation and screening of C57BL/6 ES cells

The next step in generating a BAFF^{flox} mouse involves replacing one of the endogenous WT BAFF alleles in mouse ES cells with the BAFF^{flox} allele from our targeting vector by homologous recombination. DT7-BAFF^{flox} was prepared for electroporation into ES cells by first linearizing with NotI, then precipitating and washing in ethanol, before being resuspended in sterile PBS. ES cells were then electroporated and cultured under kanamycin selection. 144 ES cell clones were then screened for correct homologous recombination events. Initially we screened our clones with the ↑loxP PCR assay (Figure 3.6, A). 80 of the 144 clones were positive for the ↑loxP site. This indicates that our targeting construct was integrated into the genomic DNA of these clones, but not necessarily in the expected location. Therefore the 80 clones were screened in a 2nd PCR assay that was designed to verify the location of our construct (neo^{r} PCR assay, Figure 3.6, B). A primer located within the neo^{r} cassette (neo1-f) was paired with a primer that was located

downstream of the homology region covered by DT7-BAFF^{flox} (g↓loxP-r). A successful homologous recombination event was predicted to generate a 2261 bp PCR product using this primer pair. Using this assay we identified six correctly targeted ES cell clones: 5, 41, 45, 61, 115, and 132 (Figure 3.6, C).

The six clones identified above were further validated by Southern blot. Sequence from the region downstream of DT7-BAFF^{flox} was scanned for repetitive elements and then used to design PCR primers that would generate a 648 bp probe (probe 4). Probe 4 sits within an *XbaI* fragment that is 6932 bp long in the WT *baff* gene. Due to a novel *XbaI* site located near the ↓*loxP* site, probe 4 should label a 3353 bp fragment upon XbaI digest of a correctly targeted *baff* allele. Using this Southern blot assay all 6 ES clones were found to be heterozygous at the *baff* gene (*baff*$^{+/flox}$) (Figure 3.6, D and E).

With successfully targeted ES cells the next step involved generating a chimeric mouse. To accomplish this *baff*$^{+/flox}$ clone #45 was injected into blastocysts (also from C57BL/6), which were then implanted into psuedo-pregnant mice (this step was carried out by Dr. Randy Thresher's group at the Animal Models Core facility). Fifteen potentially chimeric mice were born and screened for chimerism using the ↑*loxP* and *neo*^{r} PCR assays (Figures 3.7, A and B respectively). In these assays 1 male displayed a moderate degree of chimerism (#8), 1 female mouse (#10) displayed weaker chimerism, while 2 other male mice (#14 and #15) displayed questionable chimerism. These four mice were then mated to C57BL/6 mice and the transmission of the *baff*^{flox} allele to progeny was monitored using the ↑*loxP* PCR assay. Germline transmission was not detected among 149 progeny (Figure 3.7, C).

DISCUSSION

We sought to investigate the role that DC-derived BAFF plays in the autoimmunity found in *mertk*^{kd} mice. Our approach to this question required creating a mouse line in which the expression of BAFF *in vivo* could be selectively ablated in DC. Initially, this involves flanking a critical region of the endogenous *baff* gene with *loxP* sites. Such an endeavor can be broken down into 3 separate steps: 1) design of the targeting vector, 2) homologous replacement of a *baff*^{WT} allele in ES cells, and 3) chimeric mouse generation and germline transmission of the *baff*^{flox} allele.

We were able to successfully complete steps 1 and 2. Regarding step 3, chimeric mice were generated but germline transmission of the *baff*^{flox} allele from these chimeras was never detected. One important consideration in this failure was that the degree of chimerism in these mice could only be estimated based on a PCR assay rather than by coat color. The ↑*loxP* PCR assay was used to assess chimerism because blastocysts from a WT C57BL/6 mouse were used as recipients for *baff*^{flox} ES cells. A better alternative may have been to use blastocysts from a white coat mouse. Indeed, a C57BL/6 mouse line with a natural mutation in the enzyme Tyrosinase can be utilized for this very purpose[231]. Using such a strategy the strength of chimerism can be easily assessed by the amount of black in an otherwise white coat. This assessment is important because, generally speaking, the greater the degree of chimerism the greater the chance that targeted ES cells have differentiated into meiotically-active gonadal tissue and hence have the potential to transmit the *baff*^{flox} allele on to progeny.

Despite the lack of a mixed coat detection method chimeric mice were detected by PCR, yet germline transmission of the *baff*^{flox} allele was unsuccessful. The most likely reason for this failure is the ES cells themselves. The potential for ES cells to differentiate into gonadal tissue is a property that can vary significantly among various ES cell lines. Moreover, this potential is generally thought to decrease during *in vitro* manipulations, a property that also varies from line to line. ES cell lines from the 129 mouse strains have traditionally been used to make knockout mice due to what many regard as their exceptional germline potential. The drawback of such an approach is that mice made on the 129 genetic background need to be backcrossed several generations (at least 6) before results can be compared to other WT strains, such as C57BL/6, with any confidence. To avoid these lengthy backcrossing steps we chose to use C57BL/6 ES cells. At first it might seem sacrificing the reliability of 129 ES cells for the speed of C57BL/6 ES cells may have been a poor choice. However, when these 2 approaches were compared in parallel knockouts of the same gene C57BL/6 ES cells performed comparable to 129 in terms of their germline transmission outcomes[232]. Regarding future attempts at generating a BAFF^{flox} mouse, since the homology region of DT7-BAFF^{flox} is derived from a C57BL/6 genomic library we are invested in continuing with a C57BL/6 ES cell line. In fact DT7-BAFF^{flox} has recently been reintroduced into a new line of C57BL/6 ES cells and screening of these clones is currently under way.

Provided that successful germline transmission of the *baff*^{flox} allele is achieved the next step will be to remove the *frt*-flanked *neo*^{r} cassette from the last intron of the *baff* gene (see figure 3.6, B). *Neo*^{r} was introduced along with the ↓*loxP* site as part

of PL451 to select for both positive DY380 clones and positive ES cell clones. Once a mouse carrying the *baff*^{flox} allele has been made the *neo*^{r} is no longer necessary and should be removed by FLP-*frt* recombination. To achieve this we have obtained FLP-Tg mice in which FLP recombinase is driven by the *actin* promoter. Homozygous *baff*^{flox} mice will be mated to FLP-Tg mice so that Neo^{r} can be removed. Among the heterozygous *baff*$^{flox/+}$ progeny from this cross we expect half to have had their *neo*^{r} cassette removed. These mice will then be intercrossed to regenerate homozygous *baff*^{flox} mice.

Once *neo*^{r} has been removed from our *baff*^{flox} mice they will be mated to Cre-Tg mice. A line of *baff*^{flox} / *mertk*^{kd} mice will be also be generated and mated to Cre-Tg mice as well. As mentioned in the *Introduction* section, we intend to use our *baff*^{flox} mice to answer two experimental questions about autoimmunity in *mertk*^{kd} mice: what is the role of DC-derived BAFF, and can BAFF ablation in aging *mertk*^{kd} mice prevent, or reverse, autoAb production. Our choice of Cre-Tg mice will reflect these experimental goals.

For removal of BAFF from DC there are several lines of Cre-Tg mice that are known to be active in DC. Cre-Tg mice using the *lysM* [233, 234] or *cd11b* [235, 236] gene promoters have been used for their selectivity toward myeloid lineage cell types. In some cases these mice have been used to address questions relating to DC biology. Nevertheless, because these lines have Cre expression in a broader range of cell types, such as macrophage and granulocytes, they are not our first choice for deletion of *baff* in DC. Moreover, by using *cd11b*-Cre mice *baff* deletion is likely not to occur in the CD8^{+}CD11b^{-} DC subset, yet these cells do express MerTK

and therefore may be playing a role in autoAb production in *mertk*^{kd} mice. To study DC-derived BAFF more specifically we hope to mate the *baff*^{flox} mice to *cd11c*-driven Cre mice. These mice have reportedly been made[237] but data using them has yet to be published.

We also wish to have temporal control over Cre expression so that BAFF expression can be ablated only when aging *mertk*^{kd} mice are producing autoAb. To do this we plan to take advantage of a tetracycline-inducible Cre expression system. These models require two transgenes, a gene encoding the reverse tetracycline-inducible transactivator (rtTA), and a *cre* gene regulated by the *tetO* operator sequence. Only after the tetracycline analog doxycyline is added can the rtTA protein binding to the *tetO* sequence thereby inducing *cre* expression[238]. This requires adding 2 additional transgenes (rtTA and *tetO-cre*) to our baff^{flox} mice, which can sometimes result in mosaicism. Alternatively, an auto-inducible system exists in which both rtTA and Cre are driven from the same doxycycline-inducible bidirectional *tetO* element (DAI-Cre transgenics). These mice display low leakiness (Cre/*lox* recombination in the absence of doxycycline) and high Cre activity in multiple tissues upon induction [239].

If BAFF ablation in DC is successful at preventing autoAb in *mertk*^{kd} mice it would suggest a numerically minor cell population (DC) has the ability to regulate the tolerance status of a much larger one (B cells). Such a disparity in cell-to-cell ratios indicates that micro-anatomical relationships are likely to play an important role. The splenic marginal zone (MZ) is one possible location where DC may be participating in the breakdown of B cell tolerance. MZ B cell numbers are elevated approximately

2-fold in *mertk*^{kd} mice and are a reservoir of autoreactive B cells in *mertk*^{kd} mice carrying an IgM transgene specific for the SLE antigen, Sm [49]. The larger MZ B cell population may be due to the elevated number of, and elevated BAFF-production by, DC in *mertk*^{kd} mice [240]. In BAFF/anti-HEL/HEL triple transgenic animals autoreactive B cells are allowed to populate the MZ only when BAFF is present in excess, although in this case BAFF overexpression was global and not DC-derived[151]. Intriguingly however, DC have been shown to promote the differentiation of MZ B cells into plasmablasts via a BAFF/APRIL-dependent mechanism [23]. Thus DC-derived BAFF in *mertk*^{kd} mice may not only be permitting the residence of autoreactive B cells in the MZ, but possibly aid in their differentiation into autoAb-secreting cells as well.

If BAFF production by DC turns out not to be required for autoimmunity in *mertk*^{kd} mice we will refocus our attention on other potential causes for the breakdown in B cell tolerance. Since BAFF production by non-hematopoetic cells is required for maintenance of the resting B cell pool stromal cells may play a role in autoimmunity. However, serum BAFF (which is derived from non-hematopoetic cells[198]) levels are not elevated in *mertk*^{kd} mice [240], suggesting that this pool of BAFF-producing cells is not driving autoimmunity. Future experiments involving bone marrow chimeric mice will increase our understanding of this issue. Alternatively, autoimmunity in *mertk*^{kd} mice may turn out to be BAFF-independent, regardless of the source cell type. Indeed, when SLE-prone NZB 2328 mice were crossed to *baff*$^{-/-}$ mice anti-dsDNA antibodies could still be detected in older animals [241]. A lack of a requirement for BAFF would favor a model in which autoimmunity

in *mertk*^{kd} mice is driven strictly by availability of excess antigen (uncleared apoptotic cells). It would be interesting to see if *mertk*^{kd} mice reach a certain age at which the capacity for the spleen to clear apoptotic cells is saturated.

Baff^{flox} mice will be a valuable tool for understanding the role of BAFF in both protective B cell responses and autoimmune disease. The versatility of such a mouse will be limited only by the wide array of Cre-Tg mice currently available. For example, there is a suggestive role for BAFF in multiple sclerosis (MS) [242, 243]. Applying *baff*^{flox} mice (in which Cre is driven by brain-specific promoters) to an MS model could greatly increase our understanding of BAFF's role in this disease.

Table 3.1

Primer name	Sequence (5'→3')
fragment A'-f	TTGGCAGGAGGTCTGTTAAG
fragment A'-r	CCAGAACAAGATTGGGACCT
↑*loxp*-f1	AAGTTGGTGGTGGCCTCACTT
↑*loxP*-r1	**CCGGAATTC**GAGTACCTGTTCCTCTGCACAACA
↑*loxP*-f2	CCGGGATCCTCAGGAAATAGCCAGTGTGCAGAAC
↑*loxP*-r2	CTCCATTGGGCTATCTGCCAAACA
↓*loxP*-f1	AAGGCAAGTCTAAGGTAGATGCCC
↓*loxP*-r1	**CCGGAATTC**CCCAGAAGGCTCTCAGGTTTC
↓*loxP*-f2	CCGGGATCCTTCTCTGTCAGCTTCACTGCCT
↓*loxP*-r2	ACATTATGATGTTATGACCTGTCCTGTC
neo1-f	TCGCCTTCTTGACGAGTTCT
g↓*loxP*-r	CATACCTTAAAATATGCATTTAACCTG
exon 5/6-f	TCTCATGAGTAATTCTCTCTCTGCT
exon 5/6-r	GGAATAAGATTCCCCAGCAC
probe4-f	AGTGAAGCGTGAATGCTGTG
probe4-r	ACCTGGAAAAGAGCGTGTGT

Table 3.1 PCR primers used to make and validate DT-BAFF^{flox} All PCR primers are written in 5'→3' direction. Extra bases added to 5' ends for novel EcoRI and BamHI sites are written in bold or underlined, respectively.

Table 3.2

PCR product	Primer-f	Primer-r	Size (bp)
fragment A'	fragment A'-f	fragment A'-r	6959
↑*loxp*-1	↑*loxp*-f1	↑*loxP*-r1	123
↑*loxP*-2	↑*loxP*-f2	↑*loxP*-r2	135
↓*loxp*-1	↓*loxP*-f1	↓*loxP*-r1	107
↓*loxP*-2	↓*loxP*-f2	↓*loxP*-r2	120
↑*loxP* assay	↑*loxp*-f1	↑*loxP*-r2	WT=275 targeted=338
↓*loxP* assay	↓*loxP*-f1	↓*loxP*-r2	230
↑*loxP*(PL452)	↑*loxp*-f1	↑*loxP*-r2	2135
↓*loxP*(PL451)	↓*loxP*-f1	↓*loxP*-r2	2110
exon 5/6 assay	exon 5/6-f	exon 5/6-r	440
hybrid *loxP* assay	↑*loxp*-f1	↓*loxP*-r2	315
probe 4	probe 4-f	probe 4-r	648

Table 3.2 PCR products generated during the creation and validation of DT-BAFF^{flox} Shown are the names, constituent primers, and size of each PCR product referred to throughout the *Results* section.

Figure 3.1

A)

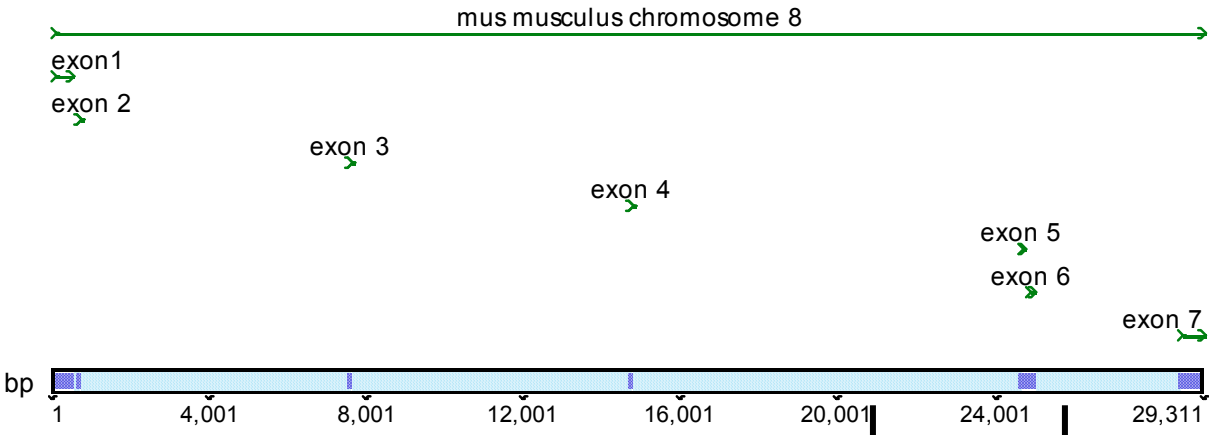

B)

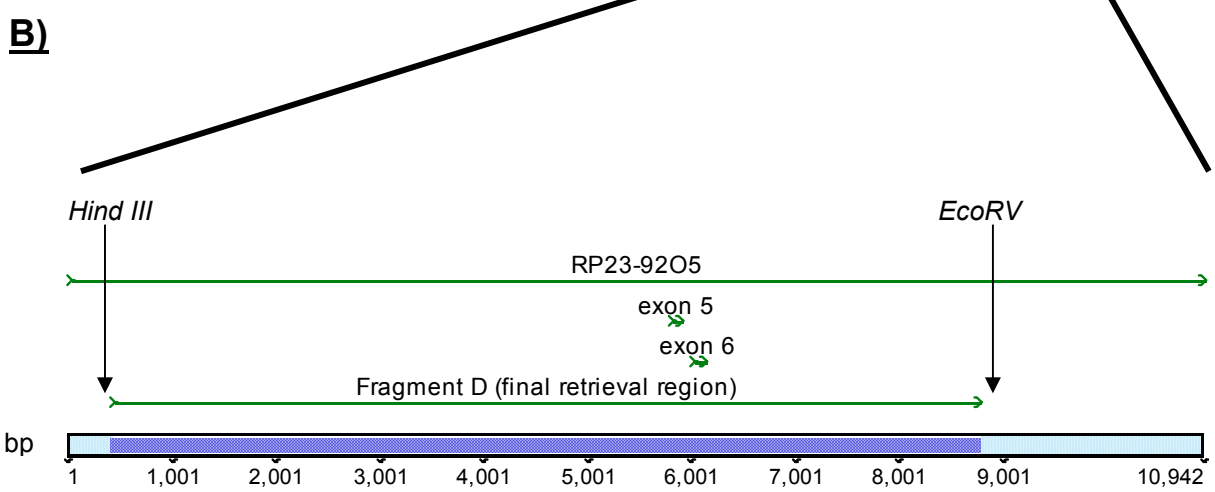

Figure 3.1 Genomic organization of the murine *baff* gene A) The location of exons 1-7 within the *baff* gene on mouse chromosome 8. B) Enlargement of the exon 5-6 area of the *baff* gene. The span of homologous DNA that was retrieved for the DT7-BAFF targeting vector is shown (Fragment D). Scale bars represent base pairs (bp).

Figure 3.2

A)

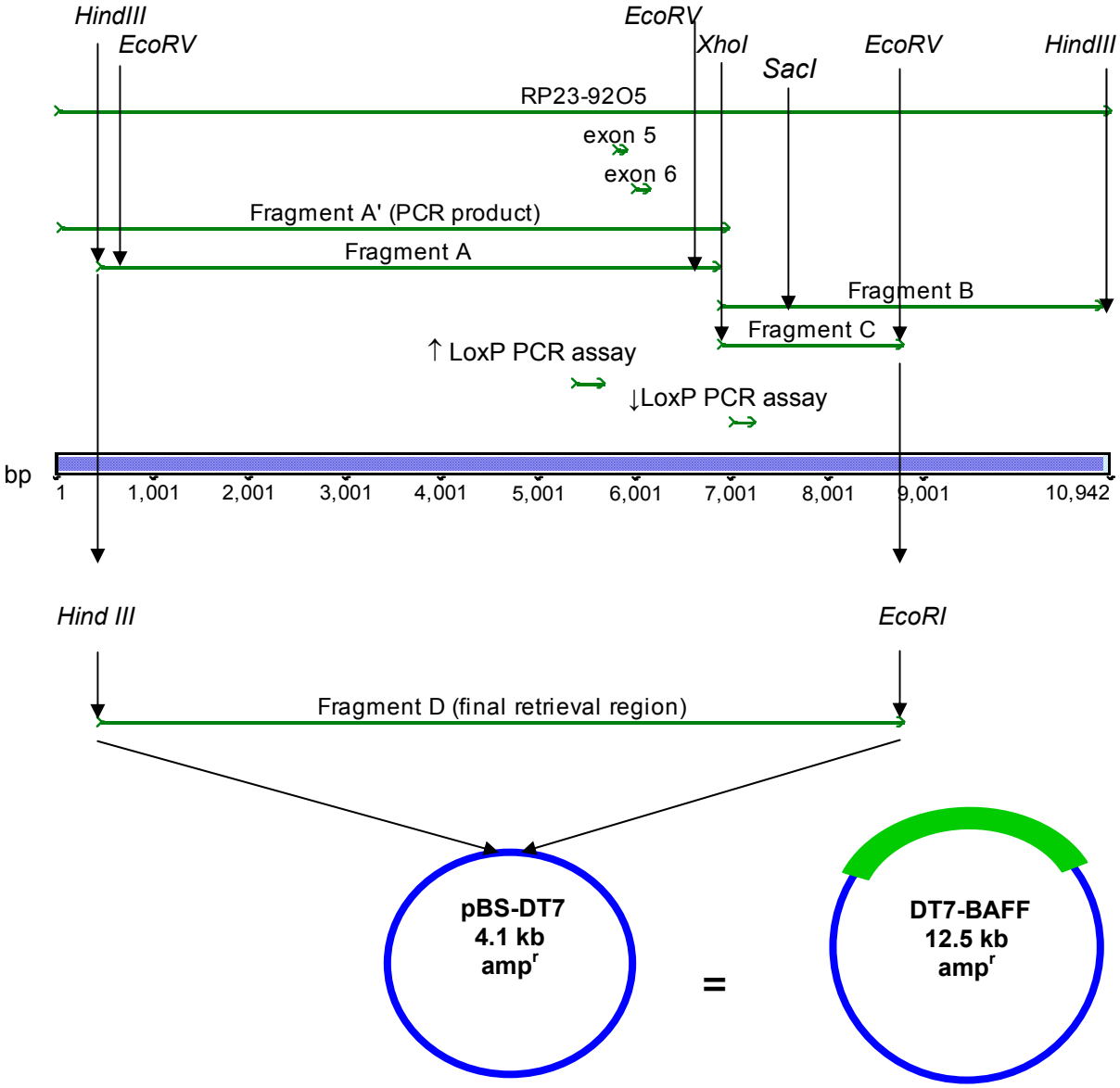
HindIII
EcoRV
EcoRV
XhoI
SacI
EcoRV
HindIII
RP23-92O5
exon 5
exon 6
Fragment A' (PCR product)
Fragment A
Fragment B
Fragment C
↑ LoxP PCR assay
↓LoxP PCR assay
bp
1
1,001
2,001
3,001
4,001
5,001
6,001
7,001
8,001
9,001
10,942
Hind III
EcoRI
Fragment D (final retrieval region)
pBS-DT7
4.1 kb
amp^r
=
DT7-BAFF
12.5 kb
amp^r

Figure 3.2, continued

B)

Figure 3.2, continued

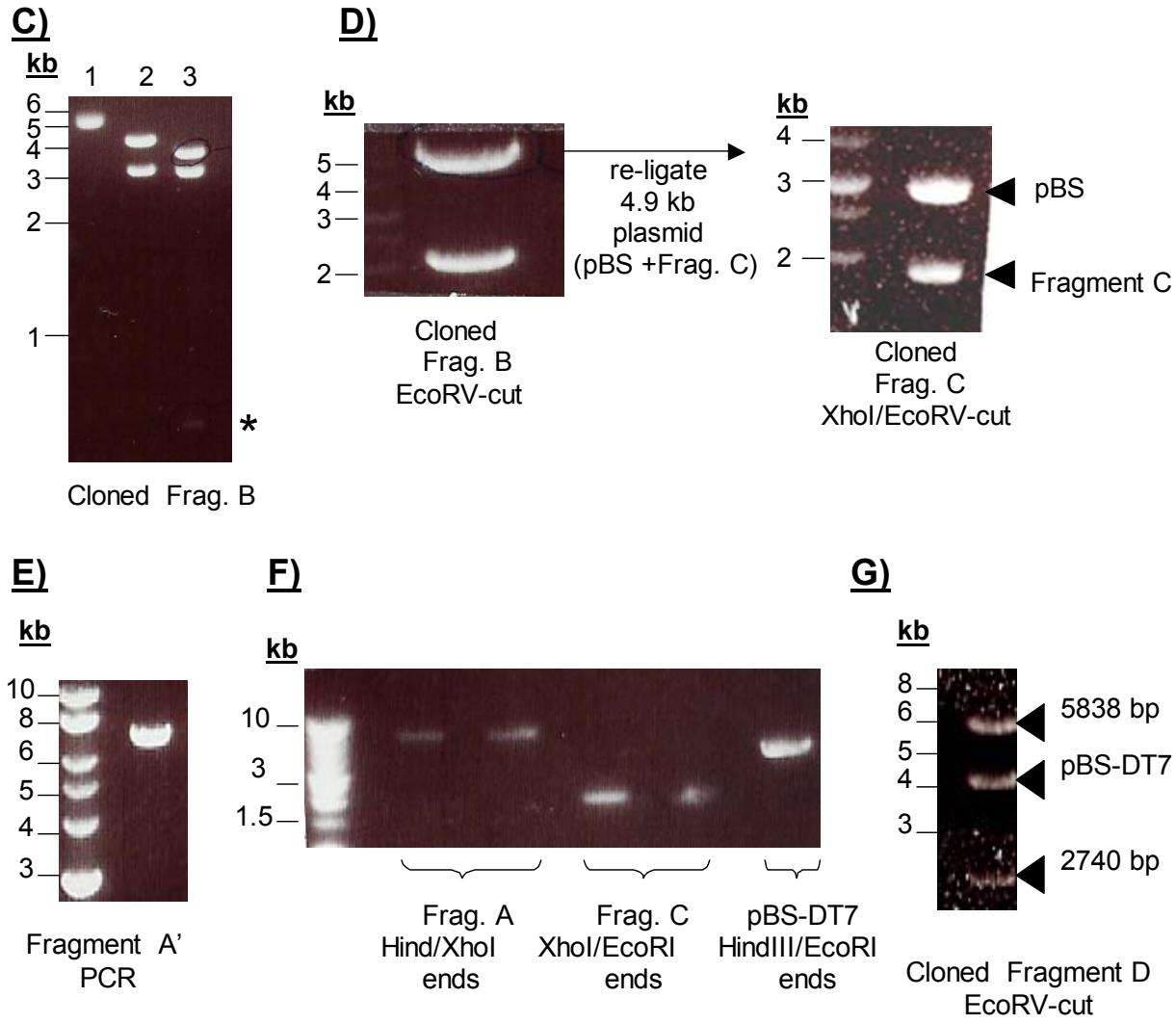

Figure 3.2 Subcloning Fragment D into pBS-DT7 A) Fragments A and C, isolated from the BAC clone RP23-92O5, were joined to form Fragment D. Also shown are the locations of ↑loxP and ↓loxP PCR assays. B) Schematic of pBS-DT7. The *HindIII* and *EcoRI* sites used to insert Fragment D are shown. C) Fragment B in pBS: uncut plasmid (lane 1), HindIII/XhoI digest (lane 2), HindIII/XhoI/SacI digest (lane3). The * indicates the position of a 579 bp band that is unique to lane 3. D) Fragment C isolated by removing 2067 bp from Fragment B. E) PCR of Fragment A' from BAC RP23-92O5. F) Fragments A and C (after gel purification), and pBS-DT7 prepared for triple ligation. G) Verification of Fragment D cloned in pBS-DT7 by EcoRV restriction digest.

Figure 3.3

A)

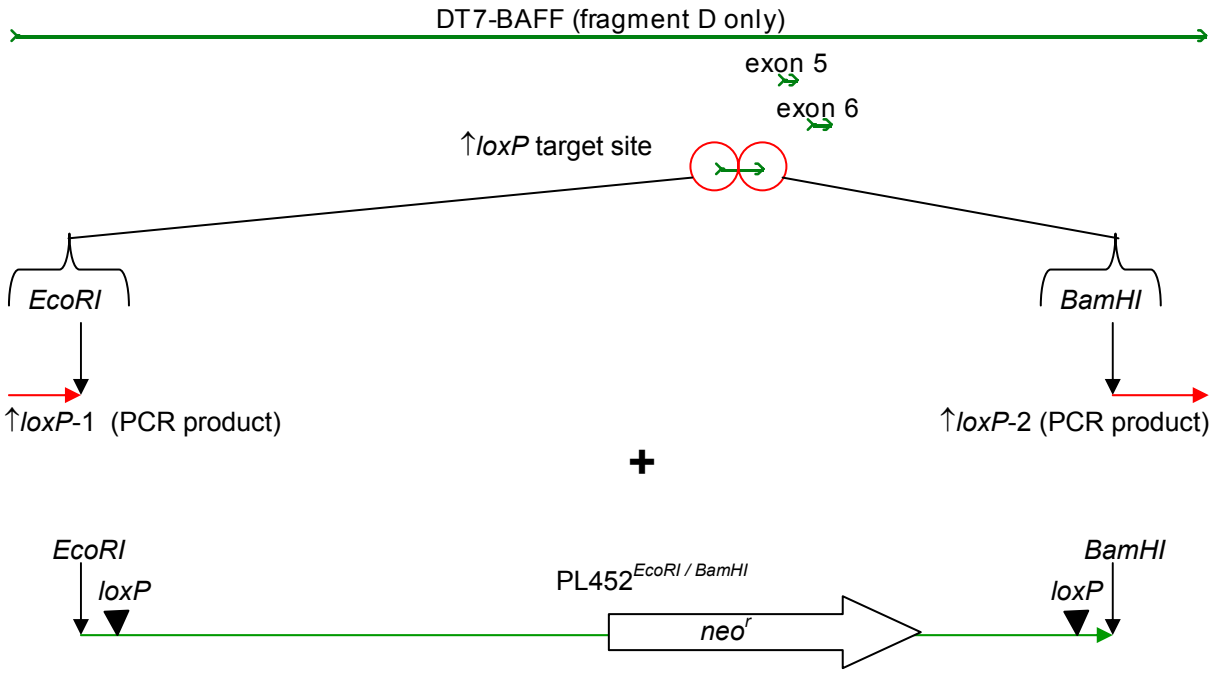

B)

Ligate and perform PCR across entire fragment using outermost primer pair (↑*loxP*-f1 and ↑*loxP*-r2) to generate ↑*loxP*(PL452)

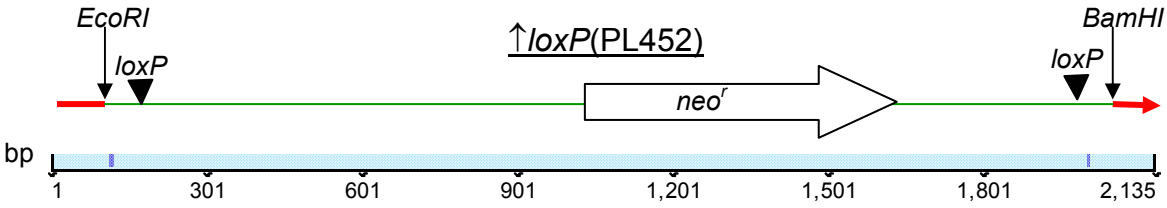

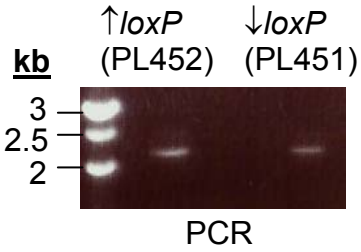

Figure 3.3, continued

C)

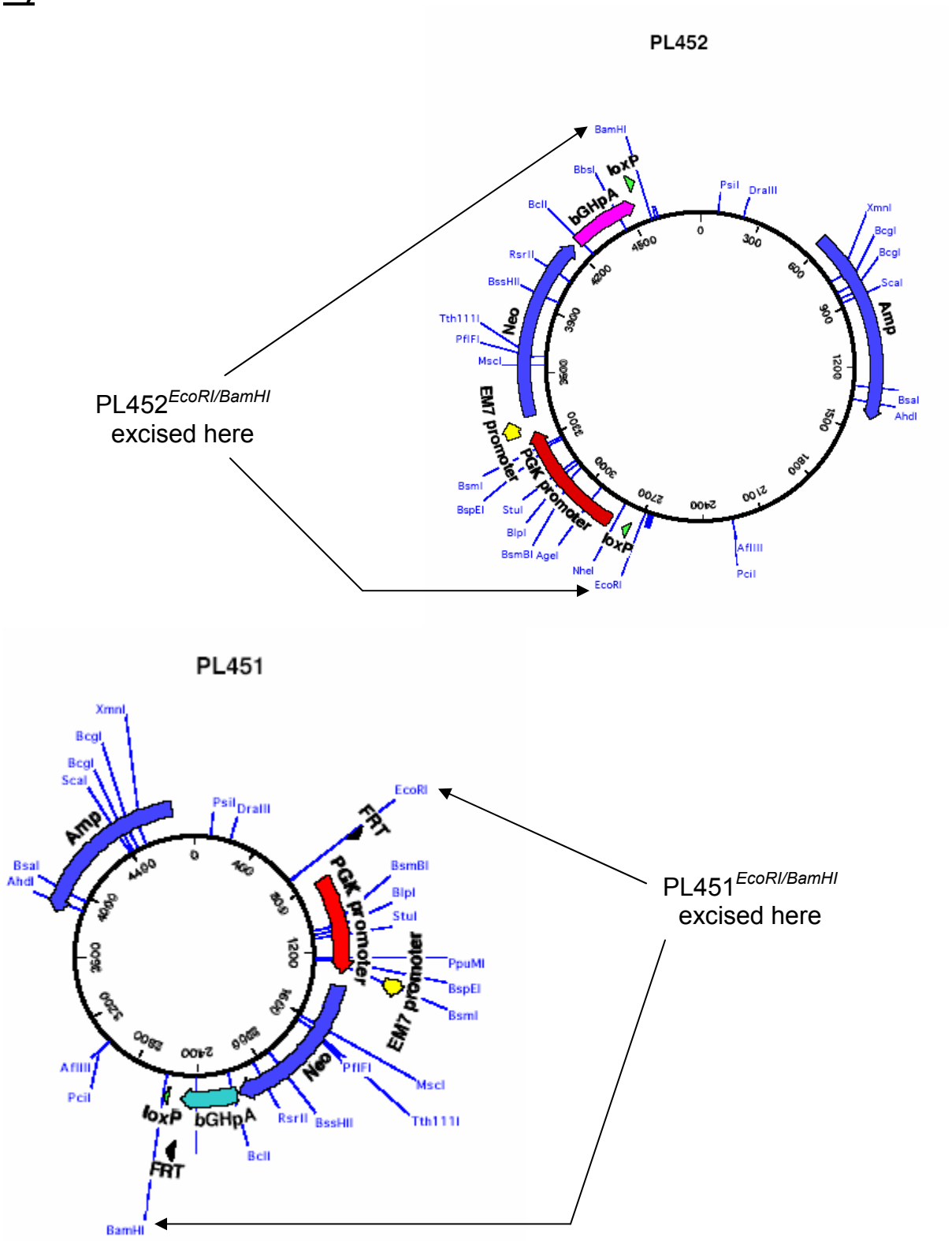

Figure 3.3, Continued

Figure 3.3 Generation of *loxP* fragments for site-specific integration A) The intended integration site for the ↑*loxP* site upstream of exons 5 and 6 is shown. PCR products ↑*loxP*-1 and ↑*loxP*-2 were generated from this area (red circles), and contain novel *EcoRI* and *BamHI* sites, respectively. The fragment of PL452 containing the *loxP* -flanked *neo*^{r} cassette is shown with *EcoRI* and *BamH*I sticky ends. Arrowheads denote position of *loxP* sites. B) Digested PCR products ↑*loxP*-1 and ↑*loxP*-2 were ligated to the PL452$^{EcoRI/BamHI}$ fragment to generate ↑*loxP*(PL452), which was then amplified by PCR (bottom gel). Shown in red are the regions homologous to the intended ↑*loxP* target site in pBS-DT7. The ↓*loxP*(PL451) fragment, targeted for integration downstream of exons 5 and 6, was prepared in a similar manner. Scale bar represent base pairs (bp). C) Schematics of the parent plasmids PL452 and PL451, from which PL452$^{EcoRI/BamHI}$ and PL452$^{EcoRI/BamHI}$ were derived, respectively. PL452 has a *neo*^{r} cassette flanked by 2 *loxP* sites, while PL451 has a *neo*^{r} cassette flanked by 2 *frt* sites, and a single *loxP* site external to the *frt* sites.

Figure 3.4

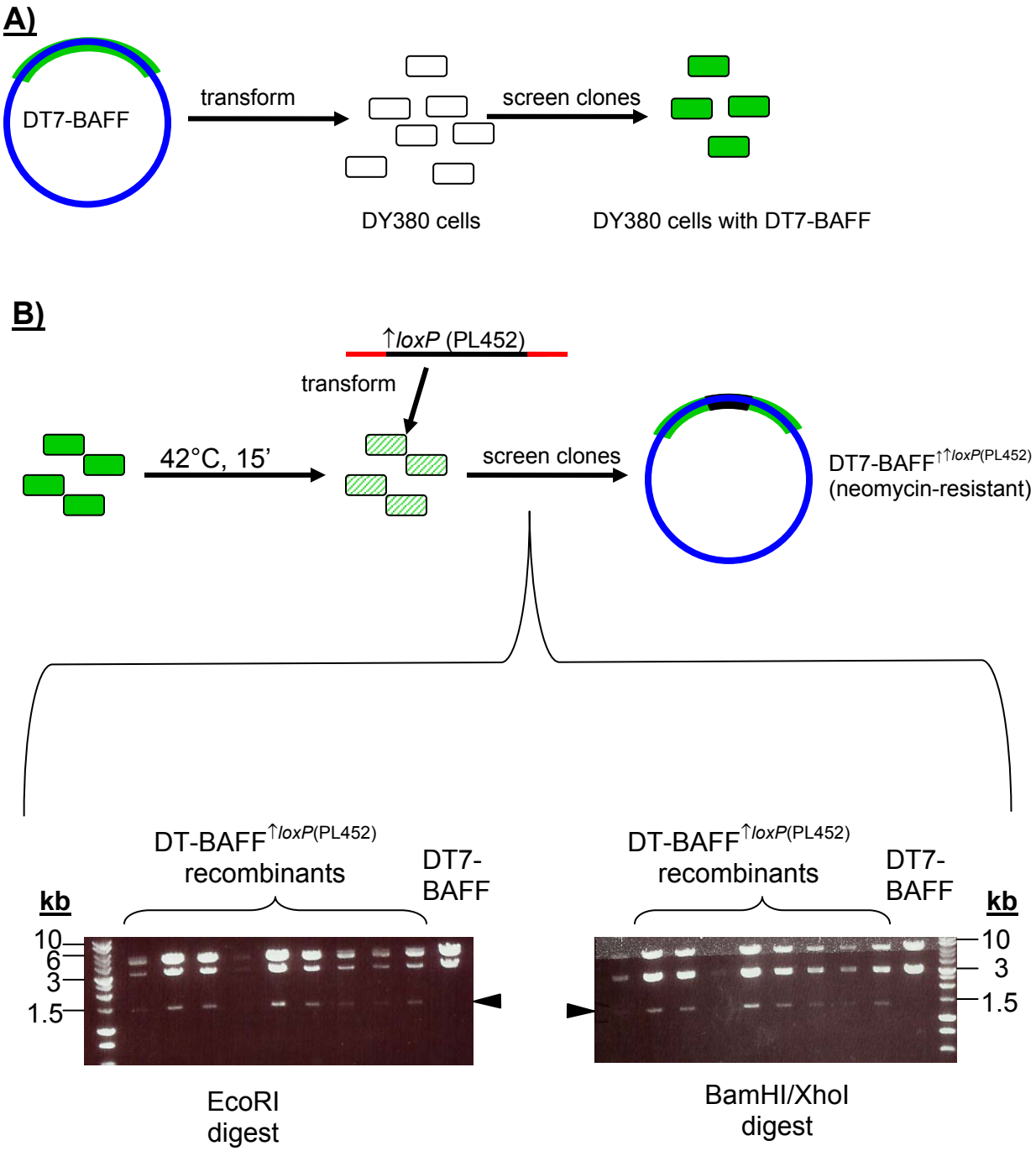
A)
DT7-BAFF
transform
screen clones
DY380 cells
DY380 cells with DT7-BAFF
B)
↑loxP (PL452)
transform
42°C, 15'
screen clones
DT7-BAFF↑↑loxP(PL452)
(neomycin-resistant)
DT-BAFF↑loxP(PL452)
recombinants
DT7-
BAFF
kb
10
6
3
1.5
EcoRI
digest
DT-BAFF↑loxP(PL452)
recombinants
DT7-
BAFF
kb
10
3
1.5
BamHI/XhoI
digest

Figure 3.4, continued

C)

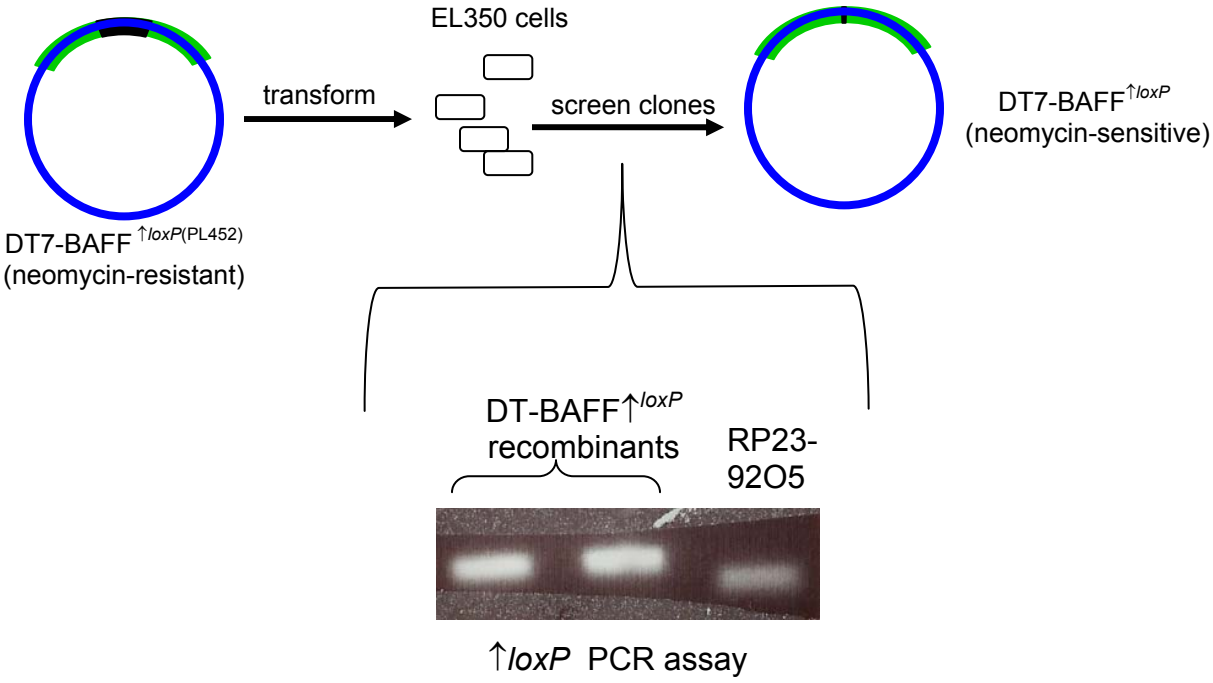

D)

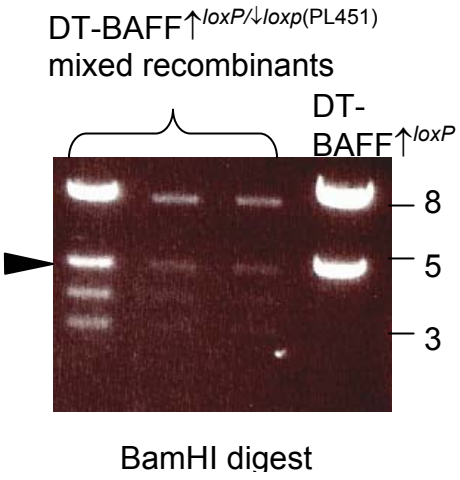

E)

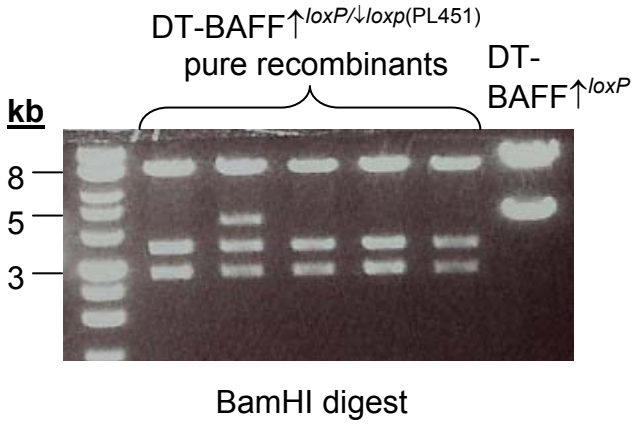

Figure 3.4, continued

Figure 3.4 *loxP* sites are introduced into DT7-BAFF by homologous recombination A) DT7-BAFF is introduced into DY380 cells by electroporation. B) Genes required for homologous recombination are induced in DT7-BAFF^{+} DY380 clones by growing at 42°C for 15 minutes. ↑*loxP*(PL452) is introduced by electroporation. Kanamycin-resistant clones are screed for proper integration of ↑*loxP*(PL452) by digest with EcoRI (*left*) or BamHI/XhoI (*right*). Bands indicative of correct placement of ↑*loxP*(PL452) are 1402 bp and 1340 bp for EcoRI or BamHI/XhoI (respectively), which were absent in the parent plasmid DT7-BAFF (arrowheads). C) The majority of PL452, including the neo^{r} cassette, is removed by Cre/*lox* recombination in EL350 cells. 92 bp of extra sequence, including a single *loxP* site, remain (↑*loxP* site). This size increase can be detected using the ↑*loxP* PCR assay. D) Step B above was repeated for ↓*loxP*(PL451). Correct placement of this piece in DT-BAFF$^{\uparrow loxP/\downarrow loxP(PL451)}$ is indicated by new bands of 2844 bp and 3562 bp in BamHI digest. However also present is a 4444 bp band (arrowhead) which should only be seen in similar digest of the parent plasmid DT-BAFF$^{\uparrow loxP}$, indicating that the colonies are not pure. E) Pure clones of DT-BAFF$^{\uparrow loxP/\downarrow loxP(PL451)}$ were obtained by transforming JM109 cells. The 4444 bp band is absent in 4 out of 5 clones digested with BamHI.

Figure 3.5

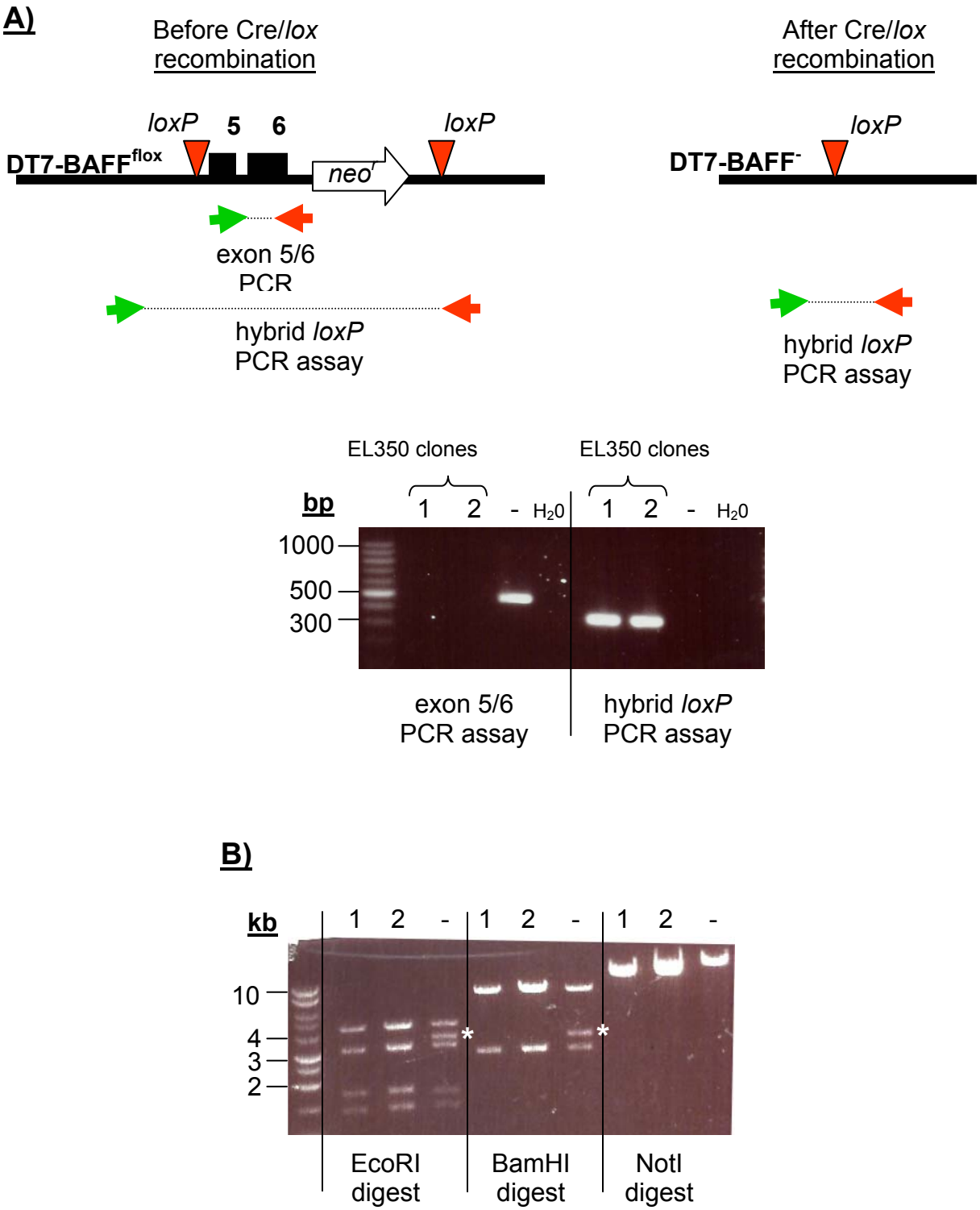
A)
Before Cre/lox recombination
After Cre/lox recombination
loxP
5
6
loxP
DT7-BAFF^flox
neo^r
loxP
DT7-BAFF^-
exon 5/6 PCR
hybrid loxP PCR assay
hybrid loxP PCR assay
EL350 clones
EL350 clones
bp
1
2
-
H20
1
2
-
H20
1000
500
300
exon 5/6 PCR assay
hybrid loxP PCR assay
B)
kb
1
2
-
1
2
-
1
2
-
10
4
3
2
*
*
EcoRI digest
BamHI digest
NotI digest

Figure 3.5, continued

Figure 3.5 *loxP* sites in DT7-BAFF^{flox} are functional A) Schematic showing the location of PCR primers for the exon 5/6 PCR assay and hybrind *loxP* PCR assay. Cre/*lox* recombination in EL350 cells eliminates the binding sites for the exon 5/6 PCR assay primers, while also bringing the hybrid *loxP* PCR assay primer binding sites in close proximity (315 bp). Shown are 2 EL350 clones that underwent successful Cre/*lox* recombination, as determined by both of these PCR assays. The parent plasmid DT7-BAFF^{flox} (-) and water template (H_20) are also included for comparison. B) The same two EL350 clones were also digested with EcoRI, BamHI*, or* NotI. The loss of 3632 bp and 3562 bp bands in the EcoRI and BamHI digests, respectively, (white *) confirms that Cre/*lox* recombination has taken place. A reduction in the size of the linearized plasmids can also be seen in the NotI digest.

Figure 3.6

A)

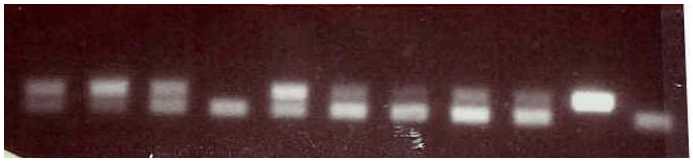

↑*loxP* PCR assay

B)

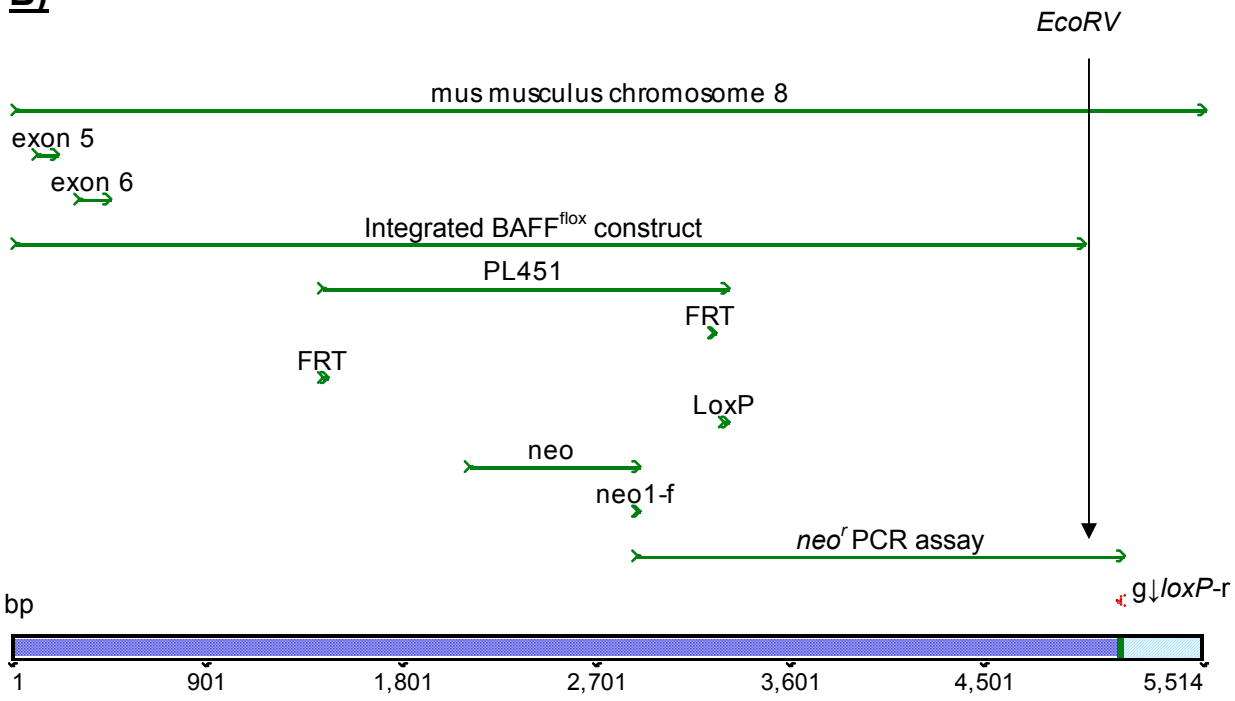

C)

*neo*ʳ PCR assay

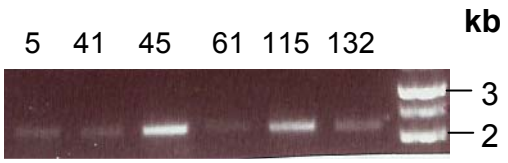

*neo*ʳ PCR assay

Figure 3.6, continued

D)

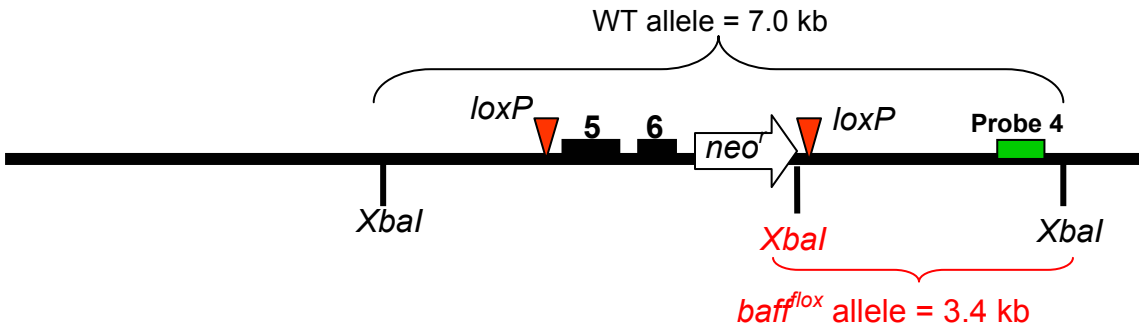

E)

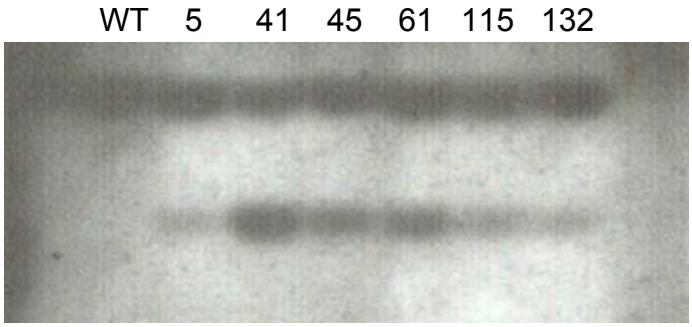

Figure 3.6 *baff*^{flox} allele is established in mouse ES cells by homologous recombination A) A sample gel showing application of the ↑*loxP* PCR assay to screen the 144 ES cell clones for presence of *baff*^{flox} allele. DT-BAFF^{flox} (+) and RP23-92O5 (-) were used as positive and negative controls, respectively. B) Schematic showing the location of primers used for the *neo*^{r} PCR assay (neo1-f and g*loxP*-r). Notice how the gloxP-r primer sits outside of the homology region covered by DT-BAFF^{flox}, the end of which is demarcated by the *EcoRV* restriction site. C). The *neo*^{r} PCR assay was used to screen only the ES clones that gave a positive result in the ↑*loxP* PCR assay. In a sample gel one positive (115) among many negative clones is shown (*left)*. The 6 positive clones (5, 41, 45, 61, 115, 132) were re-confirmed (*right*). D) Schematic showing the size bands expected from the WT and *baff*^{flox} alleles of the *baff* locus after XbaI restriction digest. The novel *XbaI* site is indicated in red. E) Southern blot confirming that the 6 ES cell clones identified by PCR are *baff*$^{flox/+}$ heterozygotes.

Figure 3.7

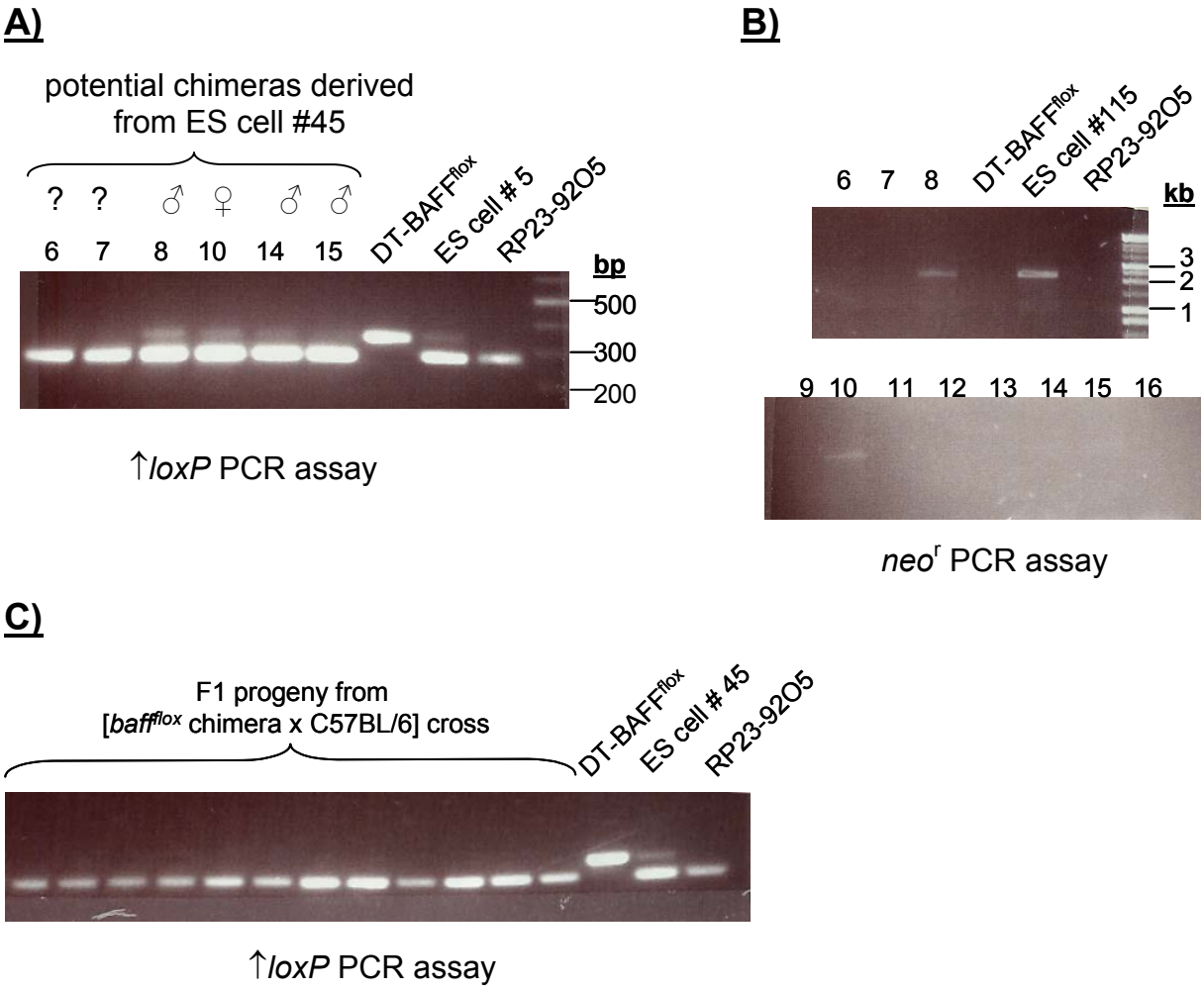

Figure 3.7 Chimeric mice did not transmit the *baff*^{flox} allele through the germline A) A sample gel of the ↑*loxP* PCR assay performed on 15 potential chimeric mice born from ES cell #45-implanted females. Pups 6 and 7 are negative, while 8, 10, 14, and 15 show varying degrees of chimerism. The gender of each pup is also shown. The vector DT-BAFF^{flox}, targeted ES cell #5, and the BAC clone RP23-92O5 are included as controls. B) Chimeras from A. were confirmed with *neo*^{r} PCR assay. Mice 14 and 15 are questionable positives. ES cell #115 is included as a positive control. C) Sample gel showing 12 of the 149 F1 progeny from the [*baff*^{flox} chimera x C57BL/6] cross screened for germline transmssion by the ↑*loxP* PCR assay.

CHAPTER 4: Discussion and Future Directions

This dissertation describes our efforts to understand what role DC play in the autoimmunity observed in *mertk*^{kd} mice. We took a "candidate mechanism" approach to this question by focusing on the production of BAFF by DC and its place in DC-B cell interactions. Our experimental observations and conclusions mostly result from *in vitro* experiments. However, an attempt to gain further insight into the consequences of BAFF production by DC *in vivo* was also undertaken by creating the DT-BAFF^{flox} targeting vector. In the future this vector can be used to make a conditional *baff*^{null} mouse which will yield a wealth of knowledge concerning the importance of BAFF in a wide range of disease models.

One of the primary conclusions from our *in vitro* work was that production of BAFF is dysregulated in DC lacking MerTK. This is an exciting result considering that, in contrast to BAFF's effects on B cells, BAFF production by any cell type has thus far been understudied. SOCS1 is the only protein that has been associated with controlling the production of BAFF by healthy (non-cancerous) cells. [206]. Now that we have established that MerTK is also involved in controlling BAFF expression future work can focus on how this is accomplished mechanistically and what involvement there is for SOCS1 in this regulation.

A surprising discovery made during this work was how strictly BAFF production is controlled in WT DC. We found that LPS and IFNγ, two inducers of BAFF by human DC, were ineffective at eliciting BAFF from mouse BMDC (Figure 2.5 A). In order to fully understand how *baff* expression is regulated finding a *baff* induction stimulus for mouse DC is critical. Immune complexes of chromatin and autoAb were found to accomplish this task[199] so it will be interesting to see how

C57BL/6 and *mertk*^{kd} BMDC compare in their response to immune complexes. Additionally, other *baff* inducers in human DC and MΦ that were not tested in our system and could be tested in the future include type I-IFNs and IL-10[130, 161, 200]. Intriguingly, we show that apoptotic cells are potent inducers of BAFF from DC in the absence of MerTK (Figure 2.5B). A plausible model is that apoptotic cells are recognized by DC via TAM family members. While Axl and Tyro3 are needed for DC phagocytosis[79], MerTK is responsible for inhibiting BAFF expression to prevent unwanted activation of autoreactive B cells.

One approach to understanding the signaling mechanism that is used by MerTK to regulate BAFF production is to consider what transcription factors control *baff* expression. Due to its established place downstream of MerTK in DC, NF-κB would seem like a good place to begin. Although NF-κB was not directly examined in this research, when considered in the context of what is known about how NF-κB relates to MerTK and BAFF, our results raise an important question. Namely, does MerTK regulation of *baff* expression take place by inhibiting NF-κB activation as has been demonstrated previously[31]? Several apparent paradoxes between our data and the published literature suggest that MerTK may regulate baff expression independently of its inhibition of NF-κB.

Roland Tisch's group has demonstrated that *mertk*^{kd} BMDC are indistinguishable from WT BMDC in there basal activation state and their ability to mature in response to LPS. Our results concur with published data on this point. What is novel, and unexpected if NF-κB activates *baff* expression, is that despite not showing evidence of a heightened activation state resting *mertk*^{kd} spDC and BMDC

produce excess BAFF compared to C57BL/6 DC (Figures 2.3 and 2.5). Thus, whereas the consequence of lacking *mertk* was previously only thought to become apparent when DC are pre-treated with apoptotic cells, our data suggests that MerTK may also function as a negative regulator of resting DC in the absence of this pre-treatment. In addition, we found that apoptotic cells, a known inhibitor of NF-κB activation in DC, further induce BAFF production by *mertk*^{kd} BMDC (Figure 2.5 B). Moreover, BAFF production was not elicited from C57BL/6 BMDC after stimulation with LPS (a known activator of NF-κB), even though they were responsive to LPS in terms of costimulatory molecule upregulation (Figure 2.5 A). So exogenous treatments that inhibit NF-κB (apoptotic cells) stimulate further BAFF production by *mertk*^{kd} BMDC, and treatments that activate NF-κB (LPS) do not stimulate BAFF production by C57BL/6 BMDC. Taken together this data suggests that BAFF production by DC may be independent of NF-κB activation.

Our finding that BAFF production was not elicited from C57BL/6 DC by LPS has also been reported in a previous study using mouse DC [199]. However, data collected from human cells stands in opposition to this finding. LPS has been shown to induce BAFF production in human DC and MΦ[130]. Furthermore, in two independent studies using reporter constructs containing putative NF-κB sites in the promoter for the human *baff* gene were shown to be functionally important[244, 245]. These pieces of empirical evidence suggest that NF-κB is in fact involved in the transcription of *baff*, at least in human cells.

To gain further insight into the discrepancies between the induction of BAFF production by mouse and human cells we decided to compare putative transcription

factor (TF)-binding sites in the *baff* promoter in both species. Rather than scanning each promoter independently for putative sites, which can generate many false positives, we turned towards a technique which restricts the search for TF-binding sites to regions of DNA which are conserved among species. Because of their persistence throughout evolution, TF-binding sites identified in this manner are more likely to be functionally important.

The free web-based tools at dcode.org were used to identify evolutionary conserved regions (ECRs) within the *baff* promoter of primates and rodents. At first we compared nearly 10 kb of upstream sequence between two primate species humans and monkey. As seen in Figure 4.1 there are several ECRs in the promoter regions between these two species. Within these ECRs several conserved TF-binding sites could be identified, including 3 putative NF-κB binding sites. Other conserved TF-bindings sites were also identified including: multiple STAT and SMAD family members, IRF-1 and -2, NFAT, AP-1, ELK and CREB. In contrast to the monkey, there was very little similarity across the same region of the human *baff* promoter when compared to that of mouse. Only one ECR was identified and it did not contain any putative NF-κB binding sites. This promoter analysis supports the premise that NF-κB may not regulate expression of the murine *baff* gene, and therefore helps to explain some of our findings such as the lack of BAFF production by LPS-stimulated C57BL/6 BMDC.

Although we did not find evolutionarily conserved NF-κB binding sites in the mouse *baff* promoter our analysis did uncover a different set of TF-binding sites that are shared by both primates and rodents. The interferon response factor (IRF)

family members IRF-1 and IRF-2, as well as the B lymphocyte-induced maturation protein (BLIMP-1), all have putative binding sites very close the 5' end of the *baff* gene transcript (Figure 4.1). These hits likely represent the same location on the *baff* promoter since all three of these TF have been shown to recognize the same canonical sequence [246]. IRF-1 and IRF-2 are involved in activating many genes in response to type I and type II interferons. IRF-1 is thought to act primarily as an activator while IRF-2 antagonizes IRF-1 by blocking its access to their shared DNA binding site [247]. BLIMP-1 is also a transcriptional repressor that has a well described role in B cell differentiation into plasma cells[248]. However BLIMP-1 is also expressed in myeloid lineage cells and functions in their differentiation as well [249, 250]. Beyond this little is known about what function BLIMP-1 has in myeloid lineage cells such as DC.

Assuming the conserved binding site for IRF-1, IRF-2 and BLIMP-1 does in fact regulate *baff* gene expression how would this fit with an increased level of BAFF production in *mertk*^{kd} DC? Since IRF-2 and BLIMP-1 are both transcriptional repressors they may be important negative regulators of *baff* expression in the resting state. In C57BL/6 DC MerTK may positively regulate the expression of these two genes, thereby keeping the *baff* gene inactive. In *mertk*^{kd} DC on the other hand, there may be a paucity of these repressors which allows IRF-1 to bind the same promoter site and drive *baff* expression. A recent report involving PI3K and BLIMP-1 in B cells suggests a potential mechanism for how MerTK may keep these repressors elevated. Recall that, upon DC engagement of apoptotic cells MerTK binds to PI3K, more specifically to the δ, but not α or β, isoform of the p110 subunit

(PI3Kδ) [31]. In B cells BLIMP-1 participates in a PI3Kδ-dependent pathway that inhibits Ig class switching [251], indicating that a functional association exists between these two proteins. A plausible model for *baff* regulation therefore may be that, in DC, recruitment of PI3Kδ by MerTK increases BLIMP-1 function (probably via increasing its transcription), which in turn represses *baff* gene transcription by binding to the site identified in Figure 4.1. However, p110δ was only found to bind MerTK following apoptotic cell treatment of DC [31], suggesting that the elevated BAFF produced by unstimulated *mertk*^{kd} DC is not due to a lack of PI3Kδ activation by MerTK. An alternative possibility is that a low burden of apoptotic cells from the expected amount of cell death *in vitro* provides a much smaller, and undetectable, association between MerTK and PI3K. This tonic signaling could be sufficient to mediate the repression of BAFF production that is seen in C57BL/6 BMDC, and absent from *mertk*^{kd} DC. Future experimentation to advance this model should include: validating the putative IRF-1/IRF-2/BLIMP-1 binding site with reporter constructs or chromatin immunoprecipitation, comparing the relative levels of IRF-1, IRF-2, and BLIMP-1 in C57BL/6 and *mertk*^{kd} DC, genetic or pharmacologic inhibition of PI3K, and using the *prdm1*^{flox} mouse [248] to generate DC lacking BLIMP-1 (*prdm1* gene codes for BLIMP-1 protein).

BAFF is a pro-survival factor for B cells, both *in vivo* and in culture. We thought it was prudent, therefore, to see if higher BAFF production by *mertk*^{kd} DC translated into better survival for neighboring B cells. From these experiments we can draw three conclusions: 1) DC augment the survival of resting B cells *in vitro,* 2) MerTK does not influence the outcome of this phenomenon, and 3) it takes place

independently of BAFF production by DC. In contrast to numerous studies of activation metrics after stimulation of Ag-specific B cells by Ag-loaded DC, the survival of resting B cells after culture with DC has never been directly measured. To our knowledge the demonstration of a pro- survival effect on B cells by DC is novel. Although further work is needed to determine what, if any, importance this has *in vivo*, at a minimum it deserves consideration when interpreting other DC-B cell coculture data.

The finding that *mertk*^{kd} DC do not provide better survival support to B cells is unexpected but is in agreement with the lack of a need for BAFF production by DC in this process (Figure 2.7). It suggests that DC enhancement of B cell survival is not a pivotal event in the autoimmuninty seen in *mertk*^{kd} mice. However, DC may still be participants in the breach of tolerance by B cells in these mice. This could occur through the collection and display of Ag by DC or indirectly by the activation of autoreactive CD4^{+} T cells which eventually provide CD40L to B cells. Unlike stromal cell-derived BAFF, which is copious enough to be detected systemically *in vivo*, DC-derived BAFF probably has a much smaller range of action and isn't needed to maintain the B cell numbers in the steady-state [198]. Therefore provision of BAFF to B cells by DC may only be important and moreover, only take place, during responses to foreign- or self-Ag. Non-constitutive BAFF production by DC is exemplified by the lack of BAFF made *ex vivo* by C57BL/6 spDC (Figures 2.5). DC have been shown to drive Ag-specific B cells to differentiate into plasmablasts via a BAFF (or APRIL)-dependent mechanism [23]. Therefore, it is plausible that *mertk*^{kd} DC may perform this task better than C57BL/6 or *baff*$^{-/-}$ DC since they produce BAFF

constitutively. Efforts were made to establish an *in vitro* system in which in the stimulation of self-Ag (Sm) specific 2-12Tg B cells by apoptotic cell-fed C57BL/6, *mertk*^{kd}, and *baff* DC could be compared. Results from these experiments are too preliminary to draw conclusions from but future work on this topic should be yield valuable information regarding the ability of DC to break autoreactive B cell tolerance mechanisms.

Alternatively, it is possible that DC do not participate in, or at least do not impact the outcome of, autoimmunity in *mertk*^{kd} mice. The disease process in *mertk*^{kd} mice could simply be due to an abundance of self-Ag due to poor apoptotic cell clearance. This, deficit, however is not apparent in resting *mertk*^{kd} mice, only being observed following a challenge with extraordinary burdens of apoptotic cells [117, 122]. However, these studies were done in younger mice, which likely had negative or low autoAb levels. A rigorous quantification of apoptotic cell numbers generated spontaneously in aging *mertk*^{kd} mice will need to be undertaken to see if a clearance deficit becomes observable later in life when autoAb levels are high.

To fully understand if DC are playing a role in autoimmune *mertk*^{kd} mice a more acute model of autoAb induction will have to be established. The slow, prolonged, and not fully penetrant, autoAb phenotype in *mertk*^{kd} mice makes understanding specific biological events difficult. If autoAb production could be initiated acutely and to a similar degree in all *mertk*^{kd} mice at a desired time, then asking questions about progression towards autoimmunity *in vivo* becomes much more feasible. An attempt to initiate acute autoAb production by injecting young *mertk*^{kd} mice with apoptotic cells was unsuccessful [122]. Future efforts should be

directed towards optimizing this protocol or looking for other means of inducing autoAb acutely. Once an acute model is established the role of DC can be addressed using *cd11c*-DTR mice [252]. These mice express the receptor for *Diptheria* toxin under the control of the *cd11c* gene promoter. When the toxin is administered *in vivo* $CD11c^+$ cells are selectively eliminated. The effect is transient (days) due to toxicity, so having an acute model of autoimmunity is critical.

The phenotype of a lupus-like disease in $mertk^{kd}$ mice raises the question of whether or not MerTK has any involvement in SLE. Due to its highly polygenic nature a lot of research effort has been invested in understanding the genetics of SLE [207, 208]. Althogh the *mertk* gene itself has not been specifically associated with SLE it does lie close (10-30 MB) to markers on human and murine chromosome 2 showing linkages to both SLE and disease in the (NZBxNZW)F1 mouse model, respectively [208, 253, 254]. However these regions contain multiple genes other than *mertk*, some of which are located closer to the genetic markers than *mertk*, such as IL-1, which could be responsible for the linkage.

When *mertk* itself was searched for single nucleotide polymorphisms (SNP) associated with SLE no linkage meeting statistical significance was found. However the authors did uncover a significant association between several SNPs and a decreased risk for leukopenia and lymphopenia among SLE patients [255]. One of these SNPs results in a R→K substitution in one of the fibronectin type III domains. It is unclear what, if any, functional significance this substitution has at the molecular level, nor how it might impact white blood cell counts in SLE patients. Given its association with retinitis pigmentosa [118, 119], the chances of finding additional

evidence of a genetic association between *mertk* and SLE may be improved by focusing on patients with ocular problems. To summarize, although it is premature to label *mertk* as an SLE-associated gene, it does have the potential to be given its proximity to genetic markers on chromosome 2. At a minimum, it is safe to say that polymorphisms in *mertk* have the potential to impact certain facets of the disease such lymphopenia.

We set out to test the hypothesis that MerTK functions as a negative regulator of DC function, such that it impacts the outcome of interactions between DC and B cells. The conclusions reached by these experiments only partially support this hypothesis. Our finding that DC from *mertk*^{kd} mice constitutively produce BAFF supports this hypothesis in that the lack of *mertk* causes an increase in a DC function. BAFF is a potent B cell tropic cytokine with a well-documented ability to induce autoimmunity when produced in excess. Therefore, elevated BAFF production by *mertk*^{kd} DC provides a mechanistic explanation for how DC might potentially impact B cell autoimminity. The conclusions reached form our coculture experiments, however, have led us to refute the hypothesis that MerTK impacts DC-B cell interactions, at least in terms of resting B cell survival. This was the likely outcome since the pro-survival benefit that DC provide to B cells was found to be BAFF-independent. Thus, the assay we had developed was not sensitive to elevated BAFF production by BMDC. However, these results leave open the possibility that the importance of MerTK and BAFF become more apparent in experiments where DC initiate B cell responses by delivering cognate antigen.

Figure 4.1

A)

Human vs. monkey *baff* promoter region

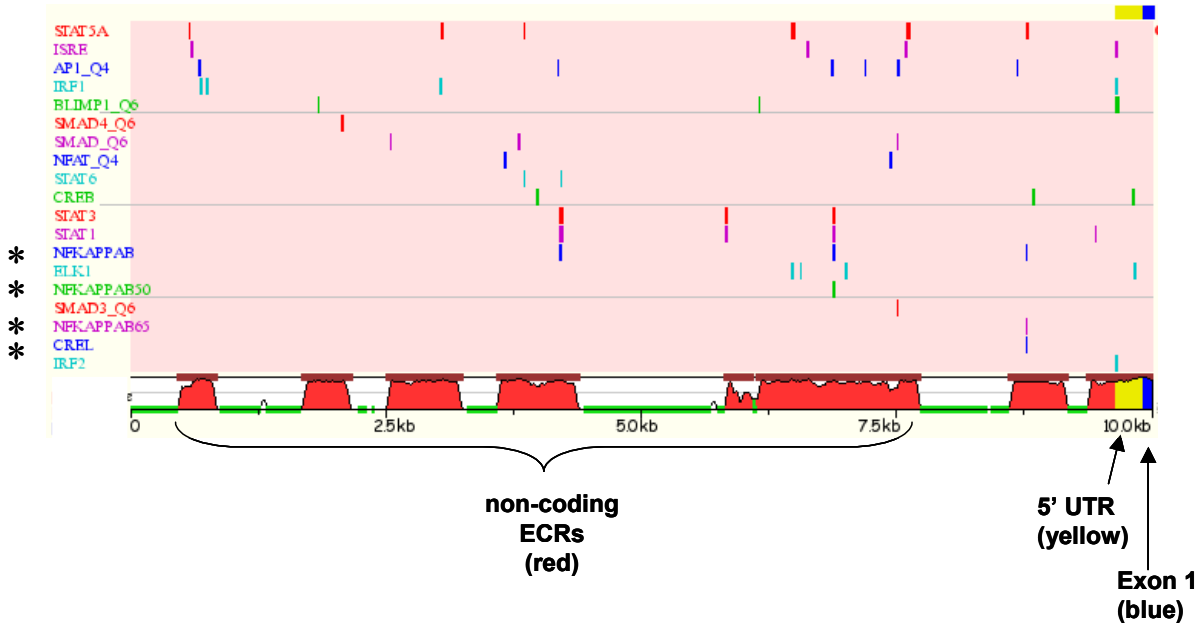

B)

Human vs. mouse *baff* promoter region

C)

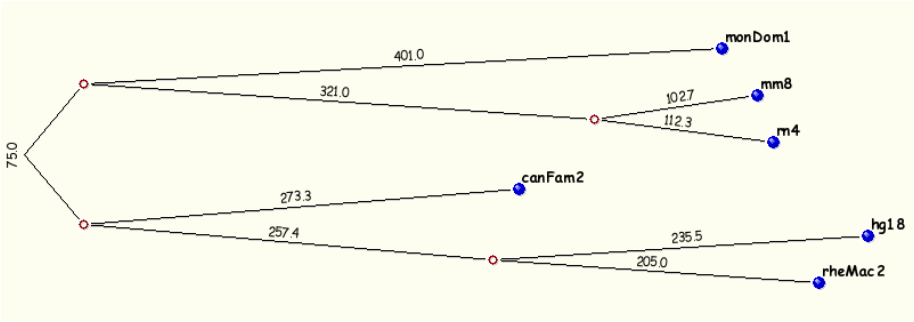

Figure 4.1, continued

Figure 4.1 NF-κB binding sites are found in the primate, but not mouse, *baff* gene promoter Comparative analysis for shared transcription factor (TF) binding sites between the human and rhesus monkey (A), or human and mouse (B) *baff* gene promoters. 10 kb were scanned including the 5' UTR and first exon of the baff gene, which are highlighted in A. The search for *cis*-regulatory elements was restricted to regions of strong sequence homology between species in non-coding DNA. These are referred to as ECRs (evolutionary conserved regions) and are highlighted in red. A list of "immune related" TF binding sites that were identified are listed on the left side of schematic, while there positions in the sequence are indicated by the similarly colored bars. Identified NF-κB binding sites are highlighted (*). These TF binding sites were not identified in the mouse *baff* promoter. C) The phylogentic relationship of six different mammals as determined by the same 10 kb region. This analysis and these graphics were produced using web-based ECR browser tools at http://www.dcode.org [256].

References

1. Janeway C., T.P., *Immunobiology. The Immune System in Health and Disease*. 3 ed. 1997, London, New York: Current Biology Ltd., Garland Publishing Inc.

2. Casola, S., *Control of peripheral B-cell development.* Curr Opin Immunol, 2007. **19**(2): p. 143-9.

3. Martin, F. and J.F. Kearney, *Marginal-zone B cells.* Nat Rev Immunol, 2002. **2**(5): p. 323-35.

4. Wang, H. and S.H. Clarke, *Regulation of B-cell development by antibody specificity.* Curr Opin Immunol, 2004. **16**(2): p. 246-50.

5. Rubin E., F.J., *Pathology*. 3rd ed. 1999, Philadelphia, PA: Lippincott-Raven.

6. Shortman, K. and Y.J. Liu, *Mouse and human dendritic cell subtypes.* Nat Rev Immunol, 2002. **2**(3): p. 151-61.

7. Shortman, K. and S.H. Naik, *Steady-state and inflammatory dendritic-cell development.* Nat Rev Immunol, 2007. **7**(1): p. 19-30.

8. Fogg, D.K., et al., *A clonogenic bone marrow progenitor specific for macrophages and dendritic cells.* Science, 2006. **311**(5757): p. 83-7.

9. Geissmann, F., *The origin of dendritic cells.* Nat Immunol, 2007. **8**(6): p. 558-60.

10. Ardavin, C., *Origin, precursors and differentiation of mouse dendritic cells.* Nat Rev Immunol, 2003. **3**(7): p. 582-90.

11. Liu, K., et al., *Origin of dendritic cells in peripheral lymphoid organs of mice.* Nat Immunol, 2007. **8**(6): p. 578-83.

12. Naik, S.H., et al., *Intrasplenic steady-state dendritic cell precursors that are distinct from monocytes.* Nat Immunol, 2006. **7**(6): p. 663-71.

13. Banchereau, J. and R.M. Steinman, *Dendritic cells and the control of immunity.* Nature, 1998. **392**(6673): p. 245-52.

14. Villadangos, J.A. and W.R. Heath, *Life cycle, migration and antigen presenting functions of spleen and lymph node dendritic cells: limitations of the Langerhans cells paradigm.* Semin Immunol, 2005. **17**(4): p. 262-72.

15. Reis e Sousa, C., *Toll-like receptors and dendritic cells: for whom the bug tolls.* Semin Immunol, 2004. **16**(1): p. 27-34.

16. Iwasaki, A. and R. Medzhitov, *Toll-like receptor control of the adaptive immune responses.* Nat Immunol, 2004. **5**(10): p. 987-95.

17. Reis e Sousa, C., *Dendritic cells in a mature age.* Nat Rev Immunol, 2006. **6**(6): p. 476-83.

18. Bretscher, P.A., *A two-step, two-signal model for the primary activation of precursor helper T cells.* Proc Natl Acad Sci U S A, 1999. **96**(1): p. 185-90.

19. Sharpe, A.H. and G.J. Freeman, *The B7-CD28 superfamily.* Nat Rev Immunol, 2002. **2**(2): p. 116-26.

20. Bergtold, A., et al., *Cell surface recycling of internalized antigen permits dendritic cell priming of B cells.* Immunity, 2005. **23**(5): p. 503-14.

21. Qi, H., et al., *Extrafollicular activation of lymph node B cells by antigen-bearing dendritic cells.* Science, 2006. **312**(5780): p. 1672-6.

22. Huang, N.N., et al., *B cells productively engage soluble antigen-pulsed dendritic cells: visualization of live-cell dynamics of B cell-dendritic cell interactions.* J Immunol, 2005. **175**(11): p. 7125-34.

23. Balazs, M., et al., *Blood dendritic cells interact with splenic marginal zone B cells to initiate T-independent immune responses.* Immunity, 2002. **17**(3): p. 341-52.

24. Wykes, M., et al., *Dendritic cells interact directly with naive B lymphocytes to transfer antigen and initiate class switching in a primary T-dependent response.* J Immunol, 1998. **161**(3): p. 1313-9.

25. Xu, W., et al., *Dendritic cell and macrophage subsets in the handling of dying cells.* Immunobiology, 2006. **211**(6-8): p. 567-75.

26. Scheinecker, C., et al., *Constitutive presentation of a natural tissue autoantigen exclusively by dendritic cells in the draining lymph node.* J Exp Med, 2002. **196**(8): p. 1079-90.

27. Steinman, R.M., et al., *The induction of tolerance by dendritic cells that have captured apoptotic cells.* J Exp Med, 2000. **191**(3): p. 411-6.

28. Albert, M.L., et al., *Immature dendritic cells phagocytose apoptotic cells via alphavbeta5 and CD36, and cross-present antigens to cytotoxic T lymphocytes.* J Exp Med, 1998. **188**(7): p. 1359-68.

29. Sauter, B., et al., *Consequences of cell death: exposure to necrotic tumor cells, but not primary tissue cells or apoptotic cells, induces the maturation of immunostimulatory dendritic cells.* J Exp Med, 2000. **191**(3): p. 423-34.

30. Stuart, L.M., et al., *Inhibitory effects of apoptotic cell ingestion upon endotoxin-driven myeloid dendritic cell maturation.* J Immunol, 2002. **168**(4): p. 1627-35.

31. Sen, P., et al., *Apoptotic cells induce Mer tyrosine kinase-dependent blockade of NF-kappaB activation in dendritic cells.* Blood, 2007. **109**(2): p. 653-60.

32. Chen, X., et al., *Phosphatidylserine regulates the maturation of human dendritic cells.* J Immunol, 2004. **173**(5): p. 2985-94.

33. Ip, W.K. and Y.L. Lau, *Distinct maturation of, but not migration between, human monocyte-derived dendritic cells upon ingestion of apoptotic cells of early or late phases.* J Immunol, 2004. **173**(1): p. 189-96.

34. Frisoni, L., et al., *Nuclear autoantigen translocation and autoantibody opsonization lead to increased dendritic cell phagocytosis and presentation of*

nuclear antigens: a novel pathogenic pathway for autoimmunity? J Immunol, 2005. **175**(4): p. 2692-701.

35. Inaba, K., et al., *Efficient presentation of phagocytosed cellular fragments on the major histocompatibility complex class II products of dendritic cells.* J Exp Med, 1998. **188**(11): p. 2163-73.

36. Iyoda, T., et al., *The CD8+ dendritic cell subset selectively endocytoses dying cells in culture and in vivo.* J Exp Med, 2002. **195**(10): p. 1289-302.

37. Liu, K., et al., *Immune tolerance after delivery of dying cells to dendritic cells in situ.* J Exp Med, 2002. **196**(8): p. 1091-7.

38. Blander, J.M. and R. Medzhitov, *Toll-dependent selection of microbial antigens for presentation by dendritic cells.* Nature, 2006. **440**(7085): p. 808-12.

39. Emanuel Rubin, J.L.F., *Pathology*. 3rd ed. 1999, Philadelphia, PA: Lippincott-Raven.

40. Klippel, J., *Primer on the Rheumatic Diseases*. 12 ed. 2001, Atlanta, GA: The Arthritis Foundation.

41. Trager, J. and M.M. Ward, *Mortality and causes of death in systemic lupus erythematosus.* Curr Opin Rheumatol, 2001. **13**(5): p. 345-51.

42. Riemekasten, G. and B.H. Hahn, *Key autoantigens in SLE.* Rheumatology (Oxford), 2005. **44**(8): p. 975-82.

43. Kerr, J.F., A.H. Wyllie, and A.R. Currie, *Apoptosis: a basic biological phenomenon with wide-ranging implications in tissue kinetics.* Br J Cancer, 1972. **26**(4): p. 239-57.

44. Vaux, D.L. and S.J. Korsmeyer, *Cell death in development.* Cell, 1999. **96**(2): p. 245-54.

45. Casciola-Rosen, L.A., G. Anhalt, and A. Rosen, *Autoantigens targeted in systemic lupus erythematosus are clustered in two populations of surface structures on apoptotic keratinocytes.* J Exp Med, 1994. **179**(4): p. 1317-30.

46. Cocca, B.A., A.M. Cline, and M.Z. Radic, *Blebs and apoptotic bodies are B cell autoantigens.* J Immunol, 2002. **169**(1): p. 159-66.

47. Mevorach, D., et al., *Systemic exposure to irradiated apoptotic cells induces autoantibody production.* J Exp Med, 1998. **188**(2): p. 387-92.

48. Radic, M., T. Marion, and M. Monestier, *Nucleosomes are exposed at the cell surface in apoptosis.* J Immunol, 2004. **172**(11): p. 6692-700.

49. Qian, Y., H. Wang, and S.H. Clarke, *Impaired clearance of apoptotic cells induces the activation of autoreactive anti-Sm marginal zone and B-1 B cells.* J Immunol, 2004. **172**(1): p. 625-35.

50. Caricchio, R., L. McPhie, and P.L. Cohen, *Ultraviolet B radiation-induced cell death: critical role of ultraviolet dose in inflammation and lupus autoantigen redistribution.* J Immunol, 2003. **171**(11): p. 5778-86.

51. Jevnikar, A.M., M.J. Grusby, and L.H. Glimcher, *Prevention of nephritis in major histocompatibility complex class II-deficient MRL-lpr mice.* J Exp Med, 1994. **179**(4): p. 1137-43.

52. Steinberg, A.D., et al., *Effects of thymectomy or androgen administration upon the autoimmune disease of MRL/Mp-lpr/lpr mice.* J Immunol, 1980. **125**(2): p. 871-3.

53. Wofsy, D., et al., *Treatment of murine lupus with monoclonal anti-T cell antibody.* J Immunol, 1985. **134**(2): p. 852-7.

54. Kaliyaperumal, A., et al., *Nucleosomal peptide epitopes for nephritis-inducing T helper cells of murine lupus.* J Exp Med, 1996. **183**(6): p. 2459-69.

55. Lu, L., et al., *Major peptide autoepitopes for nucleosome-specific T cells of human lupus.* J Clin Invest, 1999. **104**(3): p. 345-55.

56. Riemekasten, G., et al., *Identification and characterization of SmD183-119-reactive T cells that provide T cell help for pathogenic anti-double-stranded DNA antibodies.* Arthritis Rheum, 2003. **48**(2): p. 475-85.

57. Riemekasten, G., et al., *T cell reactivity against the SmD1(83-119) C terminal peptide in patients with systemic lupus erythematosus.* Ann Rheum Dis, 2002. **61**(9): p. 779-85.

58. Burlingame, R.W., et al., *Genesis and evolution of antichromatin autoantibodies in murine lupus implicates T-dependent immunization with self antigen.* J Clin Invest, 1993. **91**(4): p. 1687-96.

59. Graham, D.K., et al., *Cloning and developmental expression analysis of the murine c-mer tyrosine kinase.* Oncogene, 1995. **10**(12): p. 2349-59.

60. O'Bryan, J.P., et al., *axl, a transforming gene isolated from primary human myeloid leukemia cells, encodes a novel receptor tyrosine kinase.* Mol Cell Biol, 1991. **11**(10): p. 5016-31.

61. Budagian, V., et al., *Soluble Axl is generated by ADAM10-dependent cleavage and associates with Gas6 in mouse serum.* Mol Cell Biol, 2005. **25**(21): p. 9324-39.

62. Sather, S., et al., *A soluble form of the Mer receptor tyrosine kinase inhibits macrophage clearance of apoptotic cells and platelet aggregation.* Blood, 2007. **109**(3): p. 1026-33.

63. Graham, D.K., et al., *Cloning and mRNA expression analysis of a novel human protooncogene, c-mer.* Cell Growth Differ, 1994. **5**(6): p. 647-57.

64. Chen, C., et al., *Mer receptor tyrosine kinase signaling participates in platelet function.* Arterioscler Thromb Vasc Biol, 2004. **24**(6): p. 1118-23.

65. Prasad, D., et al., *TAM receptor function in the retinal pigment epithelium.* Mol Cell Neurosci, 2006. **33**(1): p. 96-108.

66. Behrens, E.M., et al., *The mer receptor tyrosine kinase: expression and function suggest a role in innate immunity.* Eur J Immunol, 2003. **33**(8): p. 2160-7.

67. Caraux, A., et al., *Natural killer cell differentiation driven by Tyro3 receptor tyrosine kinases.* Nat Immunol, 2006. **7**(7): p. 747-54.

68. Graham, D.K., et al., *Ectopic expression of the proto-oncogene Mer in pediatric T-cell acute lymphoblastic leukemia.* Clin Cancer Res, 2006. **12**(9): p. 2662-9.

69. Yeoh, E.J., et al., *Classification, subtype discovery, and prediction of outcome in pediatric acute lymphoblastic leukemia by gene expression profiling.* Cancer Cell, 2002. **1**(2): p. 133-43.

70. Lu, Q. and G. Lemke, *Homeostatic regulation of the immune system by receptor tyrosine kinases of the Tyro 3 family.* Science, 2001. **293**(5528): p. 306-11.

71. Schlessinger, J., *Cell signaling by receptor tyrosine kinases.* Cell, 2000. **103**(2): p. 211-25.

72. Chen, J., K. Carey, and P.J. Godowski, *Identification of Gas6 as a ligand for Mer, a neural cell adhesion molecule related receptor tyrosine kinase implicated in cellular transformation.* Oncogene, 1997. **14**(17): p. 2033-9.

73. Nagata, K., et al., *Identification of the product of growth arrest-specific gene 6 as a common ligand for Axl, Sky, and Mer receptor tyrosine kinases.* J Biol Chem, 1996. **271**(47): p. 30022-7.

74. Godowski, P.J., et al., *Reevaluation of the roles of protein S and Gas6 as ligands for the receptor tyrosine kinase Rse/Tyro 3.* Cell, 1995. **82**(3): p. 355-8.

75. Ohashi, K., et al., *Stimulation of sky receptor tyrosine kinase by the product of growth arrest-specific gene 6.* J Biol Chem, 1995. **270**(39): p. 22681-4.

76. Stitt, T.N., et al., *The anticoagulation factor protein S and its relative, Gas6, are ligands for the Tyro 3/Axl family of receptor tyrosine kinases.* Cell, 1995. **80**(4): p. 661-70.

77. Varnum, B.C., et al., *Axl receptor tyrosine kinase stimulated by the vitamin K-dependent protein encoded by growth-arrest-specific gene 6.* Nature, 1995. **373**(6515): p. 623-6.

78. Manfioletti, G., et al., *The protein encoded by a growth arrest-specific gene (gas6) is a new member of the vitamin K-dependent proteins related to protein S, a negative coregulator in the blood coagulation cascade.* Mol Cell Biol, 1993. **13**(8): p. 4976-85.

79. Seitz, H.M., et al., *Macrophages and dendritic cells use different axl/mertk/tyro3 receptors in clearance of apoptotic cells.* J Immunol, 2007. **178**(9): p. 5635-42.

80. Hafizi, S. and B. Dahlback, *Gas6 and protein S. Vitamin K-dependent ligands for the Axl receptor tyrosine kinase subfamily.* Febs J, 2006. **273**(23): p. 5231-44.

81. Sasaki, T., et al., *Structural basis for Gas6-Axl signalling.* Embo J, 2006. **25**(1): p. 80-7.

82. Tanabe, K., et al., *Roles of gamma-carboxylation and a sex hormone-binding globulin-like domain in receptor-binding and in biological activities of Gas6.* FEBS Lett, 1997. **408**(3): p. 306-10.

83. Sasaki, T., et al., *Crystal structure of a C-terminal fragment of growth arrest-specific protein Gas6. Receptor tyrosine kinase activation by laminin G-like domains.* J Biol Chem, 2002. **277**(46): p. 44164-70.

84. Hasanbasic, I., I. Rajotte, and M. Blostein, *The role of gamma-carboxylation in the anti-apoptotic function of gas6.* J Thromb Haemost, 2005. **3**(12): p. 2790-7.

85. Nakano, T., et al., *Cell adhesion to phosphatidylserine mediated by a product of growth arrest-specific gene 6.* J Biol Chem, 1997. **272**(47): p. 29411-4.

86. Furie, B. and B.C. Furie, *The molecular basis of blood coagulation.* Cell, 1988. **53**(4): p. 505-18.

87. Lemke, G. and Q. Lu, *Macrophage regulation by Tyro 3 family receptors.* Curr Opin Immunol, 2003. **15**(1): p. 31-6.

88. Ling, L. and H.J. Kung, *Mitogenic signals and transforming potential of Nyk, a newly identified neural cell adhesion molecule-related receptor tyrosine kinase.* Mol Cell Biol, 1995. **15**(12): p. 6582-92.

89. Ling, L., D. Templeton, and H.J. Kung, *Identification of the major autophosphorylation sites of Nyk/Mer, an NCAM-related receptor tyrosine kinase.* J Biol Chem, 1996. **271**(31): p. 18355-62.

90. Guttridge, K.L., et al., *Mer receptor tyrosine kinase signaling: prevention of apoptosis and alteration of cytoskeletal architecture without stimulation or proliferation.* J Biol Chem, 2002. **277**(27): p. 24057-66.

91. Georgescu, M.M., et al., *Biological effects of c-Mer receptor tyrosine kinase in hematopoietic cells depend on the Grb2 binding site in the receptor and activation of NF-kappaB.* Mol Cell Biol, 1999. **19**(2): p. 1171-81.

92. Mahajan, N.P. and H.S. Earp, *An SH2 domain-dependent, phosphotyrosine-independent interaction between Vav1 and the Mer receptor tyrosine kinase: a mechanism for localizing guanine nucleotide-exchange factor action.* J Biol Chem, 2003. **278**(43): p. 42596-603.

93. Chimini, G. and P. Chavrier, *Function of Rho family proteins in actin dynamics during phagocytosis and engulfment.* Nat Cell Biol, 2000. **2**(10): p. E191-6.

94. Manetz, T.S., et al., *Vav1 regulates phospholipase cgamma activation and calcium responses in mast cells.* Mol Cell Biol, 2001. **21**(11): p. 3763-74.

95. Todt, J.C., B. Hu, and J.L. Curtis, *The receptor tyrosine kinase MerTK activates phospholipase C gamma2 during recognition of apoptotic thymocytes by murine macrophages.* J Leukoc Biol, 2004. **75**(4): p. 705-13.

96. Rebecchi, M.J. and S.N. Pentyala, *Structure, function, and control of phosphoinositide-specific phospholipase C.* Physiol Rev, 2000. **80**(4): p. 1291-335.

97. Wu, Y., et al., *A role for Mer tyrosine kinase in alphavbeta5 integrin-mediated phagocytosis of apoptotic cells.* J Cell Sci, 2005. **118**(Pt 3): p. 539-53.

98. Albert, M.L., J.I. Kim, and R.B. Birge, *alphavbeta5 integrin recruits the CrkII-Dock180-rac1 complex for phagocytosis of apoptotic cells.* Nat Cell Biol, 2000. **2**(12): p. 899-905.

99. Finnemann, S.C. and E.F. Nandrot, *MerTK activation during RPE phagocytosis in vivo requires alphaVbeta5 integrin.* Adv Exp Med Biol, 2006. **572**: p. 499-503.

100. Bonizzi, G. and M. Karin, *The two NF-kappaB activation pathways and their role in innate and adaptive immunity.* Trends Immunol, 2004. **25**(6): p. 280-8.

101. Camenisch, T.D., et al., *A novel receptor tyrosine kinase, Mer, inhibits TNF-alpha production and lipopolysaccharide-induced endotoxic shock.* J Immunol, 1999. **162**(6): p. 3498-503.

102. Sosic, D., et al., *Twist regulates cytokine gene expression through a negative feedback loop that represses NF-kappaB activity.* Cell, 2003. **112**(2): p. 169-80.

103. Sharif, M.N., et al., *Twist mediates suppression of inflammation by type I IFNs and Axl.* J Exp Med, 2006. **203**(8): p. 1891-901.

104. Hu, B., et al., *Recognition and phagocytosis of apoptotic T cells by resident murine tissue macrophages require multiple signal transduction events.* J Leukoc Biol, 2002. **71**(5): p. 881-9.

105. Leverrier, Y. and A.J. Ridley, *Requirement for Rho GTPases and PI 3-kinases during apoptotic cell phagocytosis by macrophages.* Curr Biol, 2001. **11**(3): p. 195-9.

106. Fukao, T., et al., *PI3K-mediated negative feedback regulation of IL-12 production in DCs.* Nat Immunol, 2002. **3**(9): p. 875-81.

107. Agrawal, A., et al., *Altered innate immune functioning of dendritic cells in elderly humans: a role of phosphoinositide 3-kinase-signaling pathway.* J Immunol, 2007. **178**(11): p. 6912-22.

108. Leverrier, Y., et al., *Class I phosphoinositide 3-kinase p110beta is required for apoptotic cell and Fcgamma receptor-mediated phagocytosis by macrophages.* J Biol Chem, 2003. **278**(40): p. 38437-42.

109. Mark Wallet and R. Tisch, *Personal Communication*.

110. Lu, Q., et al., *Tyro-3 family receptors are essential regulators of mammalian spermatogenesis.* Nature, 1999. **398**(6729): p. 723-8.

111. Dowling, J.E. and R.L. Sidman, *Inherited retinal dystrophy in the rat.* J Cell Biol, 1962. **14**: p. 73-109.

112. Mullen, R.J. and M.M. LaVail, *Inherited retinal dystrophy: primary defect in pigment epithelium determined with experimental rat chimeras.* Science, 1976. **192**(4241): p. 799-801.

113. D'Cruz, P.M., et al., *Mutation of the receptor tyrosine kinase gene Mertk in the retinal dystrophic RCS rat.* Hum Mol Genet, 2000. **9**(4): p. 645-51.

114. Nandrot, E., et al., *Homozygous deletion in the coding sequence of the c-mer gene in RCS rats unravels general mechanisms of physiological cell adhesion and apoptosis.* Neurobiol Dis, 2000. **7**(6 Pt B): p. 586-99.

115. Vollrath, D., et al., *Correction of the retinal dystrophy phenotype of the RCS rat by viral gene transfer of Mertk.* Proc Natl Acad Sci U S A, 2001. **98**(22): p. 12584-9.

116. Duncan, J.L., et al., *An RCS-like retinal dystrophy phenotype in mer knockout mice.* Invest Ophthalmol Vis Sci, 2003. **44**(2): p. 826-38.

117. Scott, R.S., et al., *Phagocytosis and clearance of apoptotic cells is mediated by MER.* Nature, 2001. **411**(6834): p. 207-11.

118. Gal, A., et al., *Mutations in MERTK, the human orthologue of the RCS rat retinal dystrophy gene, cause retinitis pigmentosa.* Nat Genet, 2000. **26**(3): p. 270-1.

119. Tschernutter, M., et al., *Clinical characterisation of a family with retinal dystrophy caused by mutation in the Mertk gene.* Br J Ophthalmol, 2006. **90**(6): p. 718-23.

120. Bijl, M., P.C. Limburg, and C.G. Kallenberg, *New insights into the pathogenesis of systemic lupus erythematosus (SLE): the role of apoptosis.* Neth J Med, 2001. **59**(2): p. 66-75.

121. Mebius, R.E. and G. Kraal, *Structure and function of the spleen.* Nat Rev Immunol, 2005. **5**(8): p. 606-16.

122. Cohen, P.L., et al., *Delayed apoptotic cell clearance and lupus-like autoimmunity in mice lacking the c-mer membrane tyrosine kinase.* J Exp Med, 2002. **196**(1): p. 135-40.

123. Radic, M.Z., et al., *Heterogeneous nuclear ribonucleoprotein P2 is an autoantibody target in mice deficient for Mer, Axl, and Tyro3 receptor tyrosine kinases.* J Immunol, 2006. **176**(1): p. 68-74.

124. Gould, W.R., et al., *Gas6 receptors Axl, Sky and Mer enhance platelet activation and regulate thrombotic responses.* J Thromb Haemost, 2005. **3**(4): p. 733-41.

125. Angelillo-Scherrer, A., et al., *Deficiency or inhibition of Gas6 causes platelet dysfunction and protects mice against thrombosis.* Nat Med, 2001. **7**(2): p. 215-21.

126. Schneider, P., et al., *BAFF, a novel ligand of the tumor necrosis factor family, stimulates B cell growth.* J Exp Med, 1999. **189**(11): p. 1747-56.

127. Gross, J.A., et al., *TACI and BCMA are receptors for a TNF homologue implicated in B-cell autoimmune disease.* Nature, 2000. **404**(6781): p. 995-9.

128. Moore, P.A., et al., *BLyS: member of the tumor necrosis factor family and B lymphocyte stimulator.* Science, 1999. **285**(5425): p. 260-3.

129. Mukhopadhyay, A., et al., *Identification and characterization of a novel cytokine, THANK, a TNF homologue that activates apoptosis, nuclear factor-*

kappaB, and c-Jun NH2-terminal kinase. J Biol Chem, 1999. **274**(23): p. 15978-81.

130. Nardelli, B., et al., *Synthesis and release of B-lymphocyte stimulator from myeloid cells.* Blood, 2001. **97**(1): p. 198-204.

131. Scapini, P., et al., *G-CSF-stimulated neutrophils are a prominent source of functional BLyS.* J Exp Med, 2003. **197**(3): p. 297-302.

132. Oren, D.A., et al., *Structural basis of BLyS receptor recognition.* Nat Struct Biol, 2002. **9**(4): p. 288-92.

133. Liu, Y., et al., *Crystal structure of sTALL-1 reveals a virus-like assembly of TNF family ligands.* Cell, 2002. **108**(3): p. 383-94.

134. Gavin, A.L., et al., *DeltaBAFF, an alternate splice isoform that regulates receptor binding and biopresentation of the B cell survival cytokine, BAFF.* J Biol Chem, 2003. **278**(40): p. 38220-8.

135. Gavin, A.L., et al., *deltaBAFF, a splice isoform of BAFF, opposes full-length BAFF activity in vivo in transgenic mouse models.* J Immunol, 2005. **175**(1): p. 319-28.

136. Gross, J.A., et al., *TACI-Ig neutralizes molecules critical for B cell development and autoimmune disease. impaired B cell maturation in mice lacking BLyS.* Immunity, 2001. **15**(2): p. 289-302.

137. Schiemann, B., et al., *An essential role for BAFF in the normal development of B cells through a BCMA-independent pathway.* Science, 2001. **293**(5537): p. 2111-4.

138. Shulga-Morskaya, S., et al., *B cell-activating factor belonging to the TNF family acts through separate receptors to support B cell survival and T cell-independent antibody formation.* J Immunol, 2004. **173**(4): p. 2331-41.

139. Tardivel, A., et al., *The anti-apoptotic factor Bcl-2 can functionally substitute for the B cell survival but not for the marginal zone B cell differentiation activity of BAFF.* Eur J Immunol, 2004. **34**(2): p. 509-18.

140. Khare, S.D., et al., *Severe B cell hyperplasia and autoimmune disease in TALL-1 transgenic mice.* Proc Natl Acad Sci U S A, 2000. **97**(7): p. 3370-5.

141. Mackay, F., et al., *Mice transgenic for BAFF develop lymphocytic disorders along with autoimmune manifestations.* J Exp Med, 1999. **190**(11): p. 1697-710.

142. Parry, T.J., et al., *Pharmacokinetics and immunological effects of exogenously administered recombinant human B lymphocyte stimulator (BLyS) in mice.* J Pharmacol Exp Ther, 2001. **296**(2): p. 396-404.

143. Batten, M., et al., *BAFF mediates survival of peripheral immature B lymphocytes.* J Exp Med, 2000. **192**(10): p. 1453-66.

144. Craxton, A., et al., *Macrophage- and dendritic cell--dependent regulation of human B-cell proliferation requires the TNF family ligand BAFF.* Blood, 2003. **101**(11): p. 4464-71.

145. Do, R.K., et al., *Attenuation of apoptosis underlies B lymphocyte stimulator enhancement of humoral immune response.* J Exp Med, 2000. **192**(7): p. 953-64.

146. Hsu, B.L., et al., *Cutting edge: BLyS enables survival of transitional and mature B cells through distinct mediators.* J Immunol, 2002. **168**(12): p. 5993-6.

147. Mongini, P.K., et al., *APRIL and BAFF promote increased viability of replicating human B2 cells via mechanism involving cyclooxygenase 2.* J Immunol, 2006. **176**(11): p. 6736-51.

148. Huang, X., et al., *Homeostatic cell-cycle control by BLyS: Induction of cell-cycle entry but not G1/S transition in opposition to p18INK4c and p27Kip1.* Proc Natl Acad Sci U S A, 2004. **101**(51): p. 17789-94.

149. Miller, J.P., J.E. Stadanlick, and M.P. Cancro, *Space, selection, and surveillance: setting boundaries with BLyS.* J Immunol, 2006. **176**(11): p. 6405-10.

150. Lesley, R., et al., *Reduced competitiveness of autoantigen-engaged B cells due to increased dependence on BAFF.* Immunity, 2004. **20**(4): p. 441-53.

151. Thien, M., et al., *Excess BAFF rescues self-reactive B cells from peripheral deletion and allows them to enter forbidden follicular and marginal zone niches.* Immunity, 2004. **20**(6): p. 785-98.

152. Brink, R., *Regulation of B cell self-tolerance by BAFF.* Semin Immunol, 2006. **18**(5): p. 276-83.

153. Stohl, W., et al., *B lymphocyte stimulator overexpression in patients with systemic lupus erythematosus: longitudinal observations.* Arthritis Rheum, 2003. **48**(12): p. 3475-86.

154. Zhang, J., et al., *Cutting edge: a role for B lymphocyte stimulator in systemic lupus erythematosus.* J Immunol, 2001. **166**(1): p. 6-10.

155. Cheema, G.S., et al., *Elevated serum B lymphocyte stimulator levels in patients with systemic immune-based rheumatic diseases.* Arthritis Rheum, 2001. **44**(6): p. 1313-9.

156. Tan, S.M., et al., *Local production of B lymphocyte stimulator protein and APRIL in arthritic joints of patients with inflammatory arthritis.* Arthritis Rheum, 2003. **48**(4): p. 982-92.

157. Groom, J., et al., *Association of BAFF/BLyS overexpression and altered B cell differentiation with Sjogren's syndrome.* J Clin Invest, 2002. **109**(1): p. 59-68.

158. Mariette, X., et al., *The level of BLyS (BAFF) correlates with the titre of autoantibodies in human Sjogren's syndrome.* Ann Rheum Dis, 2003. **62**(2): p. 168-71.

159. Emmerich, F., et al., *High-level serum B-cell activating factor and promoter polymorphisms in patients with idiopathic thrombocytopenic purpura.* Br J Haematol, 2007. **136**(2): p. 309-14.

160. Mackay, I.R., J. Groom, and C.R. Mackay, *Levels of BAFF in serum in primary biliary cirrhosis and autoimmune diabetes.* Autoimmunity, 2002. **35**(8): p. 551-3.

161. Litinskiy, M.B., et al., *DCs induce CD40-independent immunoglobulin class switching through BLyS and APRIL.* Nat Immunol, 2002. **3**(9): p. 822-9.

162. Castigli, E., et al., *TACI and BAFF-R mediate isotype switching in B cells.* J Exp Med, 2005. **201**(1): p. 35-9.

163. Tangye, S.G., et al., *BAFF, APRIL and human B cell disorders.* Semin Immunol, 2006. **18**(5): p. 305-17.

164. Culton, D.A., et al., *Early preplasma cells define a tolerance checkpoint for autoreactive B cells.* J Immunol, 2006. **176**(2): p. 790-802.

165. Avery, D.T., et al., *BAFF selectively enhances the survival of plasmablasts generated from human memory B cells.* J Clin Invest, 2003. **112**(2): p. 286-97.

166. Gorelik, L., et al., *Cutting edge: BAFF regulates CD21/35 and CD23 expression independent of its B cell survival function.* J Immunol, 2004. **172**(2): p. 762-6.

167. Marsters, S.A., et al., *Interaction of the TNF homologues BLyS and APRIL with the TNF receptor homologues BCMA and TACI.* Curr Biol, 2000. **10**(13): p. 785-8.

168. Wu, Y., et al., *Tumor necrosis factor (TNF) receptor superfamily member TACI is a high affinity receptor for TNF family members APRIL and BLyS.* J Biol Chem, 2000. **275**(45): p. 35478-85.

169. Thompson, J.S., et al., *BAFF-R, a newly identified TNF receptor that specifically interacts with BAFF.* Science, 2001. **293**(5537): p. 2108-11.

170. Yan, M., et al., *Identification of a novel receptor for B lymphocyte stimulator that is mutated in a mouse strain with severe B cell deficiency.* Curr Biol, 2001. **11**(19): p. 1547-52.

171. Bossen, C. and P. Schneider, *BAFF, APRIL and their receptors: structure, function and signaling.* Semin Immunol, 2006. **18**(5): p. 263-75.

172. Xu, S. and K.P. Lam, *B-cell maturation protein, which binds the tumor necrosis factor family members BAFF and APRIL, is dispensable for humoral immune responses.* Mol Cell Biol, 2001. **21**(12): p. 4067-74.

173. Mackay, F., et al., *BAFF AND APRIL: a tutorial on B cell survival.* Annu Rev Immunol, 2003. **21**: p. 231-64.

174. Ng, L.G., et al., *B cell-activating factor belonging to the TNF family (BAFF)-R is the principal BAFF receptor facilitating BAFF costimulation of circulating T and B cells.* J Immunol, 2004. **173**(2): p. 807-17.

175. Schneider, P., *The role of APRIL and BAFF in lymphocyte activation.* Curr Opin Immunol, 2005. **17**(3): p. 282-9.

176. Sasaki, Y., et al., *TNF family member B cell-activating factor (BAFF) receptor-dependent and -independent roles for BAFF in B cell physiology.* J Immunol, 2004. **173**(4): p. 2245-52.

177. von Bulow, G.U., J.M. van Deursen, and R.J. Bram, *Regulation of the T-independent humoral response by TACI.* Immunity, 2001. **14**(5): p. 573-82.

178. Yan, M., et al., *Activation and accumulation of B cells in TACI-deficient mice.* Nat Immunol, 2001. **2**(7): p. 638-43.

179. Seshasayee, D., et al., *Loss of TACI causes fatal lymphoproliferation and autoimmunity, establishing TACI as an inhibitory BLyS receptor.* Immunity, 2003. **18**(2): p. 279-88.

180. Sakurai, D., et al., *TACI attenuates antibody production costimulated by BAFF-R and CD40.* Eur J Immunol, 2007. **37**(1): p. 110-8.

181. Castigli, E., et al., *TACI is mutant in common variable immunodeficiency and IgA deficiency.* Nat Genet, 2005. **37**(8): p. 829-34.

182. Salzer, U., et al., *Mutations in TNFRSF13B encoding TACI are associated with common variable immunodeficiency in humans.* Nat Genet, 2005. **37**(8): p. 820-8.

183. Treml, L.S., J.E. Crowley, and M.P. Cancro, *BLyS receptor signatures resolve homeostatically independent compartments among naive and antigen-experienced B cells.* Semin Immunol, 2006. **18**(5): p. 297-304.

184. O'Connor, B.P., et al., *BCMA is essential for the survival of long-lived bone marrow plasma cells.* J Exp Med, 2004. **199**(1): p. 91-8.

185. Claudio, E., et al., *BAFF-induced NEMO-independent processing of NF-kappa B2 in maturing B cells.* Nat Immunol, 2002. **3**(10): p. 958-65.

186. Kayagaki, N., et al., *BAFF/BLyS receptor 3 binds the B cell survival factor BAFF ligand through a discrete surface loop and promotes processing of NF-kappaB2.* Immunity, 2002. **17**(4): p. 515-24.

187. Morrison, M.D., et al., *An atypical tumor necrosis factor (TNF) receptor-associated factor-binding motif of B cell-activating factor belonging to the TNF family (BAFF) receptor mediates induction of the noncanonical NF-kappaB signaling pathway.* J Biol Chem, 2005. **280**(11): p. 10018-24.

188. Hatada, E.N., et al., *NF-kappa B1 p50 is required for BLyS attenuation of apoptosis but dispensable for processing of NF-kappa B2 p100 to p52 in quiescent mature B cells.* J Immunol, 2003. **171**(2): p. 761-8.

189. Enzler, T., et al., *Alternative and classical NF-kappa B signaling retain autoreactive B cells in the splenic marginal zone and result in lupus-like disease.* Immunity, 2006. **25**(3): p. 403-15.

190. Sasaki, Y., et al., *Canonical NF-kappaB activity, dispensable for B cell development, replaces BAFF-receptor signals and promotes B cell proliferation upon activation.* Immunity, 2006. **24**(6): p. 729-39.

191. Craxton, A., et al., *BAFF regulates B cell survival by downregulating the BH3-only family member Bim via the ERK pathway.* J Exp Med, 2005. **202**(10): p. 1363-74.

192. Patke, A., et al., *BAFF controls B cell metabolic fitness through a PKC beta- and Akt-dependent mechanism.* J Exp Med, 2006. **203**(11): p. 2551-62.

193. Oliver, P.M., et al., *Loss of the proapoptotic protein, Bim, breaks B cell anergy.* J Exp Med, 2006. **203**(3): p. 731-41.

194. Mecklenbrauker, I., et al., *Regulation of B-cell survival by BAFF-dependent PKCdelta-mediated nuclear signalling.* Nature, 2004. **431**(7007): p. 456-61.

195. Woodland, R.T., M.R. Schmidt, and C.B. Thompson, *BLyS and B cell homeostasis.* Semin Immunol, 2006. **18**(5): p. 318-26.

196. Mongini, P.K., et al., *Innate immunity and human B cell clonal expansion: effects on the recirculating B2 subpopulation.* J Immunol, 2005. **175**(9): p. 6143-54.

197. Xu, L.G., et al., *Identification of downstream genes up-regulated by the tumor necrosis factor family member TALL-1.* J Leukoc Biol, 2002. **72**(2): p. 410-6.

198. Gorelik, L., et al., *Normal B cell homeostasis requires B cell activation factor production by radiation-resistant cells.* J Exp Med, 2003. **198**(6): p. 937-45.

199. Boule, M.W., et al., *Toll-like receptor 9-dependent and -independent dendritic cell activation by chromatin-immunoglobulin G complexes.* J Exp Med, 2004. **199**(12): p. 1631-40.

200. Ogden, C.A., et al., *Enhanced apoptotic cell clearance capacity and B cell survival factor production by IL-10-activated macrophages: implications for Burkitt's lymphoma.* J Immunol, 2005. **174**(5): p. 3015-23.

201. Hase, H., et al., *BAFF/BLyS can potentiate B-cell selection with the B-cell coreceptor complex.* Blood, 2004. **103**(6): p. 2257-65.

202. Balogh, P., et al., *Ontogeny of the follicular dendritic cell phenotype and function in the postnatal murine spleen.* Cell Immunol, 2001. **214**(1): p. 45-53.

203. Wu, J., et al., *Follicular dendritic cell-derived antigen and accessory activity in initiation of memory IgG responses in vitro.* J Immunol, 1996. **157**(8): p. 3404-11.

204. Collins, C.E., et al., *B lymphocyte stimulator (BLyS) isoforms in systemic lupus erythematosus: disease activity correlates better with blood leukocyte BLyS mRNA levels than with plasma BLyS protein levels.* Arthritis Res Ther, 2006. **8**(1): p. R6.

205. Diaz-de-Durana, Y., et al., *TACI-BLyS signaling via B-cell-dendritic cell cooperation is required for naive CD8+ T-cell priming in vivo.* Blood, 2006. **107**(2): p. 594-601.

206. Hanada, T., et al., *Suppressor of cytokine signaling-1 is essential for suppressing dendritic cell activation and systemic autoimmunity.* Immunity, 2003. **19**(3): p. 437-50.

207. Harley, J.B., J.A. Kelly, and K.M. Kaufman, *Unraveling the genetics of systemic lupus erythematosus.* Springer Semin Immunopathol, 2006. **28**(2): p. 119-30.

208. Kelly, J.A., K.L. Moser, and J.B. Harley, *The genetics of systemic lupus erythematosus: putting the pieces together.* Genes Immun, 2002. **3 Suppl 1**: p. S71-85.

209. Goodnow, C.C., *Immunology. Discriminating microbe from self suffers a double toll.* Science, 2006. **312**(5780): p. 1606-8.

210. Kumar, K.R., et al., *Regulation of B cell tolerance by the lupus susceptibility gene Ly108.* Science, 2006. **312**(5780): p. 1665-9.

211. Pisitkun, P., et al., *Autoreactive B cell responses to RNA-related antigens due to TLR7 gene duplication.* Science, 2006. **312**(5780): p. 1669-72.

212. Napirei, M., et al., *Features of systemic lupus erythematosus in Dnase1-deficient mice.* Nat Genet, 2000. **25**(2): p. 177-81.

213. Hanayama, R., et al., *Autoimmune disease and impaired uptake of apoptotic cells in MFG-E8-deficient mice.* Science, 2004. **304**(5674): p. 1147-50.

214. Ishimoto, Y., et al., *Promotion of the uptake of PS liposomes and apoptotic cells by a product of growth arrest-specific gene, gas6.* J Biochem (Tokyo), 2000. **127**(3): p. 411-7.

215. Kalled, S.L., *Impact of the BAFF/BR3 axis on B cell survival, germinal center maintenance and antibody production.* Semin Immunol, 2006. **18**(5): p. 290-6.

216. Rolink, A.G., et al., *BAFF is a survival and maturation factor for mouse B cells.* Eur J Immunol, 2002. **32**(7): p. 2004-10.

217. Bondanza, A., et al., *Cutting edge: dissociation between autoimmune response and clinical disease after vaccination with dendritic cells.* J Immunol, 2003. **170**(1): p. 24-7.

218. Chen, M., et al., *Dendritic cell apoptosis in the maintenance of immune tolerance.* Science, 2006. **311**(5764): p. 1160-4.

219. Georgiev, M., et al., *Mature dendritic cells readily break tolerance in normal mice but do not lead to disease expression.* Arthritis Rheum, 2005. **52**(1): p. 225-38.

220. Ma, L., et al., *Systemic autoimmune disease induced by dendritic cells that have captured necrotic but not apoptotic cells in susceptible mouse strains.* Eur J Immunol, 2005. **35**(11): p. 3364-75.

221. O'Keeffe, M., et al., *Dendritic cell precursor populations of mouse blood: identification of the murine homologues of human blood plasmacytoid pre-DC2 and CD11c+ DC1 precursors.* Blood, 2003. **101**(4): p. 1453-9.

222. Blanco, P., et al., *Induction of dendritic cell differentiation by IFN-alpha in systemic lupus erythematosus.* Science, 2001. **294**(5546): p. 1540-3.

223. Kamath, A.T., et al., *Developmental kinetics and lifespan of dendritic cells in mouse lymphoid organs.* Blood, 2002. **100**(5): p. 1734-41.

224. Crowley, J.E., et al., *Homeostatic niche specification among naive and activated B cells: a growing role for the BLyS family of receptors and ligands.* Semin Immunol, 2005. **17**(3): p. 193-9.

225. *More information on the plasmids PL451and PL452 or the bacterial strains DY380 and EL350 can be found at http://recombineering.ncifcrf.gov/.*

.

226. Rozen, S. and H. Skaletsky, *Primer3 on the WWW for general users and for biologist programmers.* Methods Mol Biol, 2000. **132**: p. 365-86.

227. Smit AFA, H.R., Green P, *RepeatMasker Open-3.0*. 1996-2004.

228. Gordon, N.C., et al., *BAFF/BLyS receptor 3 comprises a minimal TNF receptor-like module that encodes a highly focused ligand-binding site.* Biochemistry, 2003. **42**(20): p. 5977-83.

229. Kim, H.M., et al., *Crystal structure of the BAFF-BAFF-R complex and its implications for receptor activation.* Nat Struct Biol, 2003. **10**(5): p. 342-8.

230. Liu, Y., et al., *Ligand-receptor binding revealed by the TNF family member TALL-1.* Nature, 2003. **423**(6935): p. 49-56.

231. Liu, P., et al., *Embryonic lethality and tumorigenesis caused by segmental aneuploidy on mouse chromosome 11.* Genetics, 1998. **150**(3): p. 1155-68.

232. Seong, E., et al., *To knockout in 129 or in C57BL/6: that is the question.* Trends Genet, 2004. **20**(2): p. 59-62.

233. Chong, M.M., et al., *Suppressor of cytokine signaling-1 in T cells and macrophages is critical for preventing lethal inflammation.* Blood, 2005. **106**(5): p. 1668-75.

234. Hazenbos, W.L., et al., *GPI-anchor deficiency in myeloid cells causes impaired FcgammaR effector functions.* Blood, 2004. **104**(9): p. 2825-31.

235. Dziennis, S., et al., *The CD11b promoter directs high-level expression of reporter genes in macrophages in transgenic mice.* Blood, 1995. **85**(2): p. 319-29.

236. Ferron, M. and J. Vacher, *Targeted expression of Cre recombinase in macrophages and osteoclasts in transgenic mice.* Genesis, 2005. **41**(3): p. 138-45.

237. Brockschnieder, D., et al., *An improved mouse line for Cre-induced cell ablation due to diphtheria toxin A, expressed from the Rosa26 locus.* Genesis, 2006. **44**(7): p. 322-7.

238. Lewandoski, M., *Conditional control of gene expression in the mouse.* Nat Rev Genet, 2001. **2**(10): p. 743-55.

239. Holzenberger, M., et al., *Ubiquitous postnatal LoxP recombination using a doxycycline auto-inducible Cre transgene (DAI-Cre).* Genesis, 2000. **26**(2): p. 157-9.

240. P.G. , G.M., *unpublished observations*.

241. Jacob, C.O., et al., *Paucity of clinical disease despite serological autoimmunity and kidney pathology in lupus-prone New Zealand mixed 2328 mice deficient in BAFF.* J Immunol, 2006. **177**(4): p. 2671-80.

242. Magliozzi, R., et al., *Intracerebral expression of CXCL13 and BAFF is accompanied by formation of lymphoid follicle-like structures in the meninges of mice with relapsing experimental autoimmune encephalomyelitis.* J Neuroimmunol, 2004. **148**(1-2): p. 11-23.

243. Thangarajh, M., et al., *Expression of B-cell-activating factor of the TNF family (BAFF) and its receptors in multiple sclerosis.* J Neuroimmunol, 2004. **152**(1-2): p. 183-90.

244. Fu, L., et al., *Constitutive NF-kappaB and NFAT activation leads to stimulation of the BLyS survival pathway in aggressive B-cell lymphomas.* Blood, 2006. **107**(11): p. 4540-8.

245. He, B., et al., *EBV-encoded latent membrane protein 1 cooperates with BAFF/BLyS and APRIL to induce T cell-independent Ig heavy chain class switching.* J Immunol, 2003. **171**(10): p. 5215-24.

246. Kuo, T.C. and K.L. Calame, *B lymphocyte-induced maturation protein (Blimp)-1, IFN regulatory factor (IRF)-1, and IRF-2 can bind to the same regulatory sites.* J Immunol, 2004. **173**(9): p. 5556-63.

247. Nguyen, H., J. Hiscott, and P.M. Pitha, *The growing family of interferon regulatory factors.* Cytokine Growth Factor Rev, 1997. **8**(4): p. 293-312.

248. Shapiro-Shelef, M., et al., *Blimp-1 is required for the formation of immunoglobulin secreting plasma cells and pre-plasma memory B cells.* Immunity, 2003. **19**(4): p. 607-20.

249. Chang, D.H., C. Angelin-Duclos, and K. Calame, *BLIMP-1: trigger for differentiation of myeloid lineage.* Nat Immunol, 2000. **1**(2): p. 169-76.

250. Gyory, I., et al., *Identification of a functionally impaired positive regulatory domain I binding factor 1 transcription repressor in myeloma cell lines.* J Immunol, 2003. **170**(6): p. 3125-33.

251. Omori, S.A., et al., *Regulation of class-switch recombination and plasma cell differentiation by phosphatidylinositol 3-kinase signaling.* Immunity, 2006. **25**(4): p. 545-57.

252. Jung, S., et al., *In vivo depletion of CD11c(+) dendritic cells abrogates priming of CD8(+) T cells by exogenous cell-associated antigens.* Immunity, 2002. **17**(2): p. 211-20.

253. Rahman, Z.S., et al., *A novel susceptibility locus on chromosome 2 in the (New Zealand Black x New Zealand White)F1 hybrid mouse model of systemic lupus erythematosus.* J Immunol, 2002. **168**(6): p. 3042-9.

254. Lindqvist, A.K., et al., *A susceptibility locus for human systemic lupus erythematosus (hSLE1) on chromosome 2q.* J Autoimmun, 2000. **14**(2): p. 169-78.

255. Cheong, H.S., et al., *MERTK polymorphisms associated with risk of haematological disorders among Korean SLE patients.* Rheumatology (Oxford), 2007. **46**(2): p. 209-14.

256. Ovcharenko, I., et al., *ECR Browser: a tool for visualizing and accessing data from comparisons of multiple vertebrate genomes.* Nucleic Acids Res, 2004. **32**(Web Server issue): p. W280-6.